1-1-2013

Arx Influences Cortical Function by Regulating Progenitor Cell Proliferation

Jacqueline Christine Simonet
University of Pennsylvania, jsimonet@gmail.com

Arx Influences Cortical Function by Regulating Progenitor Cell Proliferation

Abstract
Mutations in the Aristaless-related homeobox (ARX) gene are found in a spectrum of epilepsy and X-linked intellectual disability disorders in children. During development Arx is expressed in pallial ventricular zone (VZ) progenitor cells which give rise to the excitatory projection neurons of the cortex. Arx-/Y mice were shown to have decreased proliferation in the cortical VZ resulting in smaller brains; however, the basis for this reduced proliferation was not established. To determine the role of ARX on cell cycle dynamics in cortical progenitor cells, we generated cerebral cortex specific Arx mouse mutants (cKO). The loss of pallial Arx resulted in the reduction of cortical progenitor cells, particularly affected was the proliferation of intermediate progenitor cells (IPCs). The mechanism was determined to be due to an overexpression of CDKN1C, an inhibitor of cell cycle progression, in the cortical VZ and SVZ of Arx KOs throughout corticogenesis. We also identified CDKN1C through transcriptional profile analysis of Arx KO cortices and showed that ARX is a direct regulator of Cdkn1c transcription. Later in development and postnatally cKO corticies showed a reduction of upper layer but not deeper layer neurons consistent with the IPC defect. The phenotype of the adult cKO mice is different from all other Arx mutant mice. They have no discernable seizure activity and are less anxious, less social, and more active when compared to their wild type littermates. Anatomically, there are significant changes with reduced cortical thickness and a hypoplastic corpus callosum and anterior commissure both consistent with a perturbation in cortical connectivity. Together, these data suggest specific structural and behavioral anomalies, common in patients with ARX mutations, are specifically due to alterations in pallial progenitor function. Furthermore, and of considerable interest, our data demonstrate that some of the neurobehavioral features found in patients with ARX mutations are not due to on-going seizures, as is often postulated, as the confounding variable of epilepsy was eliminated in these behavior analyses.

Degree Type
Dissertation

Degree Name
Doctor of Philosophy (PhD)

Graduate Group
Cell & Molecular Biology

First Advisor
Jeffrey A. Golden

Second Advisor
Eric D. Marsh

Keywords
anxiety, behavior, cell cycle, cortex, hyperactivity, mouse

ARX INFLUENCES CORTICAL FUNCTION BY REGULATING PROGENITOR CELL PROLIFERATION

Jacqueline C. Simonet

A DISSERTATION

in

Cell and Molecular Biology

Presented to the Faculties of the University of Pennsylvania

in

Partial Fulfillment of the Requirements for the

Degree of Doctor of Philosophy

2013

Supervisor of Dissertation

Jeffrey A. Golden

Professor of Pathology at Harvard Medical School

Co-Supervisor of Dissertation

Eric D. Marsh

Assistant Professor of Neurology

Graduate Group Chairperson

Daniel S. Kessler, Associate Professor of Cell and Developmental Biology

Dissertation Committee

Michael Granto, Professor of Cell and Developmental Biology

Erika L. F. Holzbaur, Professor of Physiology

Paul A. Janmey, Professor of Physiology

Matthew B. Dalva, Associate Professor of Neuroscience at Thomas Jefferson University

ARX INFLUENCES CORTICAL FUNCTION BY REGULATING PROGENITOR CELL PROLIFERATION

ACKNOWLEDGMENT

I would like to thank my mentors Jeff Golden and Eric Marsh for their assistance in developing and executing the experiments in this document and for their excellent editing skills. I would also like to thank my committee for all of their guidance and advice over the many years and directions of my thesis work. I would like to thank my husband, Guy LeBas, for always being willing to edit drafts, listen to talks, and sometimes even assist in experiments. I would like to thank all of my current and former lab mates for all of their help over the years. Especially Will Shapiro and George Clement for mouse husbandry and genotyping. Nikki Sunnen, Dan Lysko, Ginam Cho, and Erika Lin-Hendel for all of their help planning and executing experiments and listening to my talks and offering wonderful advice. I would like to thank Dr. Kunio Kitamura for the anti-Arx antibody and Christina Bradley for her assistance with behavioral assays. As well as Elliot Bourgeois for writing the MATLAB code for home cage movement detection and Camillo Bermudez and Irfan Shehzad for their assistance with the EEG quantification.

ABSTRACT

ARX INFLUENCES CORTICAL FUNCTION BY REGULATING PROGENITOR CELL PROLIFERATION

Jacqueline Simonet

Jeffrey Golden

Eric Marsh

Mutations in the *Aristaless-related homeobox* (*ARX*) gene are found in a spectrum of epilepsy and X-linked intellectual disability disorders in children. During development *Arx* is expressed in pallial ventricular zone (VZ) progenitor cells which give rise to the excitatory projection neurons of the cortex. $Arx^{-/Y}$ mice were shown to have decreased proliferation in the cortical VZ resulting in smaller brains; however, the basis for this reduced proliferation was not established. To determine the role of ARX on cell cycle dynamics in cortical progenitor cells, we generated cerebral cortex specific *Arx* mouse mutants (cKO). The loss of pallial *Arx* resulted in the reduction of cortical progenitor cells, particularly affected was the proliferation of intermediate progenitor cells (IPCs). The mechanism was determined to be due to an overexpression of CDKN1C, an inhibitor of cell cycle progression, in the cortical VZ and SVZ of *Arx* KOs throughout corticogenesis. We also identified CDKN1C through transcriptional profile analysis of *Arx* KO cortices and showed that ARX is a direct regulator of *Cdkn1c* transcription. Later in development and postnatally cKO corticies showed a reduction of upper layer but not deeper layer neurons consistent with the IPC defect. The phenotype of the adult cKO mice is different from all other *Arx* mutant mice. They have no discernable seizure activity and are less anxious, less social, and more active when compared to their wild type littermates. Anatomically, there are significant changes with reduced cortical thickness and a hypoplastic corpus callosum and anterior commissure both consistent with a perturbation in cortical connectivity. Together, these

data suggest specific structural and behavioral anomalies, common in patients with *ARX* mutations, are specifically due to alterations in pallial progenitor function. Furthermore, and of considerable interest, our data demonstrate that some of the neurobehavioral features found in patients with *ARX* mutations are not due to on-going seizures, as is often postulated, as the confounding variable of epilepsy was eliminated in these behavior analyses.

INTELLECTUAL CONTRIBUTION

Part of this work was done in collaboration with Gaia Colasante and Vania Broccoli.

The early developmental decrease in proliferation and increase in differentiation experiments in Chapter 2 Figure 2, the gene expression profile analysis in Chapter 2 Figure 11, the in situ hybridizations in Chapter 2 Figure 12 and 13, and the luciferase reporter assays and chromatin immunoprecipitation experiments in Chapter 2 Figure 12 were done by Gaia Colasante and Vania Broccoli.

The morphological experiments in Chapter 2 Figure 1, the proliferation rate experiments in Chapter 2 Figure 3, the cell cycle length experiments in Chapter 2 Figure 5, the cell cycle exit experiments in Chapter 2 Figure 7, and the SVZ progenitor cell cycle length experiments in Chapter 2 Figure 8 were done in collaboration with Gaia Colasante and Vania Broccoli.

All of the other experiments in Chapter 2 and all of the experiments in Chapter 3 were done by Jacqueline Simonet in the laboratories of Jeffrey Golden and Eric Marsh.

Chapter 2 is published in the journal Cerebral Cortex Aug. 22, 2013 (Epub ahead of print) "ARX Regulates Cortical Intermediate Progenitor Cell Expansion and Upper Layer Neuron Formation Through Repression of Cdkn1c." and is reproduced here with their permission: http://www.oxfordjournals.org/access_purchase/publication_rights.html

At the time of submission Chapter 3 is under review for publication at Cerebral Cortex.

TABLE OF CONTENTS

LIST OF TABLES

LIST OF ILLUSTRATIONS

CHAPTER 1: Introduction

Epilepsy, intellectual disability, and other neurological disorders are major causes of childhood morbidity and mortality. The development of effective therapies relies, in part, on determining the pathogenic mechanisms of these various disorders. Complicating this process is the increasing recognition that identification of a specific genetic mutation does not, a priori, immediately elucidate the neurobiologic defect resulting in a particular disorder. In order to understand how known mutations in particular genes affect brain development and function we first need to understand how those genes function in normal brain development. My thesis work has focused on beginning to answer these questions for one particular gene, *Arx*, in the cerebral cortex of mice.

Development of the Cerebral Cortex

Understanding how changes in one gene affect cerebral cortical development requires first appreciating normal cortical development. Early in development the embryo consists of three cell layers, the inner most layer is the endoderm, the middle is the mesoderm, and the outer most layer is the ectoderm. The ectoderm gives rise to the central and peripheral nervous system along with the integumentary system. Shortly after the development of these three embryonic layers a central sheet of cells are specified as a neural plate at the dorsal midline of the embryo. The neural plate morphs into a neural tube due to proliferation, invagination, and pinching off of ectodermal cells from the surface (Alvarez IS and GC Schoenwolf 1992; Lawson A et al. 2001; Gilbert SF 2010). After the most anterior part of the neural tube has closed it begins to form bulges or

vesicles. The most anterior bulge, the prosencephalon, eventually becomes the forebrain of the embryo. As brain development proceeds this single vesicle divides in the anterior-posterior plane to become two vesicles, the telencephalon and the diencephalon. Over time the most anterior vesicle, the telencephalon, expands significantly in the medial lateral plan to become the large, bilaterally symmetric cerebral hemispheres. The cells in these vesicles will ultimately give rise to the cerebral cortex, hippocampus, basal ganglia, and olfactory bulbs. (For review see (Kandel ER et al. 2000; Gilbert SF 2010))

During these early developmental stages the telencephalon is made up of primarily progenitor cells, which continually proliferate to generate more progenitor cells (Gotz M and YA Barde 2005). The progenitor cells in the dorsal aspect of the telencephalic vesicle, also called the pallium, give rise to the cerebral cortex. These dorsal progenitor cells, termed radial glial progenitor cells (RGCs), are located adjacent to the ventricle in the ventricular zone (VZ) (Malatesta P et al. 2000; Dehay C and H Kennedy 2007) (Chapter 1; Figure 1). These RGCs produce three different types of cells: More radial glia progenitor cells, differentiated neurons, and intermediate progenitor cells (IPCs) that will form a second layer of cells further away from the ventricle called the subventricular zone (SVZ) (Noctor SC et al. 2004; Gal JS et al. 2006; Dehay C and H Kennedy 2007) (Chapter 1; Figure 1). These IPCs will divide once to several times giving rise to more IPCs and ultimately neurons (Noctor SC et al. 2004; Dehay C and H Kennedy 2007). Together the RGCs and the IPCs will give rise to all of the projection (glutamatergic excitatory) neurons, in the cerebral cortex.

Another striking feature of cerebral cortical development is that the normal six-layered neocortex develops in a highly ordered manner. The first neurons to exit the cell cycle and begin differentiation will migrate up away from the ventricle and begin to form the cortex structure by residing in what will ultimately be the deepest layer of the cortex, layer 6 (Frantz GD and SK McConnell 1996; Kandel ER et al. 2000). Subsequent neurons migrate past layer 6 neurons and begin populating what will eventually be layer 5. This inside out process of development continues until neurons populate all six layers (Frantz GD and SK McConnell 1996; Kandel ER et al. 2000). Glial cells that will support the maturation and function of these neurons are subsequently produced from the RGCs and will migrate up into all of the layers of the cortex (Bayer SA and J Altman 1991; Miller FD and AS Gauthier 2007). The outer most layer, known as the molecular layer or layer 1, is formed early in development from a unique population of neurons known as Cajal-Rietzius cells. This layer is formed prior to the deeper layers when the RGCs are still clonally proliferating. The Cajal-Rietzius cells help to direct the migration of the other neurons and glia into their appropriate layers (Meyer G et al. 2002; Hevner RF et al. 2003; Takiguchi-Hayashi K et al. 2004; Bielle F et al. 2005; Soriano E and JA Del Rio 2005).

There is currently some controversy regarding which cortical layers the IPCs contribute neurons to. As was previously described IPCs are produced by the RGCs early in development and they, in turn, replicate themselves and ultimately differentiate into neurons but not glia. Some evidence exists to support IPCs producing excitatory neurons that will reside in all layers of the cortex. Other evidence suggests that IPCs only produce superficial or upper layer neurons (for review see (Kriegstein A et al. 2006;

Pontious A et al. 2008)). The upper layer neuron hypothesis is supported mainly by the fact that upper layer molecular markers (*Cux1*, *Satb2*, *Cux2*, *Svet1*) are expressed in IPCs both before and during neurogenesis of upper layer neurons (Tarabykin V et al. 2001; Nieto M et al. 2004; Zimmer C et al. 2004; Britanova O et al. 2005). The IPCs reside in and form the SVZ during the time when the upper layer neurons are being generated. Thus the timing is right for the IPCs to give rise to upper layer neurons and not lower layer neurons (Takahashi T et al. 1999; Gotz M and L Sommer 2005). However, there is also evidence that IPCs during development produce neurons from all neocortical layers even before the SVZ is formed (Kowalczyk T et al. 2009). There is currently no direct evidence that IPCs produce only upper layer neurons versus neurons in all layers, thus this point remains to be experimentally determined.

There are more than excitatory neurons in the neocortex. Inhibitory neurons, or interneurons, comprise twenty percent of the adult neuronal population of the cerebral cortex, and are derived from a completely separate progenitor source (Faux C et al. 2010; Le Magueresse C and H Monyer 2013). These cortical interneurons develop ventrally in the subpallial compartment of the telencephalon in three regions known as the caudal, medial, and lateral ganglionic eminences (Chapter 1; Figure 1). They are embryonic structures located in what ultimately is the region of the basal ganglia in the adult (Wonders C and SA Anderson 2005; Marin O 2013). Analogous to the dorsal telencephalon, the medial ganglionic eminence progenitor cells will first divide to self replicate and later in development, beginning around embryonic day 10.5, they will begin to produce differentiated premature interneurons (Ross ME 2011; Le Magueresse C and H Monyer 2013). These developing interneurons will migrate dorsally up into the cortex

at the same time that the excitatory neurons are being produced by the RGCs and migrating radially to form the layers of the cortex (Faux C et al. 2012; Kwan KY et al. 2012; Marin O 2013) (Chapter 1; Figure 1). The interneurons integrate into the forming cortex in the same inside out manner as the excitatory neurons with the first interneurons populating the deeper layers and the last ones populating the most superficial layers (Miyoshi G and G Fishell 2011; Faux C et al. 2012; Kwan KY et al. 2012).

Once both the excitatory neurons and the interneurons have reached their final destinations they begin to send out axons to make connections with other neurons (Kandel ER et al. 2000; Lagercrantz H and T Ringstedt 2001). The excitatory neurons will make connections with adjacent neurons, neurons in other layers of the cortex, neurons in other neocortical regions, or send projections to other subcortical regions (Kandel ER et al. 2000; Innocenti GM and DJ Price 2005; Price DJ et al. 2006). The interneurons will primarily make local connections with neighboring cortical neurons since they are responsible for the coordination and regulation of cortical-cortical circuits (Kandel ER et al. 2000; Woo NH and B Lu 2006). After the axons have found their correct targets they will form synapses on the dendrites of other neurons to form complex circuits. Synapses are strengthened by activity and lost if inactive, a process called pruning (Kandel ER et al. 2000; Lagercrantz H and T Ringstedt 2001; Innocenti GM and DJ Price 2005). Through these processes the early brain is wired.

The cerebral cortex is organized into columnar functional units and groups of these units are then further organized into functional modules that control different tasks such as motor control or vision (Sansom SN and FJ Livesey 2009). Within any column of

cortex from the pial surface, the outer surface of the brain, to the ventricle the cells all have connections to each other and will all be activated together (Kandel ER et al. 2000; Sansom SN and FJ Livesey 2009). It is hypothesized that all of the cells born from a single RGC may form a column together (Kornack DR and P Rakic 1995; Sansom SN and FJ Livesey 2009). Within each column the cells in each layer make particular types of connections. In general the excitatory neurons in layers 2 and 3 project locally and to the opposite side of the cortex across the white matter tract called the corpus callosum with their axons terminating in layer 4 of the contralateral cortex (Kandel ER et al. 2000; Thomson AM and C Lamy 2007; Sansom SN and FJ Livesey 2009). Layer 4, which is the primary input layer to the cortex, also receives inputs from the thalamus. Neurons in the deeper layers, 5 and 6, primarily project to layer 1 or layer 6, but these are feedback projections rather than feed-forward (Kandel ER et al. 2000; Thomson AM and C Lamy 2007; Sansom SN and FJ Livesey 2009). Neurons in layer 5 predominately project out of the cortex to subcortical regions including down the spinal cord (Kandel ER et al. 2000; Thomson AM and C Lamy 2007; Sansom SN and FJ Livesey 2009).

Neuronal development disorders

Mutations in a variety of genes can disrupt any or all of these developmental processes and result in a spectrum of conditions. Some mutations lead to structural brain malformations while other mutations alter the circuitry, synapses, or function and lead to intellectual disability, and epilepsy. Genetic studies in a host of different brain malformations has led to the discovery of genes involved in regulating proliferation, migration, and cortical organization, among a host of other processes. Mutations have

been identified in genes involved in transcriptional regulation, cell cycle regulation, centrosome maturation and duplication, spindle formation, and DNA repair cause changes in proliferation and apoptosis of cortical progenitor cells (Barkovich AJ et al. 2012). These mutations lead to malformations such as microcephaly (small brain with fewer neurons) megalencephalies (large brain with more neurons), and focal or diffuse dysgenesis (areas of increased or decreased cortex size) (Manzini MC and CA Walsh 2011; Barkovich AJ et al. 2012).

Mutations in genes involved in structural and regulatory components of the cytoskeletal and the centrosome can cause problems with initiation, progression, and direction of migration. This leads to malformations such as periventicular heterotopia (problems with initiation of migration resulting in disorganized groups of neurons at the ventricle), subcortical heterotopia (problems with the direction of migration resulting in disorganized groups of neurons in the white matter), lissencephaly (problems with continuation and direction of migrations which results in a loss of the normal gyrated surface, a thickened neocortex, and a smooth brain), polymicrogyria (multiple small gyri), and cobblestone malformations (an overmigration of neurons resulting in disorganized groups of neurons at the pial surface of the brain) (Manzini MC and CA Walsh 2011; Barkovich AJ et al. 2012).

Mutations in genes involved in neuronal specification, projection, and the formation of synapses can cause changes in cortical organization and function. This leads to malformations such as focal dysplasia (areas of layer disorganization) and some

instances of polymicrogyria (multiple small gyri) (Manzini MC and CA Walsh 2011; Barkovich AJ et al. 2012).

The role of Arx in cortical development

Several genes do not fit neatly into any of these categories. One example is the *Aristaless-related homebox* gene (*ARX/Arx*), which is a transcription factor that is expressed in the developing hypothalamus, thalamus, basal ganglia, and cerebral cortex. It appears to regulate proliferation, specification, migration, and differentiation of various populations of neurons in these areas of the brain (Marsh ED and JA Golden 2012). *Arx* is on the X-chromosome thus most *ARX* patients are male as one normal allele is sufficient for normal brain development. There are currently 44 different mutations of *ARX* that have been found in humans (Shoubridge C et al. 2010) (Chapter 1; Figure 2). These mutations cause a spectrum of phenotypes from lissencephaly and hydranencephaly to mutations that cause no brain malformations, but do lead to intellectual disability and epilepsy.

One explanation for the different phenotypes associated with different mutations of the same gene is that mutations in different parts of the gene affect the function of the gene in different ways. In the case of *ARX*, more severe patient phenotypes, those that have brain malformations such as lissencephaly, are the result of either complete loss of function of the gene (deletions or truncations) or from mutations in the homeodomain region of the gene, which prevents Arx from to binding to DNA (Chapter 1; Figure 2). Point mutations and missense mutations that do not occur in the homeodomain tend to result in milder phenotypes that rarely include structural brain anomalies, but do include

moderate intellectual disability and epilepsy (Chapter 1; Figure 2). The exception to this rule is the polyalanine expansion mutations in the second polyalanine tract. These are the most common type occurring in about 40% of patients with an *ARX* mutation (Shoubridge C et al. 2010). These mutations can result in patients with a spectrum of phenotypes such as mild intellectual disability, moderate intellectual disability and dystonic hand movements (Parrington syndrome), moderate intellectual disability and infantile spasms, a particular type of epilepsy (West syndrome), or severe intellectual disability and early onset tonic spasms (Ohtahara syndrome) (Shoubridge C et al. 2010) (Chapter 1; Figure 2).

In order to look at the role of *Arx* in brain development and how mutations in this gene can lead to this pleiotropy of phenotypes in humans a mouse with no *Arx* expression ($Arx^{-/Y}$) was created in 2002. This $Arx^{-/Y}$ mouse dies shortly after birth most likely due to seizures or an inability to feed (Kitamura K et al. 2002). These mice have a thinner cortex and decrease proliferation in the cortex during development, but migration of the post mitotic excitatory neurons into the cortex seemed to be relatively normal (Kitamura K et al. 2002). The $Arx^{-/Y}$ mice also have abnormal nerve fiber tracts such as the corpus callosum, thalamo-cortical tract, fimbria, and hippocampal commissure (Kitamura K et al. 2002). In addition, the $Arx^{-/Y}$ mice have deficiencies in interneuron migration into the cortex and this led to mislocalization of interneurons in the cortex in addition to a loss of particular subtypes of interneurons (Kitamura K et al. 2002).

Mutant mice have also been generated with a series of *ARX* mutations seen in human patients (Kitamura K et al. 2009; Price MG et al. 2009). Two of the mutations are

point mutations in the homeodomain (P353L and P353R) and two others are expansions in the first polyalanine tract (330ins(GCG)7) and (10+7(GCG)) (Kitamura K et al. 2009; Price MG et al. 2009). In humans these mutations all produce very different phenotypes; the P353L mutation results in myoclonic epilepsy and intellectual disability, the P353R mutation results in XLAG (x-linked lissencephaly with ambiguous genetalia), and the polyalanine expansion results in West syndrome (infantile spasms and intellectual disability) (Kitamura K et al. 2009). Mice harboring the P353R ($Arx^{PR/Y}$) mutation die shortly after birth and have small brains similar to $Arx^{-/Y}$ mice (Kitamura K et al. 2009). Also similar to $Arx^{-/Y}$ mice, they have thinner cortices a loss of upper layer neurons, and an expansion of deeper layer neurons (Kitamura K et al. 2009). The $Arx^{PR/Y}$ mice also showed very little migration of interneurons into the cortex. Therefore, this mouse seems to be a good model of its human mutation and since it is similar to the $Arx^{-/Y}$ mouse, the $Arx^{-/Y}$ mouse can also be used as a model for human patients with these types of mutations.

The P353L knock-in mice ($Arx^{PL/Y}$) and the polyalanine expansion mice ($Arx^{(GCG)7/Y}$) have normal sized brains and cortices and with no change in cell layers (Kitamura K et al. 2009). Both the $Arx^{PL/Y}$ mice and the $Arx^{(GCG)7/Y}$ mice have delayed migration of their interneurons into the cortex and the $Arx^{PL/Y}$ mice have a slight reduction of interneurons in the cortex and the $Arx^{(GCG)7/Y}$ mice have a more severe reduction of interneuron numbers (Kitamura K et al. 2009). Most of the $Arx^{(GCG)7/Y}$ mice have seizures and die by around three months of age while the $Arx^{PL/Y}$ mice have a normal lifespan and did not have seizures, but did have a lower threshold when challenged with seizure inducing drugs (Kitamura K et al. 2009). In addition to their

more severe seizure phenotype the *Arx*$^{(GCG)7/Y}$ mice also have a more severe behavioral phenotype than the *Arx*$^{PL/Y}$ mice. The *Arx*$^{(GCG)7/Y}$ mice showed impaired aversive, spatial, and procedural learning whereas the *Arx*$^{PL/Y}$ mice only showed impaired aversive and spatial learning. In addition the *Arx*$^{(GCG)7/Y}$ mice were also anxious and hyperactive and the *Arx*$^{PL/Y}$ mice were not (Kitamura K et al. 2009). While recognizing these mice are not perfect models of the human phenotypes they do seem to mirror the severity of the human phenotypes. This indicates that the impairments to the function of *Arx* in each mutation is probably similar between mice and humans and therefore these mice are a reasonable model to further study the function of *ARX* and *ARX* mutations in patients.

A second polyalanine tract expansion mouse was made by again inserting 7 (GCG) codons inserted similar to the other polyalanine tract expansion mouse, but in a different location in the polyalanine tract (*Arx*$^{(GCG)10+7}$) (Price MG et al. 2009). These mice exhibit a similar behavioral and morphological phenotype to the *Arx*$^{(GCG)7/Y}$ mice. One exception to this is that the *Arx*$^{(GCG)10+7}$ mice were found to be less anxious and not hyperactive which is the opposite of the *Arx*$^{(GCG)7/Y}$ mice (Price MG et al. 2009). These mice (*Arx*$^{(GCG)7/Y}$) were shown to have seizures with similarities to the infantile spasms observed in human patients as early as nine days of age (Price MG et al. 2009). The *Arx*$^{(GCG)7/Y}$ mice also displayed social deficits in the social dominance tube test (Price MG et al. 2009). This second polyalanine tract expansion mouse (*Arx*$^{(GCG)7/Y}$) confirms that mouse models of human *ARX* mutations can be made and can serve as models for the human disease.

Arx mutant mice and human *ARX* patients have defects in many parts of their brains, but also in other parts of their bodies which led scientists to investigate where *Arx* is expressed during development and in the adult. *Arx* is first expressed in the anterior neural plate before neural tube closure. After neural tube closure it is expressed in the neural stem cells lining the bulges that will become the telencephalon (Colombo E et al. 2004). As development proceeds its expression can be found in the ventral thalamus, the floorplate of the developing spinal cord, the myotome which will give rise to the body muscles, the pancreas, the stomach, and the testes (Colombo E et al. 2004). In adults *Arx* expression is restricted to interneurons in the cerebral cortex and the olfactory bulb and adult neural stem cells (Colombo E et al. 2004).

In the developing cerebral cortex *Arx* shows distinct expression patterns in different neuronal populations. *Arx* is expressed in the medial ganglionic eminence, an embryologic structure in the ventral telencephalon is the origin of cortical interneurons (Kitamura K et al. 2002). Cortical interneurons are physiologically inhibitory and play central roles in modulating activity in cortical-cortical circuits. *Arx* expression begins in these neurons as they become post mitotic and begin migrating and continues to be expressed in the mature interneurons (Kitamura K et al. 2002; Colombo E et al. 2004).

Arx is also expressed in the dorsal telencephalic region that gives rise to projection (excitatory) neurons. Expression is observed in the cortical progenitor cells and intermediate progenitor cells (VZ and SVZ respectively) as the cells are proliferating to generate the excitatory neurons and the glia cells that will populate the cerebral cortex

(Colombo E et al. 2004). However, in contrast to the interneuron population, *Arx* is downregulated as these cells become post mitotic and begin to migrate.

Thus far much of the work on *Arx* in the brain has focused on its role in interneuron development with less focus on its role in the cortical progenitor cells. A conditional knockout mouse was engineered with floxed sites around exon 2, which contains the first part of the homeodomain (Fulp CT et al. 2008). This mouse has been used to remove *Arx* specifically from the developing interneurons ($Arx^{-/Y}$ $Dlx5/6^{Cre}$) (Marsh E et al. 2009). Male $Arx^{-/Y}$ $Dlx5/6^{Cre}$ mice all had abnormal background EEGs and spontaneous seizures, which suggests that loss of *Arx* in the interneurons is sufficient to cause epilepsy and could be the pathogenesis in human patients (Marsh E et al. 2009).

Unexpectedly, half of the female heterozygous $Arx^{-/X}$ $Dlx5/6^{Cre}$ mice had seizures and abnormal background EEGs, which is consistent with the theory that random X inactivation would cause some females to be more severely affected than others (Marsh E et al. 2009). In humans most *ARX* patients are males, since *ARX* is on the X-chromosome, and their mothers are carriers and have a normal phenotype though some of them have agenesis of the corpus callosum (Marsh E et al. 2009). However, when other female relatives of the male patients are examined two thirds of them were found to have some type of neurological symptoms (Marsh E et al. 2009). This would suggest that perhaps the mothers of the *ARX* patients might have skewed X-inactivation such that the majority of their cells are expressing the X with the normal *ARX* allele and the other female relatives either have normal X-inactivation or X-inactivation skewed towards expression of the mutant *ARX* allele. However, when the X-inactivation studies were

conducted in these female relatives skewed inactivation was not observed (Marsh E et al. 2009).

Other research on the role of *Arx* in interneurons has focused on both how it is regulated and what genes it regulates. In interneurons *Arx* expression is regulated by the transcription factors Dlx1 and 2 (Cobos I et al. 2005; Colasante G et al. 2008). *Arx* then regulates many genes involved in migration during early development, such as *Cxcr7* and *Cxcr4* (chemokine receptors used to direct migration) and specification, such as *Magel2* (Fulp CT et al. 2008; Colasante G et al. 2009; Friocourt G and JG Parnavelas 2011). Later during interneuron development *Arx* regulates genes involved in axonal projection, such as Slt2 and Sema6a (ligands involves in axon guidance) (Fulp CT et al. 2008; Colasante G et al. 2009; Friocourt G and JG Parnavelas 2011). Two microarrays have been done on *Arx* deficient developing interneurons, but so far only 3 genes (Lmo1, Ebf3, and Shox2) have been shown to be direct targets of Arx in interneurons (Fulp CT et al. 2008). Only one of these genes (Ebf3) has been shown to be necessary for the migration of interneurons (Colasante G et al. 2009).

Both of these microarrays provide *in vivo* support for the theory that Arx primarily acts as a transcriptional repressor since the majority of genes found were upregulated in the *Arx* deficient interneurons (Fulp CT et al. 2008; Colasante G et al. 2009). The array experiments confirmed earlier *in vitro* data demonstrating that Arx acts as a transcriptional repressor and binds to Groucho/transducin-like enhancer of split (TLE) proteins (McKenzie O et al. 2007). Several recent studies have begun to explore how different mutations of *Arx* can change its ability to regulate the transcription of

particular genes. Arx protein, which has a polyalanine tract expansion mutation similar to those seen in *ARX* patients, is still capable of binding to DNA but fails to repress some of the genes that it can normally repress (Nasrallah MP et al. 2012). Arx with the polyalanine tract expansion fails to repress Ebf3 or Shox2, but still represses Lmo1 in cells and knock in mice with this mutation (Nasrallah MP et al. 2012). This appears to be due to the fact that Arx with the polyalanine tract expansion mutation can no longer bind to its cofactor Tle1 and therefore can no longer repress a subset of its target genes (Nasrallah MP et al. 2012). Another study found that most point mutations in the homeodomain of *Arx*, which result in the most severe human phenotypes, fail to repress Lmo1 and Shox2 and fail to bind to DNA (Cho G et al. 2012; Shoubridge C et al. 2012). In addition point mutations in the nuclear localization signal of Arx also appear mislocalized to the cytoplasm (Shoubridge C et al. 2012). There is also some evidence that the binding of different proteins to Arx could change its affinity for particular DNA binding sites (Cho G et al. 2012). Together, these data begin to provide some insight into why different mutations of *ARX* can result in such different phenotypes.

Even though the $Arx^{-/Y}$ mice had defects in the development of both the excitatory projection neurons and the inhibitory interneurons in the cortex. Most of the research in the field has focused on the role of *Arx* in interneurons and its role in cortical progenitor cells has been less extensively studied. One exception to this is a study, which examined the role of *Arx* in the progenitor cells in the cortex using *in utero* electroporated plasmids containing either an shRNA against *Arx* or an overexpression of *Arx* into the embryonic mouse brain at embryonic day 13.5 (Friocourt G et al. 2008). When *Arx* was inactivated with the shRNA construct fewer transfected cells were found in the VZ of the cortex and

fewer of them were mitotic. In contrast, when *Arx* was overexpressed there were more transfected cells in the VZ of the cortex and more of them are stuck in the cell cycle with a longer synthesis phase of the cell cycle and a longer overall cell cycle length (Friocourt G et al. 2008). In addition, when *Arx* was either inactivated or overexpressed using these constructs *in utero* the migration of the excitatory cells into the cortex was disrupted such that they did not reach the cortex as quickly and had abnormal morphology during migration (Friocourt G et al. 2008).

This paper further supported the hypothesis that *Arx* plays a role in regulating proliferation and possibly radial migration in the development of the excitatory cells of the cortex. However, the design of their experiments makes several of the results difficult to interpret. By only observing one time point during development and knocking down or overexpressing *Arx* after cortical development has already begun there is no way to know if *Arx* has a role earlier in development or how the partially developed cortex may impact the later loss of *Arx*. As they did not follow any of the electroporated pups through to postnatal times we do not know if the radially migrating excitatory neurons are completely inhibited from reaching the cortex or whether they are simply delayed. Another problem with these experiments is the lack of specificity in the transfections or analysis of the transfected cells. It is assumed only VZ cortical progenitor cells are transfected, without confirmation. Since *Arx* expression is only altered mid way through development and only some progenitor cells are altered these experiments do not recapitulate well the dysfunction of mutant *ARX* in developing human brain.

To better analyze the role of *Arx* in the progenitor cells of the cortex and examine how loss of Arx in these cells affects cortex development and function we took advantage of our floxed allele to remove *Arx* from the cortical VZ (Fulp CT et al. 2008). To do this we mated our *Arx* floxed mice ($Arx^{F/X}$) to $Emx1^{Cre}$ mice. *Emx1* is a transcription factor that is expressed in the dorsal part of the developing telencephalon starting at embryonic day 9.5 of development. Mating these mice together produced male mice with no *Arx* expressed in their cortical progenitor cells during development, but preserved *Arx* in the interneuron precursors. We then assayed proliferation, cell cycle dynamics, and cortical layer formation in late stage embryogenesis and adult mice. We also identified a possible cell cycle regulatory gene that could be repressed by *Arx* in order to control cortical progenitor cell proliferation and differentiation and thereby control cortical layer formation. Finally, we examined the behavioral phenotype of these mice in order to determine what role the cortical malformations verses the loss of interneurons plays in the patient phenotypes. This research has led to a better understanding of the role *Arx* plays in cortical development and it has also led to a better understanding of how mutations in *Arx* cause the behavioral deficits seen in human patients.

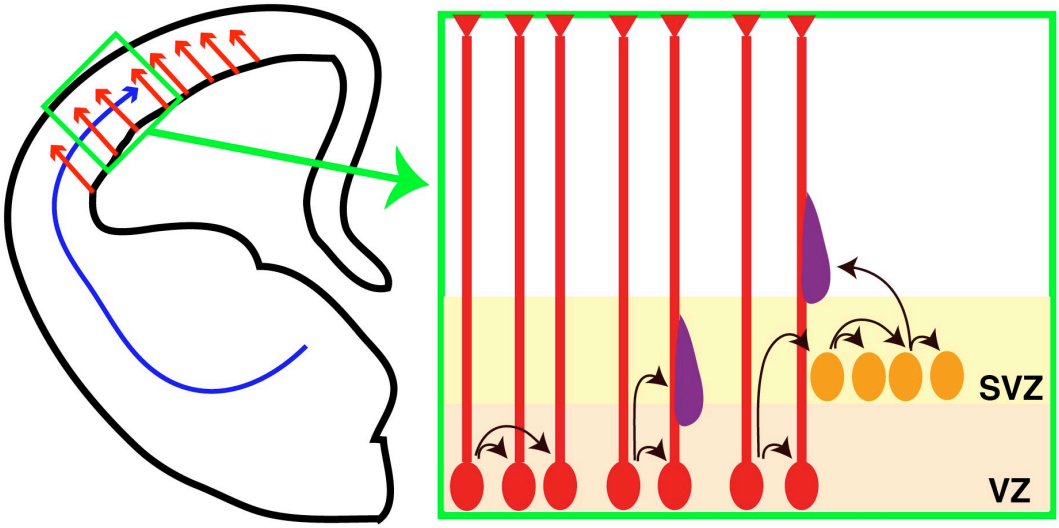

Figure 1: Cortical interneurons arise in the ventral telencephalon and migrate up into the cortex (blue arrow), while the excitatory neurons arise in the dorsal telencephalon and migrate out into the cortex (red arrows). The excitatory neurons come from two types of progenitor cells the radial glia cells (red) and intermediate progenitor cells (orange). Radial glia cells can divide to give rise to more of themselves, they can divide to produce differentiated neurons which will migrate out into the cortex, or they can divide to produce intermediate progenitor cells. Intermediate progenitor cells divide to give rise to more of themselves and to differentiated neurons.

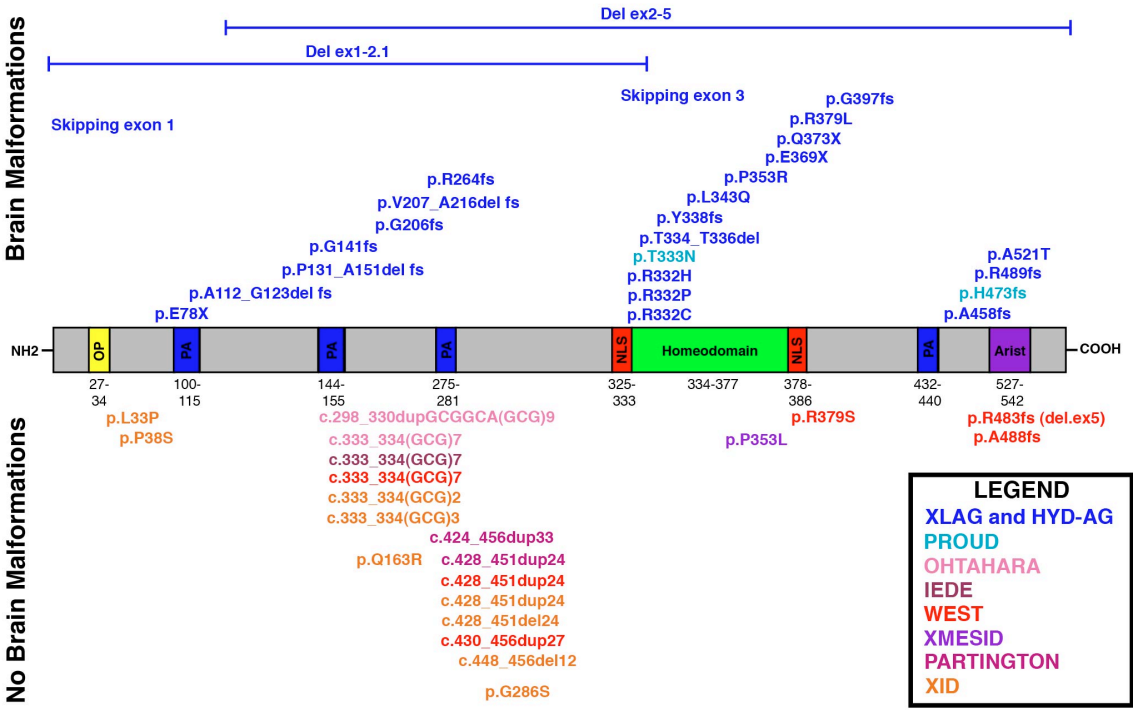

Figure 2: Schematic of the ARX protein showing the functional domains of the protein and the locations of different mutations seen in patients. ARX (Aristaless related homeobox transcription factor) has an aristaless (Arist) domain at it C-terminal, an octapeptide (OP) domain at its N-terminal, a homeodomain which binds to DNA surrounded by nuclear localization signals (NLS), and four polyalanine tracts (PA). The most severe mutations of *ARX*, which result in brain malformations; such as XLAG (X-linked lissencephaly with ambiguous genitalia), HYD-AG (hydranencephaly with ambiguous genitalia), and Proud syndrome are caused by deletions (Del), frameshifts (fs), and point mutations in the homeodomain. Less severe mutations of *ARX*, which result in epilepsy and intellectual disability syndromes; such as Ohtahara, IEDE (idiopathic infantile epileptic dyskinetic encephalopathy), West syndrome, XMESID (X-linked myoclonic seizures, spasticity and intellectual disability), Partington syndrome, and non-specific X linked intellectual disability (XID) are caused by expansions of the polyalanine tracts and by point mutations elsewhere in the gene.

CHAPTER 2: ARX regulates cortical intermediate progenitor cell expansion and upper layer neuron formation through repression of *Cdkn1c*

Introduction

Mutations in the Aristaless-related homeobox gene (*ARX*) are a common cause of X-linked intellectual disability. Over 40 different mutations have been identified in *ARX* resulting in a spectrum of disorders that vary from mild intellectual disability with no brain malformations to severe brain malformations such as lissencephaly and hydranencephaly (Gecz J et al. 2006). Currently the pathogenesis of these *ARX* related disorders are poorly defined.

During mouse cerebral cortical development *Arx* is expressed in the ventricular zone (VZ) (Colombo E et al. 2004; Friocourt G et al. 2006; Colasante G et al. 2008). *Arx* deficient mice die shortly after birth with a thin and disorganized neocortex in addition to other brain abnormalities (Kitamura K et al. 2002). The neocortical alterations appear to be the result of decreased pallial progenitor cell proliferation (Kitamura K et al. 2002; Friocourt G et al. 2008). However, it remains unclear how *Arx* regulates cortical progenitor cell proliferation, cell specification and layer formation in the neocortex.

To define the endogenous function of *Arx* in the cortical VZ, *Arx* floxed mice were mated to $Emx1^{Cre}$ mice, removing *Arx* specifically in the dorsal telencephalon. The number and proliferation rate of progenitor cells, their cell cycle length, and final cortical laminar fate were then assayed. Our data show that *Arx* regulates the expansion of both radial glial cells (RGC) and intermediate progenitor cells (IPC), with a more pronounced effect on the latter. The decrease in proliferation in the *Arx* cKO mice resulted in a loss of neurons specifically in the upper layers of the neocortex. This is consistent with the

hypothesis that IPC derived neurons contribute to all cortical layers, but predominately upper layers (Tarabykin V et al. 2001; Nieto M et al. 2004; Zimmer C et al. 2004; Sessa A et al. 2008).

We also identified a cohort of genes whose expression is consistently altered in *Arx* KO mice cortices when compared to wild type mice. Among them, *Cdkn1c*, encoding for CDKN1C, was found to be a direct target and its role in the identified IPC phenotype was analyzed. As a member of the Cip/Kip family of cyclin dependent kinase inhibitors (CDKi), CDKN1C antagonizes cell cycle progression by inhibiting G1/S transition (Sherr CJ and JM Roberts 1999). Interestingly, CDKN1C, whose expression is normally detected in the cortical SVZ, was overexpressed in both the VZ and SVZ of *Arx* KO cortices. Thus, ARX appears to regulate cortical progenitor pool expansion by repressing the premature expression of *Cdkn1c* in the cerebral cortex.

Methods

Mice

Arx conditional knockout mice ($Arx^{fl/fl}$) (Fulp et al., 2008) and *Arx* knockout mice ($Arx^{-/y}$) (Collombat P et al. 2003) were maintained on a C57Bl/6 background. Timed-pregnant mice were considered embryonic day 0.5 (E0.5) on the morning of the confirmation of the vaginal plug. To inactivate *Arx* in the dorsal telencephalon during development $Arx^{fl/y}$ mice were crossed with $Emx1^{Cre}$ animals (Jin XL et al. 2000). Genotyping of *Arx* conditional knockout and germline knockout mice was performed as described (Jin XL et al. 2000; Collombat P et al. 2003; Fulp CT et al. 2008).

Tbr2::GFP transgenic mice (Kwon GS and AK Hadjantonakis 2007) were crossed with $Arx^{fl/y}$; $Emx1^{Cre}$ animals. Mice were maintained at the Children's Hospital of Philadelphia and at the San Raffaele Scientific Institute Institutional, lab animal facilities. All experiments were approved by the Institutional Animal Care and Use Committees of the Children's Hospital of Philadelphia and of San Raffaele Scientific Institute, Milan.

BrdU administration for cell cycle dynamic analysis

BrdU was administered (50 mg/kg, i.p.) to pregnant mice 1 h before embryo harvesting to assess the S-phase labeling index. A cumulative BrdU labeling protocol was followed to determine the growth fraction (GF) (fraction of the cell population that is proliferative), to determine the time to reach the growth fraction (Tc − Ts), and, subsequently, to estimate the length of the cell cycle (Tc) and the duration of S-phase (Ts) for both radial glia and intermediate progenitors (Takahashi T et al. 1995). Pregnant mice were injected with BrdU (50 mg/kg, i.p.) starting at E13.5, with injections every 3 hours and with survival times of 0.5 h. Thus, a total of six time points were examined: 0.5 h, 3.5 h, 6.5 h, 9.5 h, 12.5 h and 15.5 h. For cell cycle exit experiment, BrdU (50 mg/kg, i.p.) was injected in a pregnant female at E13.5 and 24 hours later embryos were harvested and processed for analysis.

Histological techniques

Nissl staining

Sections were stained in a 0.1% cresyl violet solution for 5-10 minutes and then, rinsed quickly in distilled water. Thereafter, sections were dehydrated in 100% ethanol (2x5 min), dried and coverslipped with Eukitt (Electron Microscopy Science).

RNA in situ hybridizations

ISH on frozen sections was performed as previously described by (Schaeren-Wiemers N and A Gerfin-Moser 1993) with the modifications previously reported (Colombo E et al. 2007). *Cdkn1c in situ* probe was a kind gift of Dr. L. Muzio (Muzio L et al. 2002).

Immunohistochemistry

Whole heads (E11.5 and E12.5) or brains were dissected from embryonic and P1 mice and fixed over night in 4% PFA at 4°C. P14 and P30 mice were perfused with 4% PFA and then the brains were removed and fixed in 4% PFA overnight at 4°C. Fixed brains were frozen and 10um-thick coronal section were obtained. Antigen retrieval was performed in citric acid-based Antigen Unmasking Solution (Vector Laboratories) autoclaved at 105 °C for 10 minutes and BrdU staining where slides were treated with 2N HCl for 20 minutes. No antigen retrieval was performed for ARX and TBR2. Sections were then blocked for 1 hour at room temperature with 10% normal goat serum (Gibco) and 0.1% triton in PBS. Primary antibodies against ARX (rabbit, gift kindly provided by Professor Kunio Kitamura, 1:500), KI67 (rabbit, Immunological Sciences, 1:300 and mouse, BD Pharmingen, 1:200), BrdU (rat, Accurate Chemical and Scientific, 1:200), PH3 (rabbit, Chemicon, 1:100), TBR2 (rabbit, Abcam, 1:200 and Chemicon, 1:300), PAX6 (mouse, Developmental Studies Hybridoma Bank, 1:1000), CUX1 (rabbit, Santa Cruz Biotechnology, 1:50), SATB2 (mouse, Bio Matrix Research, 1:200), CTIP2 (rat, Abcam and Beckton-Dickinson 1:300), GFP (chicken, 1:2000), Caspase3 (rabbit, Cell Signaling, 1:200), and TBR1 (rabbit, Abcam, 1:25 and Chemicon, 1:400) were diluted in 10% normal goat serum and incubated on slides overnight at 4 °C. Secondary antibodies

were conjugates of Alexa Fluor 488, Alexa Fluor 594, and Alexa Fluor 647 (1:500, Invitrogen), biotinylated goat anti-mouse and anti-rabbit (Dako, 1:100). They were diluted in 10% normal goat serum and incubated on slides for 2 hours at room temperature. Biotinylated secondary antibodies were subsequently incubated with strepdavidin-Cy3 (Jackson ImmunoResearch, 1:300) in PBS. Slides were then counterstained with DAPI (Invitrogen, 1:1000), washed and mounted in Fluorescent Mounting Medium (DakoCytomation).

For the ARX/TBR2 double labeling, sections were blocked in 10% normal donkey serum (Jackson ImmunoResearch) with 0.3% triton in TBS (Tris buffered saline pH 7.4, USB Cleveland, OH; the buffer used throughout the procedure) for 30 minutes at room temperature. Anti-TBR2 antibody (Abcam, 1:200) in 10% donkey serum next was applied for 2 hours at room temperature followed by washing with TBS and then incubation with goat anti-rabbit monoclonal Fab fragments (Jackson ImmunoResearch, 1:25) in 10% donkey serum for 30 minutes at room temperature. They were then washed and secondary Alexa 594 donkey anti-goat 1:200 in 10% donkey serum in TBS was applied for 30 minutes at room temperature. For the second primary antibody the sections were again washed and blocked with the goat anti-rabbit monoclonal Fab fragments 1:25 in 10% donkey serum. After washing the anti-ARX antibody was applied overnight at 4 °C in 10% donkey serum. Finally the slides were washed and the secondary Alexa 488 donkey anti rabbit was applied at 1:200 in 10% donkey serum for 30 minutes at room temperature. The slides went through on final wash, were counterstained with DAPI and mounted.

Quantifications and statistical analysis

All quantifications on P14 cryostat brain sections were performed using a 200μm section of the dorsomedial cortex at the mid-hemispheric level from pia to white matter. For quantifications on E11.5 and P1 brain sections, cell counts were derived from 25% of the neocortex. The area of interest was derived by measuring the linear distance along the pial and ventricular surfaces of the entire lateral cortex, dividing those into quarters, and then using the total area, from pia to ventricle, in the third quartile from the dorsal midline. Quantifications on E14.5 brain sections were performed using a 150μm section of the dorsomedial and lateral cortex. At least three serial sections from three different animals for each genotype were photographed using a Leica DMR fluorescent microscope. Images were imported into Photoshop CS3 and double-positive cells were overlaid manually by color-coded dots in new layers. The number of labeled cells (dots) was calculated using the Record measurements of Photoshop CS3 and imported into Excel 2008. The percentage of labeled cells per region per section was calculated for each brain, and the final mean percentage calculated across all brains. Results were expressed as mean value ± SD and were tested for statistical significance by the two tailed, unpaired Student's t test ($p < 0.05$ level of significance).

RNA isolation, processing, and microarray analysis

The experiment was performed as previously described (Colasante G et al. 2009). Briefly, 3 pregnant Arx heterozygous dams crossed with C57Bl/6 males were sacrificed at E14.5. A total of 5 wt and 5 Arx KO embryos were harvested and after brain isolation the cerebral cortices were separated from the ventral telencephalon. Total RNA was extracted from the cortices using the Qiagen RNA micro kit (Qiagen, Valencia, CA).

cRNAs were generated and hybridized on a total of ten different MOE430v2 Affymetrix DNA chips according to the Affymetrix protocol. The chips were scanned with an Affymetrix scanner to generate digitized image data files. The data were deposited in the NCBI Gene Expression Omnibus (Edgar R, Domrachev M, Lash AE. Gene Expression Omnibus: NCBI gene expression and hybridization array data repository. Nucleic Acids Res. 2002; 30:207–10) and are accessible through GEO Series (# GSE12956).

Luciferase reporter assays

P19 cells (10^5) were seeded and transfected 24 h after plating with 400 ng of each of the following constructs in different combinations: pT81 luciferase reporter plasmids, control plasmid pCAG-iresGFP, pCAGArx-iresGFP, pCDNA3-Tle1 and 80 ng of pRL-TK-Renilla luciferase plasmid DNA (Promega) using Lipofectamine PLUS™ Reagent (Roche Diagnostics, Alameda, CA). Forty-eight hours post-transfection, cell lysis and measurement of firefly and Renilla luciferase activity was performed using the Dual-Glo Luciferase Assay System (Promega) according to the manufacturer's instructions. The firefly luciferase activity was normalized according to the corresponding Renilla luciferase activity, and luciferase activity was reported as mean relative to pCAG-iresGFP/luciferase transfection. The two *Cdkn1c* -549/-68 and -1490/-720 enhancer regions were PCR amplified from E14.5 mouse genomic DNA using the following primers: HindIII-*Cdkn1c*-F1 5'- CCCAAGCTTGCGCGCGGGCCTCCTCAC-3'; BamHI-*Cdkn1c*-R1 5'-CGCGGATCCCCAGGACCAGGACCCAGCTG-3'; HindIII-*Cdkn1c*-F2 5'- CCCAAGCTTGAGATCTAAAAGATCTGTAG-3' and BamHI-*Cdkn1c*-R2 CGCGGATCCTAGTGAATGAGGGGTTCATG-3', respectively. The amplified products were cut with HindIII and BamHI and cloned into the BamHI and HindIII sites

of pT81-TK-Luciferase, which contains the thymidine kinase minimal promoter upstream of luciferase. The (-549/-68) enhancer region carrying mutagenized ARX binding site was generated by site-directed mutagenesis with the following primers 5'-CTGAAAATACTACAGGATGCTCCTCGTGAGGAG-3' and 5'-CTCCTCACGAGGAGCATCCTGTAGTATTTTCAG-3' using the QuikChange II site-directed Mutagenesis Kit (Stratagene), according to the manufacturer's instructions.

Chromatin immunoprecipitation

E14.5 mouse embryonic cortices were isolated and single-cell suspension derived by enzymatic treatment. Cells were cross-linked with 1% formaldehyde for 10 min and chromatin prepared essentially as described previously (Ferrai C et al. 2007; Colasante G et al. 2008). The chromatin aliquots (1 ml) were incubated overnight with 1 μg of anti-GFP (Chemicon) as mock and anti-ARX(C-14) (Santa Cruz). PCR primers used are the following: PCR primers used are the following: ChIP*Ebf3*-F, 5′-GTCTATAAGTACAATGGTGACAC-3′; ChIP*Ebf3*-R, 5′-CTCCATCAAGATCCTTCTC-3′ (amplification product, 240 bp); ChIP*Cdkn1c*-F, 5′-GCGCCCCTTTATACGCGCTG 3′; ChIP*Cdkn1c*-R, 5′-TCACGTTACCGCCCGCAGAG-3′ (amplification product 200 bp); ChIP*Cdkn1a*-F 5'-GCTGTCAAAACGACCTTGAATG-3'; ChIP*Cdkn1a*-R: 5'-GGAAGGACTAACTCTTTTCCAG-3' (amplification product 220 bp); ChIP*Cdkn1b*-F 5'-CCCTGATAAGAGCGGTCAGTC-3'; ChIP*Cdkn1b*-R 5'-TTACGGAGCTTCGGTGGCTAG-3' (amplification product 250 bp). PCR products were analyzed on 2% agarose gels in TBE buffer.

Results

Reduced cerebral cortex and olfactory bulbs after deletion of *Arx* from the dorsal telencephalon

The germline loss of *Arx* in mice results in a thinner and disorganized cortex that was attributed to a primary defect in cell proliferation (Kitamura K et al. 2002). To further define the role of *Arx* in cortical progenitor cell proliferation we conditionally deleted *Arx* from the E9.5 dorsal telencephalon by crossing our $Arx^{fl/+}$ mice to $Emx1^{Cre}$ mice (Jin XL et al. 2000) (Fig. 1A, B). In $Arx^{fl/y}$; $Emx1^{Cre}$ mice (here after *Arx* cKO) no ARX protein was observed in the VZ and SVZ of the cortex by E11.5 and throughout the rest of development (Fig. 1A, B and data not shown). Morphological analyses performed at E14.5 revealed that, at this developmental stage, alterations of the gross morphology of *Arx* cKO brains are already evident. The cerebral hemispheres are reduced in size and the olfactory bulbs are smaller and characterized by an abnormally wide interspace separating them (Fig. 1C, D). Nissl staining on E14.5 coronal sections highlighted the diminution of cortical thickness affecting *Arx* cKO cerebral cortex in its whole medio-lateral extension (E14.5 relative volume (rv) *Arx* cKO/ctrl = 0.86±0.03; n=3, $p < 0.005$ (Fig. 1E, F, O). $Arx^{-/y}$ mice die perinatally (Kitamura K et al. 2002; Collombat P et al. 2003), whereas crosses between $Arx^{fl/+}$ female and $Emx1^{Cre}$ male mice recovered all expected genotypes in Mendelian ratios (data not shown). Morphological assessments at P30 of *Arx* cKO and relative control brains confirmed the analysis made at E14.5. Indeed, the cerebral hemispheres and olfactory bulbs in *Arx* cKO mice are reduced in size, whereas the cerebellum and the brain stem do not appear to be affected (Fig. 1I, J).

In addition, P30 Nissl stained coronal sections highlight an overall reduction of the cerebral cortex, most evident at the level of pyriform cortex and the hippocampus (rv P30 = 0.84±0.05; n=3, $p < 0.005$) (Fig 1K, L, O).

In the *Arx* cKO the laminar structure cannot be clearly delineated (Fig. 1M, N) and the corpus callosum was absent in *Arx* cKO brains (Fig. 1P, Q); this feature, together with the microcephaly, strongly resembles the morphologic abnormalities observed in patients with the XLAG syndrome (Kitamura K et al. 2002).

Our data indicate the loss of *Arx* in cortical progenitors recapitulates the morphologic defects observed with the germline loss of *Arx*. These data support the model by which the reduced brain size observed in *Arx* KO mice and children with loss of function *ARX* mutations, is largely or completely due to a loss of *Arx* in cortical progenitor cells.

Loss of Arx in the pallial progenitor cells reduces the proliferation rate of cortical progenitor cells

Previous data suggested a decrease in cortical progenitor cell proliferation as the basis for the reduced cerebral cortical thickness in *Arx* KO mice (Kitamura K et al. 2002). At E11.5 in cortical development there are similar numbers of progenitor cells in wild type and *Arx* cKO mice cortices as measured by the number of KI67 positive cells (ctrl: 392±33.5; cKO: 368±45.5, n=3, p=0.579: cells counted in 25% of the cortex from ventricular to pial surface)(data not shown). This suggests normal numbers of cortical progenitor cells exist early in development when the progenitor cells are being produced. However, when the same analysis was performed at E12.5 we observed a reduction in the percentage of proliferating progenitor cells (% KI67+/Hoechst, ctrl: 96.65±2.90; cKO:

87.49%±5.58, n=6, p=0.016, cells counted in a 150 μm bin from the ventricular to the pial surface)(Fig. 2C-D', G) and an increase in ßIII-tubulin positive young neurons in *Arx* cKO compared to control (% TUBB3+/Hoechst, ctrl: 10.88±2.96; cKO: 20.75±3.39, n=6, p=0.003) (Fig. 2A-B', H).

At E14.5 the cortical plate was already thinner (Fig. 1E, F) and the reduction in the total number of proliferative cells was more evident in *Arx* cKO cortices (Fig. 3A, C) (ctrl: 259±21.8; cKO: 202.5±16.3; n=6, $p < 0.001$, cells counted in a 150 μm bin from the ventricular to the pial surface). Moreover, both the types of cortical progenitor cells - RGCs and IPCs- are diminished in *Arx* cKO cortices at this embryonic stage. Indeed, we observed a reduced PAX6 labeling intensity in *Arx* cKO mice (Fig. 3D', E') in addition to a 27% reduction in the number of PAX6+ cells (ctrl: 323.6 ± 13.3; cKO: 237.5 ± 26.8; n=3, $p< 0.001$; Fig. 3J) as well as a 20 % reduction of TBR2+ cells (ctrl: 223.6±16.4; cKO: 179.3±10.8; n=3, $p< 0.001$)(Fig. 3F', G').

In order to exclude a contribution of an increase in cell-death to the reduction of cortical thickness in *Arx* cKO cortices, the apoptotic marker Caspase3 was analyzed at different embryonic stages (E13.5, E15.5, E17.5), finding no difference between *Arx* cKO and relative controls (Fig. 4).

To determine if the reduction in proliferation was affecting both types of cortical progenitor cells- RGCs and IPCs- in the same way, their rate of BrdU incorporation was measured in control and *Arx* cKO cerebral cortices after a 1 hour BrdU pulse. As expected, general reduction in BrdU incorporation (~24%) (arrows in Fig. 3F''), was found in *Arx* cKO cortices with respect to controls (ctrl: 142.3 ± 18.2; cKO: 109.0 ± 10.2; n=3, $p< 0.001$ and Fig. 3J). Interestingly, double labeling with PAX6 and BrdU revealed

little differences in the PAX6+/BrdU+ cell number between *Arx* cKO and control (ctrl: 125.6±19; cKO: 103.7±7.17; in both cases about 40% of the total PAX6+ cells; n=3, p=0.012)(Fig. 3D’’’, E’’’, J). Conversely, double labeling with TBR2 and BrdU revealed a reduction of dual labeled cells (ctrl: 52.9 ± 12.9, about 25% of the total TBR2+; cKO: 17.5 ± 2.9, about 10% of the total TBR2+; n=3, p< 0.001)(arrows in Fig. 3F’’’, G’’’, J). Consistent with these data, staining with the M-phase marker phosphohistone 3 (PH3) revealed an overall reduction of positive cells in the *Arx* cKO cerebral cortex with a greater loss in the basal area (IPCs) than the apical area (RGCs) (apical, ctrl: 122.0 ± 5.6, cKO: 107.5 ± 3.5; basal, ctrl: 39.0 ± 4.8; cKO: 11.5 ± 2.12 n=3, p< 0.001, Fig. 3H, I, H’, I’, J).

Taken together, these data indicate that at E14.5 both progenitor populations (RGCs and IPCs) are reduced in *Arx* cKO cerebral cortices and their proliferation is affected. However, BrdU incorporation rates and PH3 staining indicate that there is a disproportionate deficit in the proliferation of IPCs compared to RGCs in *Arx* cKO mice.

Cortical progenitors show a normal cell cycle length, but IPC mitoses are strongly reduced in *Arx* cKO mice.

To further understand the mechanism by which loss of *Arx* resulted in fewer proliferating cells, we tested two non-mutually exclusive hypotheses: that the cell cycle changes are related to lengthening of the cell cycle or to precocious exit of cortical progenitors from the cell cycle.

An increased cell cycle length during the neurogenic period would result in fewer cellular divisions, fewer progenitor cells and the observed reduction in BrdU incorporation. To examine neocortical cell cycle dynamics in the absence of *Arx* the

length of the cell cycle phases was estimated between E13.5 and E14.5 in wild type and *Arx* cKO mice using a cumulative BrdU pulse-labeling paradigm (Takahashi T et al. 1995). BrdU was injected intraperitoneally in gravid mothers every 3 hours up to 6 time points with survival time being 0.5 hour after the last injection. At least 2 brains of each genotype were assayed at each time point for BrdU labeling to evaluate the cell cycle parameters in the VZ precursors, where VZ was defined by two criteria: the region under the area with high density of TBR2+ cells and where cells with vertically oriented nuclei were present. Moreover TBR2/BrdU double staining was performed in order to gain information regarding the BrdU incorporation kinetic of IPCs. Representative cortical fields of control and *Arx* cKO BrdU and TBR2 labeled coronal sections are shown for 5 out the 6 time points (Fig. 5A-J).

The growth fraction (GF) in the VZ - defined as the maximum percentage of VZ progenitors entering the S-phase on the total of nuclei in the VZ - did not change between the two genotypes, and in both cases almost 100% of VZ cells were BrdU+ at the 9.5 h time point (Fig. 5G, H). The Labeling Index (LI) of VZ (BrdU+cells/total cell number) at each time point was plotted against the corresponding time after BrdU injection and from the slope of the interpolating lines, the cell cycle parameters Tc and Ts were calculated (Fig. 5N, P). Interestingly, no significant difference was found in both parameters between control and *Arx* cKO brains (ctrl: Tc=14.5 hrs and Ts= 4 hrs; cKO: Tc=14.1 hrs and Ts= 4.1 hrs).

A similar analysis of the cell cycle kinetic was performed in the SVZ. First, the GF at E13.5 was evaluated as the percentage of proliferating IPC (KI67+ TBR2+) on the total of IPCs (TBR2+) (Fig. 5K-L'). Interestingly, while about the 75% of IPCs in the

control were proliferating, only the 45% of cKO IPCs entered any cell cycle phase (% KI67+ TBR2+/TBR2, ctrl: 74.30±1.99; cKO: 45.17±2.64, n=4, $p<0.0004$). Similar reduction in the SVZ GF of *Arx* cKO was noticed also later on during cortical development (Fig. 6; E17.5 % KI67+ TBR2+/TBR2, ctrl: 16.57±2.49; cKO: 7.58±0.26). This result confirmed and completed the previous observations relative only to S and M phases of the cell cycle.

Then, LI in the SVZ was calculated as the ratio between the TBR2+ cells incorporating BrdU on the total of TBR2+ proliferating cells (BrdU+ TBR2+/Ki67+ TBR2+) and plotted against the corresponding time after BrdU injection and interpolating lines generated for both control and *Arx* cKO (Fig. 5A''-J'', O). The slope of the *Arx* cKO interpolating line resulted slightly higher, indeed cKO IPCs seemed to reach the value of GF=1 a little before the control (Tc-Ts, control: 7.8h; cKO: 6.3h). As a consequence, Tc and Ts resulted a little bit shorter in cKO IPCs with respect to control (Fig. 5P). The ratio between Ts and Tc was not significantly altered (Ts/Tc, ctrl: 0.25; cKO: 0.24), suggesting that the relative length of the different cell cycle phases was constant.

Interestingly, the same conclusions were reached by a different approach. We measured the BrdU labeling index (0.5 hour pulse) in SVZ precursors (Ki67+) at E14.5 (Arnold SJ et al. 2008), finding significant decrease in the number of proliferating Ki67+ cells/100 μm2 area in cKO SVZ with respect to control (ctrl: 19.83 ± 6.04 and cKO: 3.83 ± 1.94; n=4, $p<0.005$; Fig. 7A, B, C), comparable to the reduction in BrdU+ (Fig. 8) and PH3+ cells in cKO SVZ (Fig. 3J). Consequently, the ratio between the number of S-phase cells (BrdU+) and the total of those proliferating (Ki67+) showed no significant

difference (ctrl: 0.44 ± 0.02 and cKO: 0.40 ± 0.10; n=4, p=0.34; Fig. 8C). This last set of data again indicates that Ts/Tc ratio of *Arx* cKO SVZ precursors is comparable to control.

Consequently, the reduced BrdU incorporation observed in cumulative labeling experiment of TBR2+ cells can be attributed to a consistent reduction in the proliferation ability of *Arx* cKO SVZ progenitors and not to an alteration of their cell cycle length.

Precocious cell cycle exit in *Arx* cKO cortical progenitors

Since only about half of the pool of IPCs is able to proliferate in *Arx* cKO cortex, we predicted precocious cell cycle exit of these cells. Thus, we assessed the fraction of cells exciting the cell cycle 24 hours after a BrdU pulse (between E13.5 and E14.5). Cells remaining in the cycle are BrdU+/Ki67+, while those that have stopped cycling exhibit BrdU labeling only (Chenn A and CA Walsh 2002). At E13.5, an increase of 18% in the cells leaving the cycle is observed in *Arx* cKO progenitors (leaving fraction in ctrl: 0.49±0.06; in cKO: 0.58±0.05; n=8 for each, $p < 0.0005$; Fig. 7A'', B'', C) suggesting precocious neurogenesis. Consistent with that, more cells with undiluted BrdU exist in the *Arx* cKO when compared to control (arrowheads, Fig. 7A', B'). Although it is not possible to distinguish the contribution of RG cells and IPCs to the fraction of precociously differentiating cells, it is likely that most of those cells are IPCs, that may exit cell cycle without any round of amplification.

In order to evaluate the effects of IPC reduced proliferation in *Arx* cKO, we analyzed GFP expression in E15.5 *Arx* cKO and relative control mice crossed with *Tbr2*::GFP transgenic animals (Fig. 7D, E, D' E'), where GFP is under the control of the *Tbr2* endogenous regulatory sequences (Kwon GS and AK Hadjantonakis 2007). Due to the stability of the GFP protein in vivo, GFP fluorescence in *Tbr2*::GFP mice can be used

as a lineage tracer of the IPC progeny (Sessa A et al. 2008). We noticed an overall decrease in GFP+ cells in *Arx* cKO SVZ and cortical plate with respect to control consistent with a reduction in the amplification of IPCs in the cKO (GFP+ cells/150 um area unit, ctrl: SVZ, 55.7±5.13; IZ, 80.00±16.7; CP, 180.33±6.51; total, 316.00±15.39; cKO: SVZ, 27.70±7.37; IZ, 63.33±26.63; CP, 83.00±2.64; total 181.70± 21.01; n=4 $p<0.005$ (Fig. 7F).

Given the more pronounced effect of *Arx* ablation on IPCs than on RGCs, we sought to assess if *Arx* is also expressed in IPCs in addition to RGCs (Friocourt G et al. 2006). We performed immunofluorescence for ARX and TBR2 in wild type cortex at E14.5 and showed that ARX colocalizes with TBR2 in many cells of the VZ/SVZ (Fig. 9).

Arx cKO mice have a reduced number of upper cortical layer neurons with normal numbers of deeper layer neurons

In order to determine if the reduced proliferation of cortical progenitors has an effect on cortical lamination, we evaluated molecular markers of cortical layers at different developmental stages. First, the expression of TBR1 - labeling neurons in subplate, layer VI and few in layer V (Molyneaux BJ et al. 2007)- was evaluated in control and *Arx* cKO mice at E16.5. In *Arx* cKO the number of TBR1+ cells in layers V-VI was slightly decreased with respect to control (TBR1, ctrl layer V-VI= 98.2±6.5; cKO layer V-VI=82.0±7.8)(Fig. 10A, B). Interestingly, more neurons were found in *Arx* cKO subplate, still detectable at this stage (TBR1, ctrl: SP=36.5±4.5; cKO: SP=60.0±3.5) (arrowheads in Fig. 10A, B).

A similar difference, although more dramatic, was observed staining for CTIP2, which labels predominately layer V, but also layer VI neurons (Molyneaux BJ et al. 2007). CTIP2+ cells are already well organized in control layers V-VI, with some positive cells localized in the subplate, whereas in the *Arx* cKO they appear less compact and completely disorganized (arrowheads in Fig. 10C, D). However, the total number of CTIP2+ cells does not change between *Arx* cKO and control (CTIP2, ctrl: 166.9±4.2 and cKO: 155.7±5.7)(Fig. 10U). In order to assess upper layer stratification, we then used P1 and P14 animals. At P1 *Arx* cKO mice had a decreased number of cells labeled with SATB2 in layer II/III in the *Arx* cKO cortices with respect to controls (SATB2 ctrl: layer II/II= 131.4±18.5 and SATB2 cKO: layer II/III= 96.9±12.6; n=5, p=0.0126)(Fig. 10I, J), but not in layer IV/V (SATB2 ctrl: layer IV/V=84.0±6.8 and SATB2 cKO: layer IV/V= 77.9±7.6; n=5, p=0.547)(Fig. 10I, J). In addition, the number of cells labeled with CUX1, a marker of layer II-IV, is also decreased in the *Arx* cKO cortices (CUX1 ctrl: layer II-IV= 125.9±7.0 and CUX1 cKO: layer II-IV= 95.9±7.8; n=5, p=0.0327) (Fig. 10I-L). However, no significant difference between the *Arx* cKO and control cortices was detected for layer V and VI markers (CTIP2 ctrl: total= 97.5±7.5 and CTIP2 cKO: total= 93.2±9.6; n=3, p=0.587; TBR1 ctrl: total= 116.9±4.9 and TBR1 cKO: total= 92.1±14.2; n=3, p=0.132) (Fig. 10E- H).

At P14, a time in which laminar organization is complete, a decrease in the number of SATB2 and CUX1 positive cells persisted in layer II/III in the *Arx* cKO cortices when compared to control cortices (SATB2 ctrl: layer II/II= 29.5±2.4 layer IV= 41.4±3.8 and SATB2 cKO: layer II/III= 21.2±3.9 layer IV= 24.5±3.0; n=4, p=0.0286; CUX1 ctrl: layer II-IV= 30.5±2.1 and CUX1 cKO: layer II-IV= 24.9±3.5; n=4,

p=0.0482)(Fig. 10Q-T). However, similar numbers of CTIP2 positive and TBR1 positive cells are present in the *Arx* cKO cortices as compared to control (CTIP2 ctrl: total= 35.5±3.7 and CTIP2 cKO: total= 29.2±1.7, n=3, p=0.272; TBR1 ctrl: total= 32.7±2.1 and TBR1 cKO: total= 32.5±2.5, n=3, p=0.406)(Fig. 10M-P).

In summary, we find a reduction of upper layers (II-IV) neurons with no change in deeper layer (V-VI) neurons in *Arx* cKO mice.

Identification of genes differentially expressed in *Arx* KO versus wild type cerebral cortex by transcriptome analysis

To gain insight into the *Arx*-dependent mechanism responsible for the reduced proliferation in *Arx* cKO cortical progenitor cells observed at E14.5, we performed a gene expression profile analysis. Since all the proliferation defects observed in the *Arx* cKO cortices were also detected in *Arx* KO mouse model (data not shown), we decided to perform this experiment in *Arx* KO dorsal telencephalon. E14.5 embryonic stage was selected for analysis, as the proliferation defect was clearly detectable. Brains were harvested and the cerebral cortices were carefully dissected and processed for gene expression profiling (Fig. 11) RNA was separately extracted from the isolated tissues and used to hybridize Affymetrix microarrays (MOE430v2) containing 45,101 probe sets. Cortical tissues from *Arx* KO (n = 5) and control (n = 5) embryos were independently processed on 10 different gene-chips in order to minimize individual biological differences. Data sets obtained were then used to identify differentially expressed transcripts between *Arx* KO and wild type dorsal telencephali (Fig. 11A-I).

Using a log2 (fold-change ≥ 1 and a FDR ≤ 0.05) linear model, the analysis revealed that a total of 147 probe sets corresponding to 86 different Entrez Gene

Identifiers presented significantly different expressions between Arx KO and wild type cortices (Fig. 11A-I).

Among the full set of identified genes, 3 (DDX3Y, KDM5D and EIF2S3Y) (Fig. 6I) were considered as *Arx*-independently misregulated. In fact, they correspond to Y-linked expressing units and their upregulation in *Arx* KO tissues is indicative of a sex-biased harvest of the embryos. This was expected because all *Arx* KO embryos were males ($Arx^{-/Y}$), while wild type embryos displayed an equal probability to be males or females. The remaining 83 differentially expressed genes were grouped according to the known or predicted protein function they coded for: transcription factors (Fig. 11A); receptors (Fig. 11B); intracellular regulatory proteins (Fig. 11C); structural proteins (Fig. 11D); extracellular regulatory proteins (Fig. 11E); extracellular junctions and adhesion molecules (Fig. 11F); carriers and transporters (Fig. 11G); extracellular matrix proteins (Fig. 11H).

To ensure the reliability of our analysis, some of the misregulated genes were selected and analyzed in control and KO tissues using quantitative real-time RT-PCRs (qPCRs). In this experiment, only RNA extracted from male control embryos was used, in order to avoid any sex biased gene expression between males and females (Yang F et al. 2006).

In all cases analyzed, qPCR results confirmed previous gene-array analyses both for the up-regulated genes *RARb*, *Id1*, *Id3*, *Tub6*, *Olig2*, and *Cdkn1c* as well as the down-regulated *Pax6* gene (Fig. 11J, all normalized to ß-actin). However, the magnitude of the changes in expression levels detected by qPCRs was, in some cases, significantly higher (up to 2.5 fold) when compared to the microarray analyses (*RARb*, *Olig2*, *Cdkn1c*), while,

in other instances, the results were comparable (*Id1*, *Tub6*, *Pax6*). Interestingly, the expression of *Tbr2* was found decreased in *Arx* KO compared to control (20% reduction) in agreement with our immunohistochemistry data, even if the microarray analysis didn't show any significant alteration.

Cdkn1c is overexpressed in *Arx* KO cerebral cortex

Among the genes found to be misexpressed in *Arx* KO cerebral cortices, we noticed the upregulation of *Cdkn1c*. *Cdkn1c* encodes for CDKN1C (also known as p57/KIP2), a member of the Cip/Kip family of cyclin dipendent kinase inhibitors (CKIs). Together with the two other members of this family, CDKN1A and CDKN1B, it exerts a basilar role in the regulation of cell cycle progression of cortical progenitors at level of G1/S transition by inhibiting the cyclin/CDK complexes (Sherr CJ and JM Roberts 1999). Recently, Mairet-Coello and colleagues showed that CDKN1C overexpression in the cerebral cortex elicits precursor cell cycle exit and promotes transition from proliferation to neuronal differentiation, while opposite effects occur in CDKN1C-deficient precursors. Indeed, they reported that in mutant mice proliferation of radial glial cells (RGC) and intermediate precursors (IPC) was increased, expanding both populations, with greater effect on IPCs (Mairet-Coello G et al. 2012).

As this function is particularly consistent with the phenotype observed in *Arx* cKO brains and might underlie the reduction in the cerebral cortex volume, we focused further analyses on this gene.

In order to ascertain if *Cdkn1c* misregulation plays a role in *Arx* KO tissues, we first assessed its expression by *in situ* hybridization throughout embryonic development (E12.5-E18.5) in wild type and *Arx* KO mouse brain sections (Fig. 12A, B, D, E and Fig.

13). The expression of *Arx* was evaluated on adjacent wild type brain sections (Fig. 12C, F and Fig. 13). At E12.5 *Cdkn1c* transcript was barely detectable in the SVZ of control cortices whereas it was significantly overexpressed in both VZ and SVZ of *Arx* KO (Fig. 12A, B, arrowheads A', B'). Interestingly, the upregulation of *Cdkn1c* seemed to follow a gradient in *Arx* KO cortices, higher lateral-lower medial (Fig. 12B). Similarly, at E14.5, *Cdkn1c* is still expressed in the SVZ in control tissues (Fig. 12D, arrowheads D') and overexpression persists in *Arx* KO cortices (Fig. 12E, arrowheads E'). In contrast to E12.5, *Cdkn1c* expression clearly followed a higher medial-lower lateral gradient in both control and KO cortices (Fig. 12D, E). Beginning on E16.5, *Cdkn1c* transcript was additionally detected in cortical plate cells of both control and KO brains and at E18.5 the level of *Cdkn1c* up-regulation in *Arx* KO cortices was significantly diminished, inversely correlating with the *Arx* expression pattern at the same developmental stages (Fig. 13). Similar results were also observed in *Arx* cKO cortices.

Unexpectedly, although *Arx* is strongly expressed in the ganglionic eminences, in particular at E12.5, E14.5 and E16.5 (Fig. 12C, F and Fig. 13), its ablation in *Arx* KO mice does not induce *Cdkn1c* up-regulation in this compartment (Fig. 12B, E and Fig. 13).

In conclusion, our expression analysis of *Cdkn1c* in wild type and *Arx* KO cerebral cortices throughout the neurogenic period, showed that this gene is upregulated in *Arx* KO cortical VZ and SVZ, with a pattern that parallels *Arx* expression in control tissues. Thus, this correlation raises the possibility that *Arx* depletion directly promotes *Cdkn1c* upregulation in cKO tissues.

Cdkn1c is a direct transcriptional target of ARX

To determine if *Cdkn1c* is a direct transcriptional target of ARX, a 5 kb genomic region upstream to the murine *Cdkn1c* gene locus was screened for the presence of putative ARX binding sites. Previous studies identified palindromic sequences TAAT/ATTA spaced by 3 nucleotides (5'-ATTANNNTAAT-3') as favored binding sites for paired homeodomain proteins (Wilson D et al. 1993). Indeed, our search highlighted the presence of a unique palindromic sequence (5'-ATTAGCATAAT-3') located between bases -71/-81 upstream of the *Cdkn1c* transcription start site (named +1) (Fig. 12G). As binding sites for transcriptional regulators are usually evolutionary conserved, we performed a multiple alignment of the aforementioned genomic region among different species, finding a high level of conservation in the ARX putative binding site in mouse, rat, human and orangutan, except for the 3 spacing nucleotides that were not conserved in orangutan (Fig. 12G). A genomic region of approximately 500 bp (-549/-68) containing the putative ARX binding site and another of about 750 bp (-1490/-720 containing some TA repeats, were separately cloned, upstream to a minimal promoter, in a construct containing the *Luciferase* gene and tested for transcriptional reporter activity (Fig. 12H). The 500 bp (-549/-68)-Luc and 750 bp (-1490/-720)-Luc constructs were separately co-transfected with control plasmid pCAG-IRESGFP or pCAGArx-IRESGFP in P19 cells and the effect of ARX expression on the basal transcriptional activity of the two putative regulative sequences was evaluated. ARX co-transfection reduced the basal transcriptional activity of the 500 bp regulative region by 30% (fold increase/decrease in transcriptional activity of pCAG-ArxIRESGFP coinfected with respect to pCAG-IRESGFP coinfected: 0.67±0.04; n=3, $p<0.005$). However, higher reduction was

detected when the corepressor Tle1 (McKenzie O et al. 2007) was cotransfected in association with ARX (0.42±0.06, n=3, $p<0.005$). Surprisingly, ARX and in particular TLE1 alone are able to repress luciferase transcription; this is due to the fact that both proteins are already expressed at low levels in P19 cells (data not shown). Conversely, when pCAG-ArxIRESGFP was cotransfected with the Luciferase construct regulated by 750 bp enhancer, only a slight reduction in the basal transcriptional activity was assessed (fold increase/decrease in transcriptional activity of pCAG-ArxIRESGFP coinfected with respect to pCAG-IRESGFP coinfected (transcriptional activity; 0.94± 0.01, n=3, $p<0.05$,), even in combination with TLE1 (Fig. 12H). When the binding site 5'-ATTAGCATAAT-3' was mutagenized to 5'-AGGAGCATCCT-3', no significant reduction in Luciferase expression was appreciated in cotransfection experiments (Fig. 12H).

These results indicate that ARX exerts a specific transcriptional repression activity on this 500 bp (-549/-68) genomic region; in order to assess if this repression is direct or mediated by other factors expressed in P19 cells we performed chromatin immunoprecipitation experiments. Anti-ARX antibody was used to immunoprecipitate chromatin isolated from E14.5 telencephali; then, PCR amplification reactions, with primers designed to span the 500 bp (-549/-68) region upstream to *Cdkn1c* gene, allowed us to evaluate an enrichment of that region in the ARX immunoprecipitated chromatin with respect to IgG only and anti-GFP immunoprecipitated chromatin (Fig. 12I). Amplifications with primers spanning *Ebf3* regulatory region were also performed and used as a positive control, as *Ebf3* was previously showed to be a direct target of ARX in the ventral pallium (Fulp et al., 2008). We found enrichment of the *Cdkn1c* (and *Ebf3*)

regulatory regions when pulled down with an anti-ARX antibody but not with the anti-GFP or no antibody controls. No enrichment in ARX immunoprecipitated chromatin samples was detected amplifying for *Cdkn1a* and *Cdkn1b* regulative regions (Fig. 12I), as expected by the absence of any alteration of the two gene transcripts in *Arx* KO cortices. Taken together, these results suggest that ARX is a direct repressor of *Cdkn1c* transcription and it likely exerts this role by direct interaction with the palindromic binding site 5'-ATTAGCATAAT-3' located in the 500 bp enhancer region.

Discussion

Loss of *ARX/Arx* in both humans and mice results in a reduced size of the cerebral hemispheres. In this study, by crossing $Arx^{fl/y}$ mice with $Emx1^{Cre}$ mice, we have confirmed that the reduced brain size is largely if not completely due to the loss of *Arx* in cortical progenitor cells. Indeed, in E14.5 *Arx* cKO we observed a reduction in the number of cortical progenitor cells, both PAX6+ and TBR2+, that might be the result of the precocious RG progenitor differentiation observed at E12.5 in *Arx* cKO.

However, this cannot be the only underlying mechanism. In fact, also the proliferation rate of cortical progenitor cells is affected in *Arx* cKO and our data suggest that the IPC pool is more affected than the RGC compartment: almost all S-phase progenitors in E14.5 *Arx* cKO cortices are PAX6+ cells and only rarely TBR2+. Consistent with this, basal mitoses are dramatically reduced. Interestingly, the determination of the growth fraction at E13.5 allowed us to understand that, whereas all the cKO RG progenitors were able to proliferate at that stage, only 45% of TBR2+ cells in *Arx* cKO could enter cell cycle (versus the 75% of the control). These observations

support the hypothesis that the drastic effect on the IPC proliferation is not only due to a premature differentiation among VZ progenitors but essentially to a direct effect of ARX ablation on IPCs. In line with this, we found ARX expression in many TBR2+ cells of the VZ/SVZ.

This reduction of cortical progenitor cells led to an alteration of the cortical layering: a significant loss of cells from the superficial layers of *Arx* cKO cerebral cortex with relative preservation of the deeper layers. Our observations in this genetic model complement those found after an acute reduction of *Arx* through the *in utero* electroporation of an *Arx* shRNA in mid gestation where an increased number of progenitors exiting the cell cycle and prematurely adopting the neuronal fate were found (Friocourt G et al. 2008).

We also performed a gene expression profile analysis in wild type and *Arx* KO cerebral cortices that identified 83 misregulated genes. Interestingly, this analysis found very little overlap with the results of the same analysis that we previously performed in the ganglionic eminences (Fulp CT et al. 2008; Colasante G et al. 2009). These data reinforce the assertion that ARX exerts region specific roles in the ventral telencephalon and in the cerebral cortex through the activation/repression of different transcriptional programs (Nasrallah MP et al. 2012). In agreement with the reduction of GABAergic interneurons migrating to the cerebral cortex in *Arx* KO brains (Kitamura K et al. 2002; Colombo E et al. 2007), markers of specific interneuron subclasses (NPY, Somatostatin and also LHX6) were downregulated in KOs. However, among the several misregulated genes, we focused our attention on *Cdkn1c*, as we considered it the most interesting Arx

putative target, whose up-regulation could account for the phenotype observed in *Arx* cKO cortices (Mairet-Coello G et al. 2012).

Our characterization of the *Cdkn1c* expression pattern during normal corticogenesis found *Cdkn1c* to be expressed in the SVZ in the first phases of neurogenesis (E12.5-E14.5). At later stages it is also detected in the cortical plate (CP). Conversely, in *Arx* cKO, it is strongly upregulated in the VZ and SVZ starting at E12.5. The expression of *Cdkn1c* during corticogenesis has been debated for a long time. While early reports indicated that *Cdkn1c* mRNA is localized in the VZ, SVZ, and CP of embryonic rat cortex (van Lookeren Campagne M and R Gill 1998), CDKN1C protein has been localized in the CP, with faint expression in the IZ and no signal in the VZ/SVZ (Nguyen L et al. 2006; Itoh Y et al. 2007). A few recent studies have helped clarify this issue (Nguyen L et al. 2006; Tury A et al. 2011; Mairet-Coello G et al. 2012; Tury A et al. 2012). Using an antibody against CDKN1C, they found it is expressed mainly in differentiating postmitotic neurons, but also it colocalizes with TBR2+ cells in SVZ and with some PAX6+ in VZ. These data are fully consistent with our data on *Cdkn1c* expression obtained by *in situ* hybridizations.

Recently Tury et al. (2011) showed that CDKN1C overexpression in E14.5–15.5 rat embryos elicits precursor cell cycle exit and promotes transition from proliferation to neuronal differentiation. Comparing the neurogenic and astrogliogenic effects of CDKN1B and CDKN1C, they discovered that CDKN1C overexpression promotes more neuronal differentiation than CDKN1B (Tury A et al. 2011). The specific neurogenic effect of CDKN1C is particularly interesting in relation to its expression in IPCs, which, distinct from RGCs, generate only neurons. However, they do not clearly analyze the

specific effect of CDKN1C overexpression on the two cortical progenitor cell populations. In their follow-up work, Mairet-Coello et al. (2012), analyze the phenotype of *Cdkn1c* mutant mice, finding that proliferation of both RGCs and IPCs is increased, expanding both precursors with greater impact on IPCs.

In this context, our report is the first to describe the effect of CDKN1C overexpression on cortical progenitor cell proliferation, integrating the analysis previously performed. Interestingly, our data also support the hypothesis that CDKN1C is more relevant for IPC than RGC cell cycle exit, although CDKN1C is overexpressed in both cortical VZ and SVZ, the most dramatic effect is observed on IPC and not on RGC proliferation.

We propose a model for the Arx-dependent control of cortical progenitor cell proliferation (Fig. 14). Arx expression in the VZ and partially in the SVZ is able to repress *Cdkn1c* premature expression, allowing proliferation of RGC cells and expansion of IPCs. When *Arx* is normally downregulated, the consequent up-regulation of CDKN1C in the SVZ favors IPC cell cycle exit. In contrast, in *Arx* KO cortex, CDKN1C expression is high in the VZ resulting in a mild proliferation effect on RGC cells. More dramatic is the impact on TBR2+ IPCs; these progenitors have already such a high level of CDKN1C that directly exit the cell cycle without significant cell division.

Certainly, the presence of other alterations or compensatory mechanisms cannot be excluded in *Arx* cKO cortices. For example, the microarray analysis highlighted the up-regulation of Id1 and Id2 genes in *Arx* KO cortices. It is known that their targeted disruption in mice results in premature withdrawal of progenitor cells from the cell cycle and expression of neural-specific differentiation markers (Lyden D et al. 1999). Thus, it

is likely that their overexpression in *Arx* cKO cortices might compensate for the *Cdkn1c* up-regulation, mitigating the full phenotypic expression. Among the compensative mechanisms, we could also consider the slight acceleration of cell cycle duration in IPCs observed in *Arx* cKO.

We also demonstrated that *Cdkn1c* is a direct transcriptional target of ARX. The genomic region 5' to the murine *Cdkn1c* gene locus was screened for the presence of the ARX putative binding site and a unique palindromic sequence (5'-ATTAGCATAAT-3') was located a few bases upstream of the *Cdkn1c* transcription start site. Luciferase assays allowed us to demonstrate that ARX, together with the corepressor TLE1, is able to repress transcription through binding at the identified 500bp enhancer region. Furthermore, chromatin immunoprecipation revealed that ARX directly binds in this 500 bp *Cdkn1c* enhancer region.

Surprisingly, the ARX binding site that we identified in this study is different from the one described in our previous work (Fulp CT et al. 2008). In that work we analyzed the transcription factor binding sites (TFBSs) significantly enriched in the regulatory regions of genes whose expression increased within *Arx* KO subpallium, we identified the sequence TAATTA. In a recent study using the ChIP-chip methodology in ARX transfected N2a cells almost 50% of Arx immunoprecipitated sequences N2a cells were unequivocally enriched for TAATTA binding site in comparison to controls (Quille ML et al. 2011). In this same study, only 20% of the genes ARX immunoprecipitated in E15.5 mouse embryonic brains were found to have this binding site; furthermore, any other motif enriched in ARX-bound sequences by comparison to control sequences, could not be identified (Quille ML et al. 2011). These results suggest that whereas

overexpressed ARX seems to be recruited primarily to TAATTA, in more physiological conditions such as in embryonic brain, ARX is recruited to other less common motifs or needs other factors for DNA binding. Based on these data, the ATTAGCATAAT site we identified might be one of the in vivo binding sites to which ARX is recruited. Surprisingly, the ChIP on chip analysis performed by Quillé and colleagues revealed that ARX binds the *Cdkn1a* (p21/Cip1) promoter but not *Cdkn1c*, however this might be due to limitations of the ChIP-chip technique. Indeed, ChIP-seq experiments might allow further delineation of ARX direct transcriptional target genes.

In summary, our data indicate ARX plays a unique role in the progenitor cells of the cerebral cortex when compared to its role in the ventral forebrain. By genetically eliminating *Arx* from pallial progenitor cells we find a reduction in the number of RGC due to a premature exit from the cell cycle and significant skipping of the IPC amplification stage of corticogenesis. This defect results in the predicted deficit in upper later neurons of the cerebral cortex. We further elucidated the pathogenesis of this defect by identifying the cell cycle regulator CDKN1C as a downstream target of ARX. Our study extends our understanding of the aberrant molecular network responsible for the reduced proliferation observed in *Arx* cKO forebrains; indeed, this is a critical point for understanding the pathogenic mechanisms underlying these devastating neurologic disorders and in devising genetic or cellular therapeutic strategies to ameliorate *Arx* mutation induced pathological phenotypes.

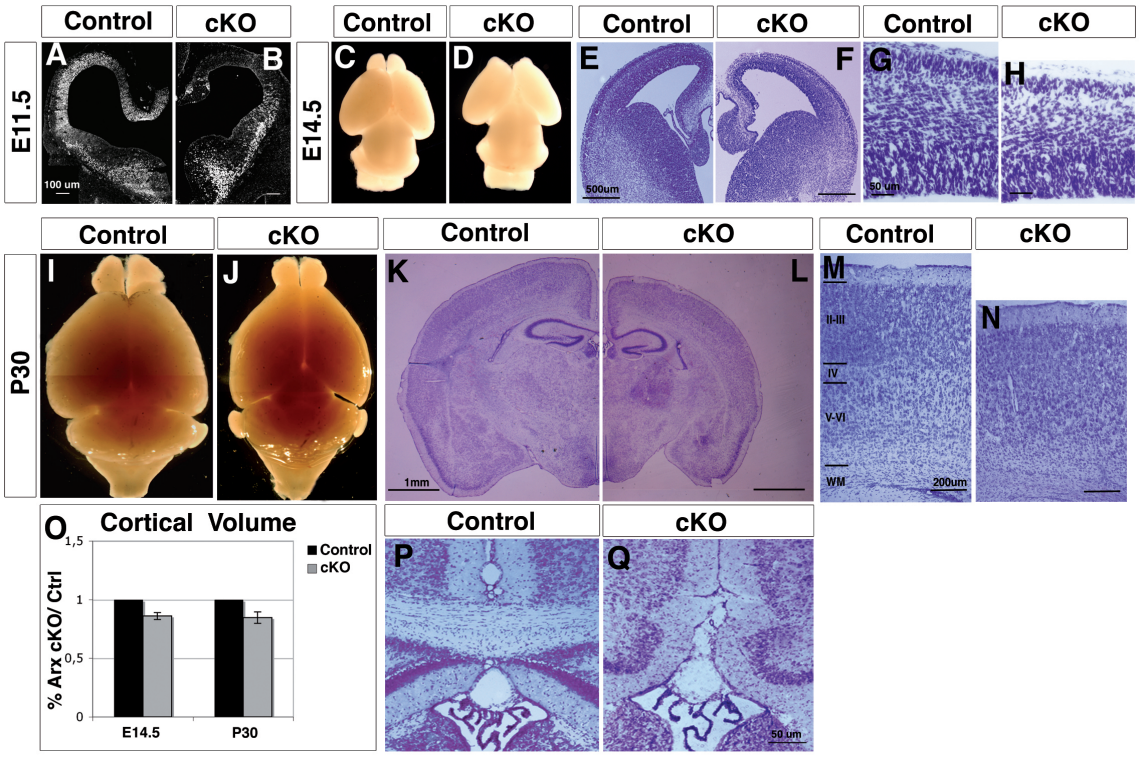

Figure 1: Reduction in cerebral cortex and olfactory bulb dimensions is observed in *Arx* cKO brains. (A, B) At E11.5 ARX expression is lost in the cortical VZ of *Arx* cKO brains when compared to control brains. (C-H) At E14.5 the *Arx* cKO brains exhibit a reduced size of the cerebral hemispheres and the olfactory bulbs (C, D). Nissl stained coronal sections (E, F) and corresponding high magnification of the cerebral cortex (G, H) highlight a diminution in the cortical thickness in the *Arx* cKO brains when compared to controls. (I-N) Morphological analysis of postnatal (P30) control and *Arx* cKO brains confirms the previous observations: cortical vesicles and olfactory bulbs are under developed, whereas the cerebellum and the brain stem do not appear to be affected (I, J); Nissl stained coronal sections reveal an overall reduction in the telencephalic structures in *Arx* cKO brains, involving the cerebral cortex and hippocampus (K, L). Magnifications of cortical areas show an increased nuclear density in the deeper layers (IV-VI) of *Arx* cKO compared to controls (M, N). (O) Quantifications of relative cortical volume (rv) at E14.5 and P30 of *Arx* cKO brains compared to controls. Error bars correspond to S.D. (P, Q) The corpus callosum is absent in *Arx* cKO brains. Cx, cortex; Hyp, hippocampus, Pyr, pyriform cortex; cc; corpus callosum.

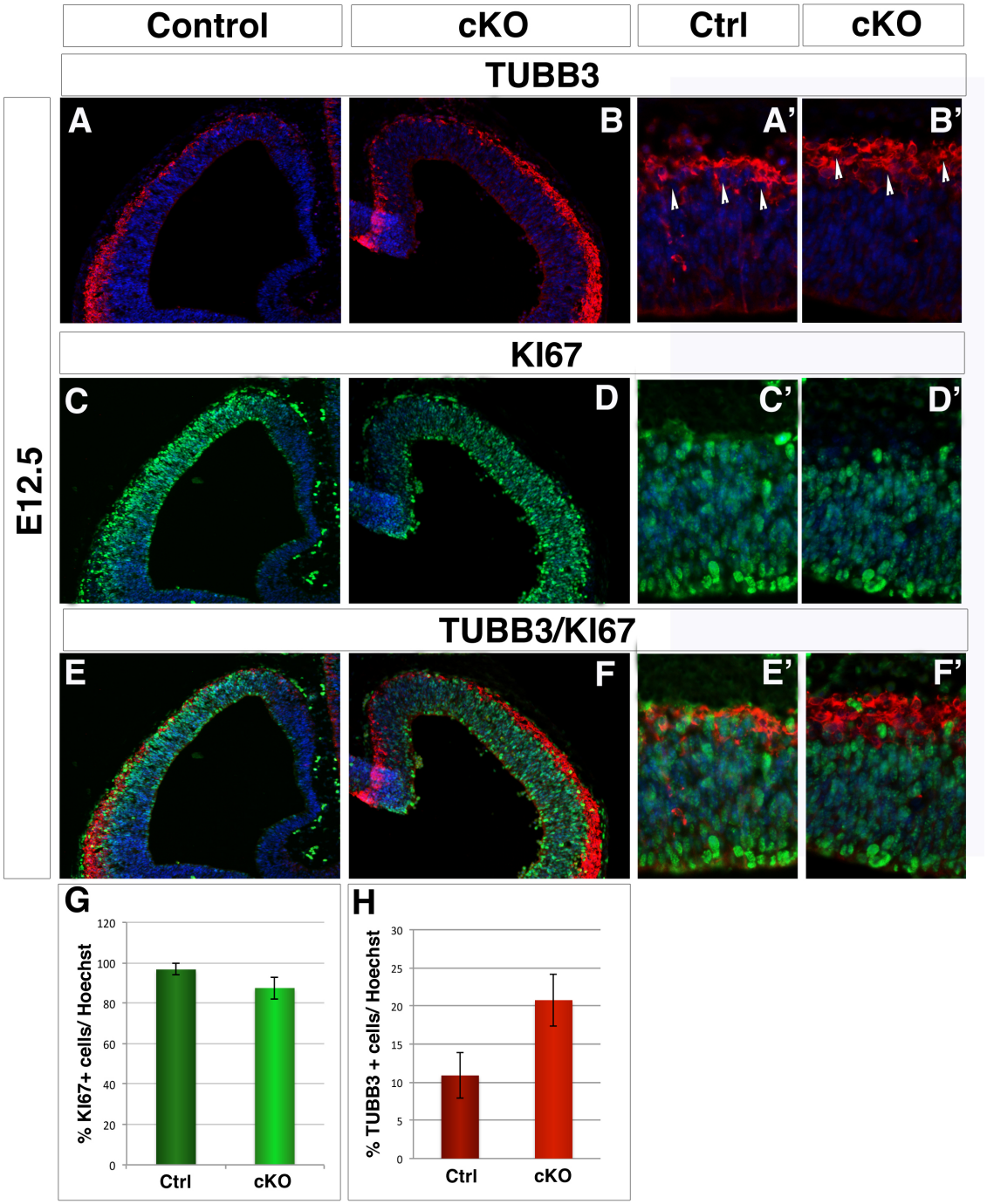

Figure 2: At E12.5 *Arx* cKO cortices display a slight decrease in cortical progenitor proliferation and increase in differentiation. Immunohistochemistry for ßIII -tubulin (TUBB3) in E12.5 control (A, A') and *Arx* cKO cortices (B, B') highlights an increase in the number of differentiated young neurons in *Arx* cKO cortex compared to control, corresponding to a slight decrease in the number of KI67+ proliferative progenitor cells (C-D'). (E-F') Merge of ßIII -tubulin and KI67 staining in control and *Arx* cKO cortex. (F) Quantification of the percentage ßIII -tubulin + and KI67+ cells at E12.5 in control and *Arx* cKO cortex.

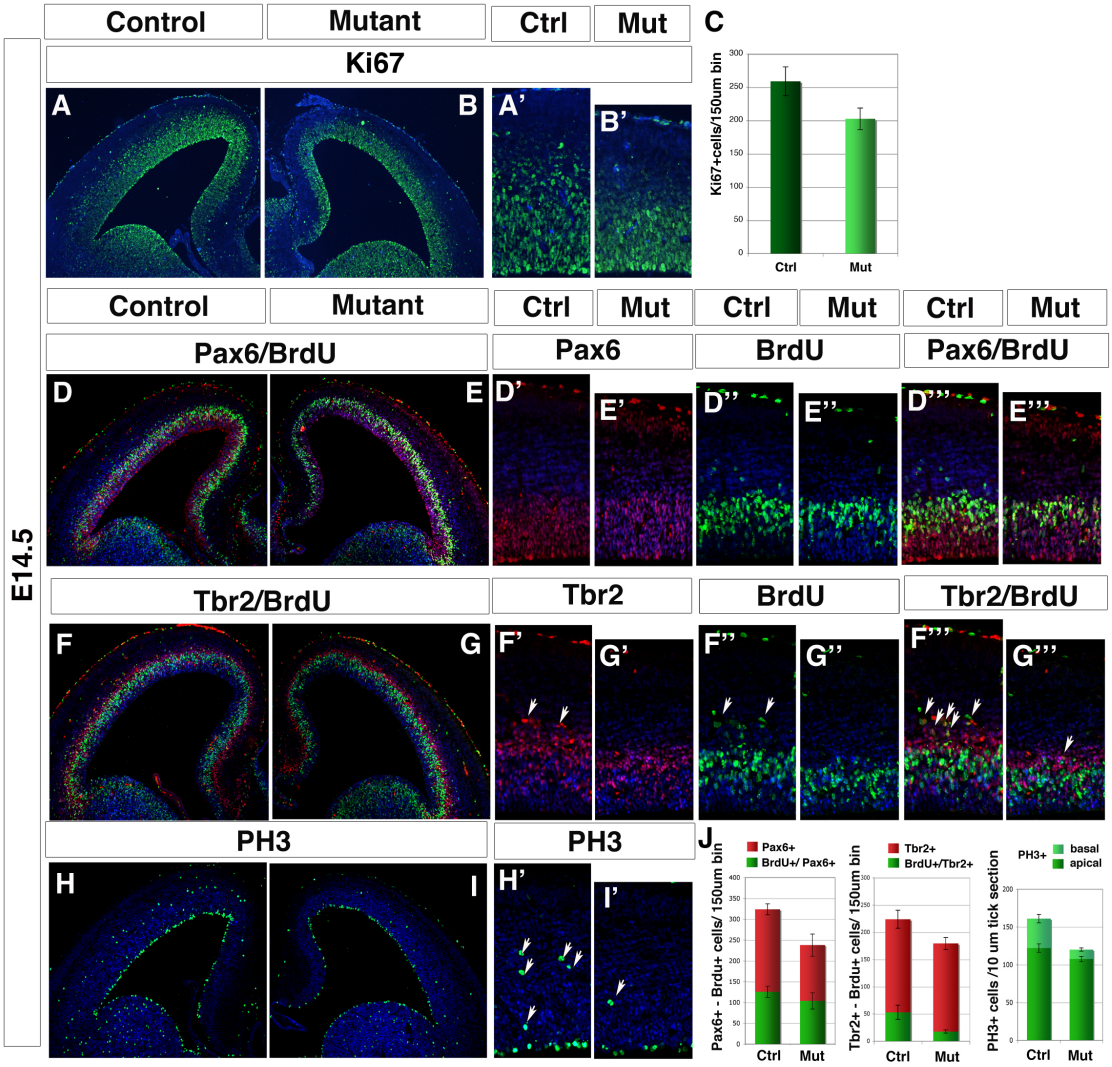

Figure 3: Proliferation rate of radial glia cells and intermediate progenitors is reduced in *Arx* cKO cerebral cortex. E14.5 coronal sections from control (left) and *Arx* cKO cortices (right) are directly compared. Ki67 stained sections (A, B) and corresponding higher magnification (E, F) reveal an overall reduction of proliferating cells in *Arx* cKO cortex compared to wild type; (C) quantifications of Ki67+ cells in a 150 µm bin extending from the ventricular to pial surface: control 259±21.8 and cKO 202.5±16.3; n=6 for each, p value < 0.001. (D, E, F, G, H, I) PAX6, TBR2, BrdU and PH3 immunolabelings performed on wild type and *Arx* cKO sections from embryos treated with 1 hour pulse of BrdU. (D'-E''') Reduction in the number and in the signal intensity of PAX6+ cells (D', E') and in the number of BrdU+ (D'', E'') in *Arx* cKO cortices compared to the control. (F'-G''') A reduction in the number of TBR2+ cells (arrowheads, F', G') and a decrease in TBR2+/BrdU+ double positive cells (arrowheads, D''', E''') in *Arx* cKO cortices compared to the control are shown (H'-I') Reduction of PH3+ cells is observed in the *Arx* cKO cerebral cortex, greater in the basal rather then in the apical region. (J) Quantifications of total PAX6+ and TBR2+ cells, dual-labeled PAX6+/BrdU+ and TBR2+/BrdU+ double positive cells and PH3+ in E14.5 wild type and *Arx* cKO cortices are shown.

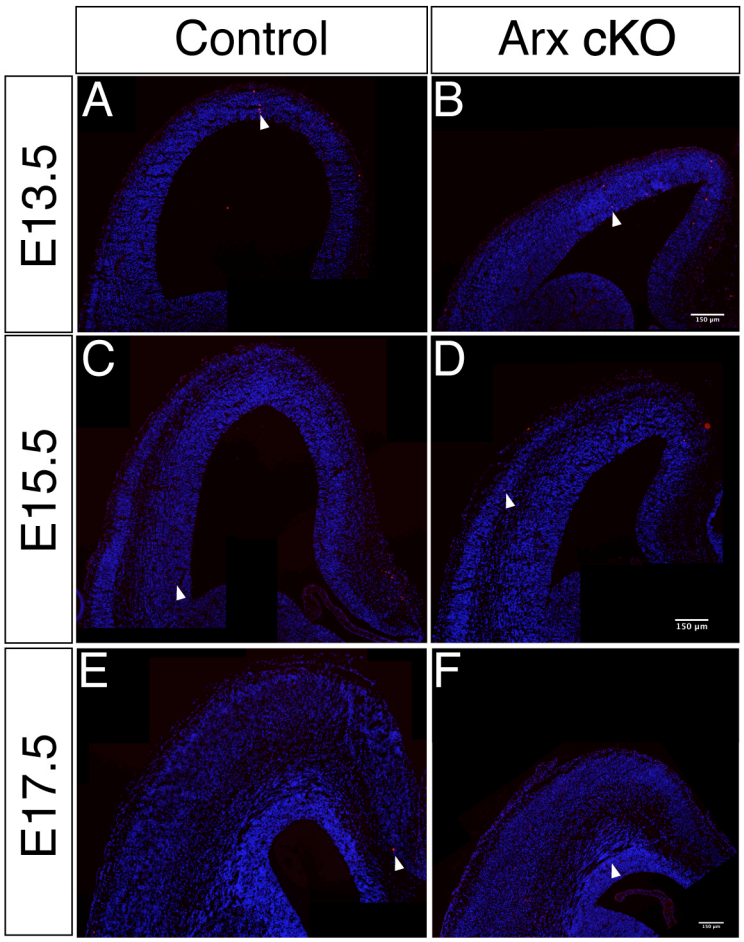

Figure 4: *Arx* cKO cerebral cortex shows no increase in apoptosis with respect to control during embryonic development. Immunohistochemistry for Caspase3 (red) in control and *Arx* cKO cortices at E13.5 (A, B), E15.5 (C, D) and E17.5 (E, F). Comparable numbers of Caspase3+ cells can be observed in both control and *Arx* cKO coronal sections.

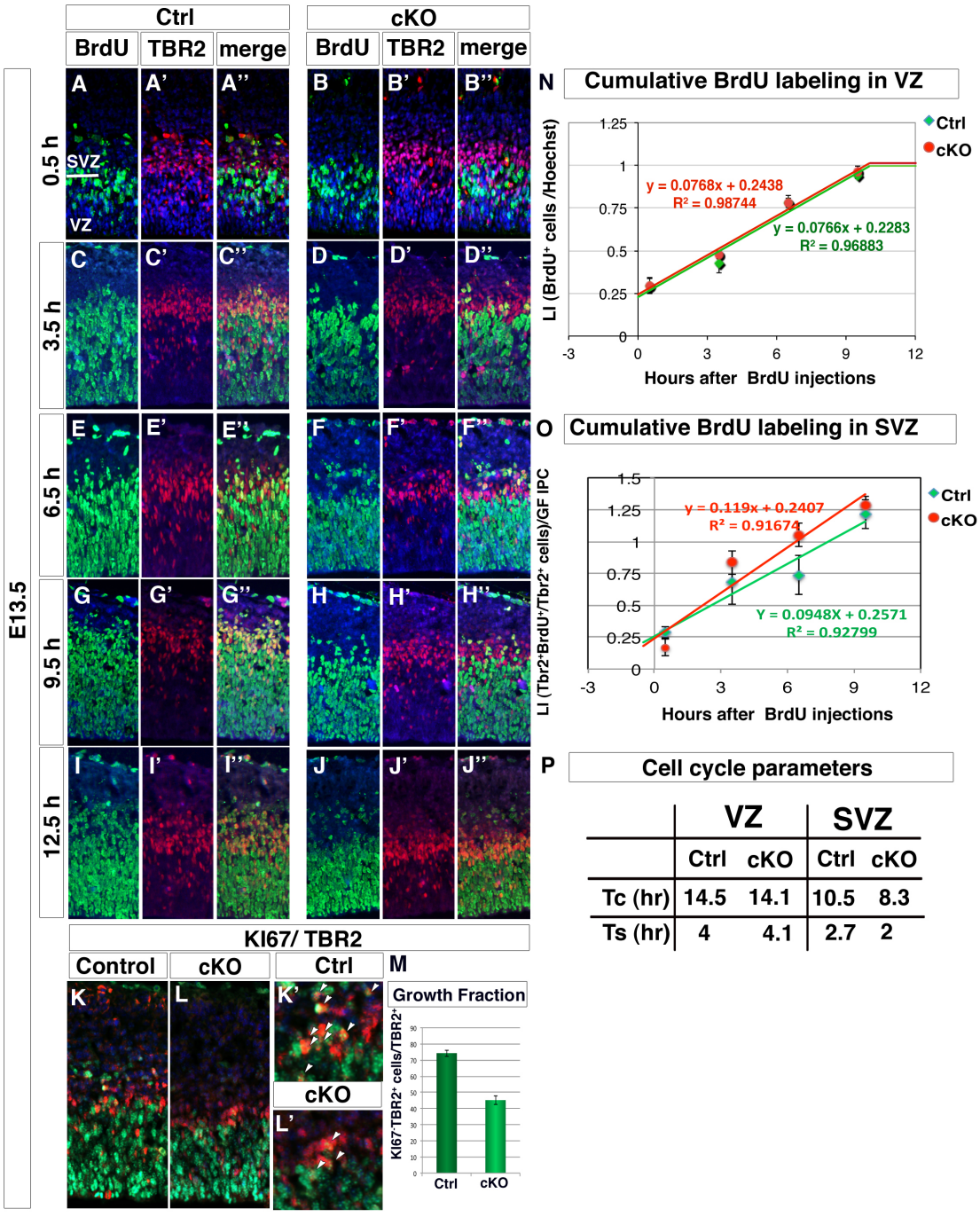

	VZ		SVZ	
	Ctrl	cKO	Ctrl	cKO
Tc (hr)	14.5	14.1	10.5	8.3
Ts (hr)	4	4.1	2.7	2

Figure 5: Cell cycle kinetic is not affected in both *Arx* cKO VZ and SVZ progenitors, but IPC growth fraction is severely reduced (A-J'') Cortical fields of BrdU and TBR2 labelings performed on control and *Arx* cKO cortices at 5 (0.5, 3.5, 6.5, 9.5 and 12.5 hours) of the 6 time points of the BrdU cumulative labeling experiment are shown. (K-M) Double labeling for TBR2 and KI67 and quantification of KI67+TBR2+ normalized on total TBR2+ cells reveals a severe reduction of the IPC proliferating fraction in *Arx* cKO with respect to control. (N-O) Labeling indices (L.I.) for both control and cKO RG and IPC progenitor (calculated as the ratio between

TBR2+ BrdU+ cells on the total of TBR2+ and normalized on the IPC growth fraction in the latter case), are plotted against correspondent BrdU labeling times and the interpolating lines are drawn. (P) Evaluation of cell cycle duration (Tc) and S-phase duration (Ts) are reported.

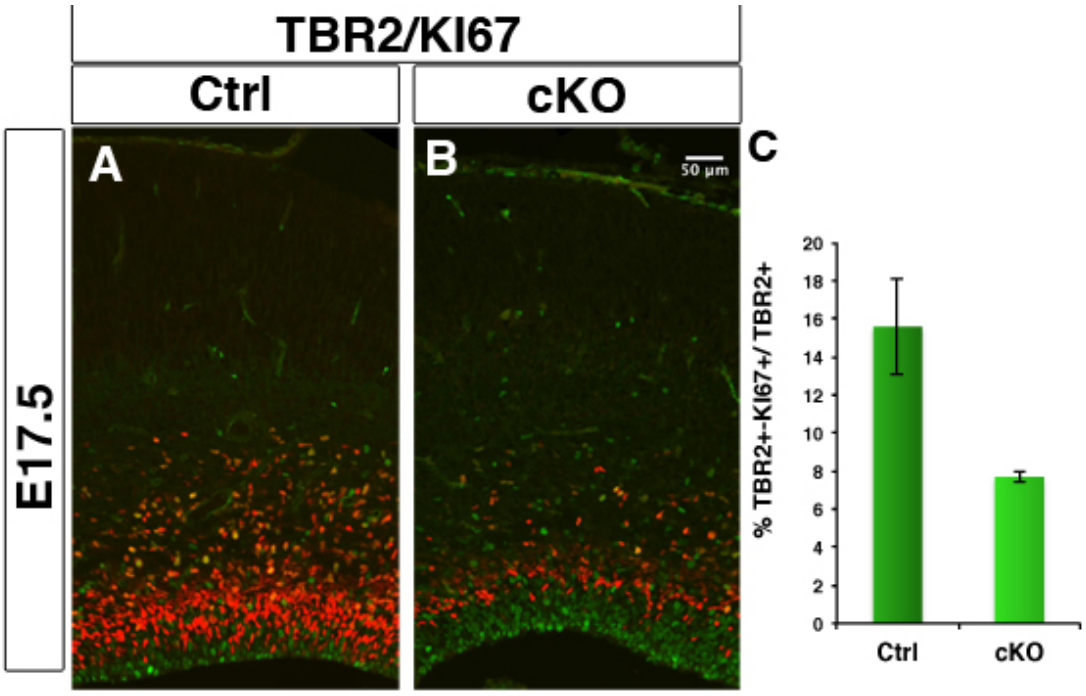

Figure 6: *Arx* cKO cortices display fewer IP proliferating cells also later on during development. Immunohistochemistry for TBR2 (red) and KI67 (green) in control (A) and *Arx* cKO (B) cortices at E17.5 revealing a decrease in TBR2+ cells in the cKO cortex with respect to control, with very little percentage of them, still proliferating (TBR2+ Ki67+). (C) Quantification of the percentage of proliferating IPC cells (TBR2+ Ki67+) on the total IPC cells (TBR2+) in both the control and cKO cortex (ctrl: 15.57±2.50; cKO: 7.69±0.26, n=4 each, p=0.0458, t test)

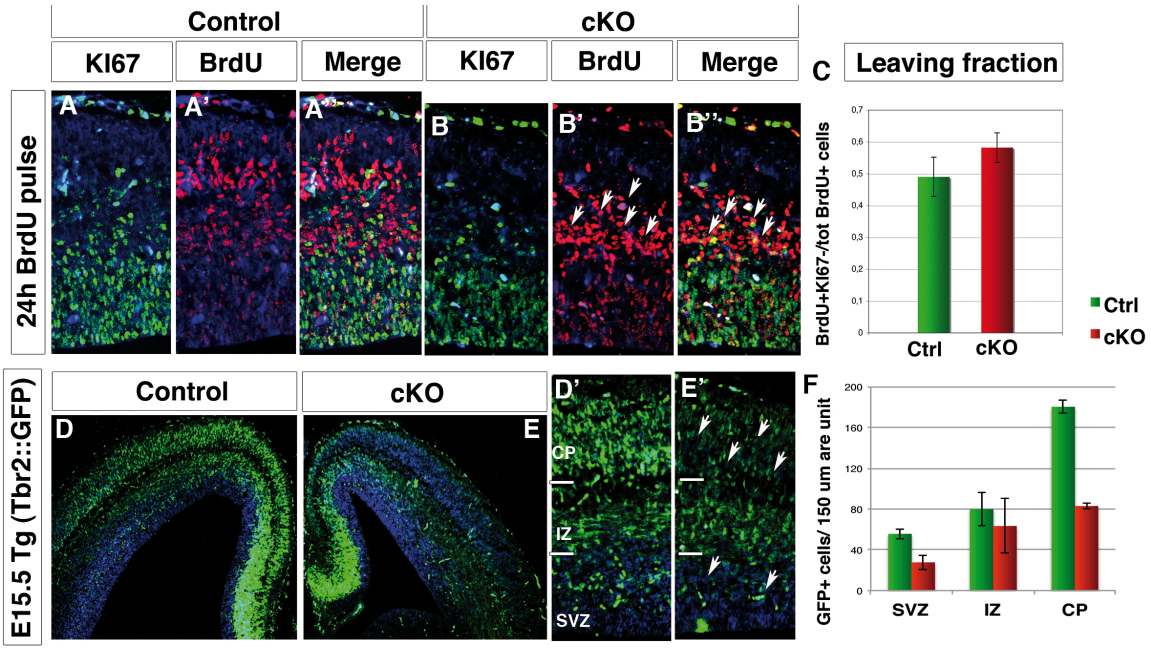

Figure 7: Increased cell cycle exit affects *Arx* cKO progenitors and the progeny of TBR2+ cells is reduced. (A,B) E14.5 control and *Arx* cKO cortical sections were double labeled for Ki67 and BrdU, following BrdU injection at E13.5. (C) Quantification of the proportion of cells leaving the cycle (leaving fraction: BrdU+Ki67-/tot BrdU+ cells). (D, E) E15.5 coronal sections and relative higher magnifications (D', E') of control and *Arx* cKO in the transgenic background *Tbr2*::GFP analyzed for GFP expression reveal a reduction in number and intensity of GFP+ cells in *Arx* cKO SVZ , subplate (SP) and cortical plate (CP) (F).

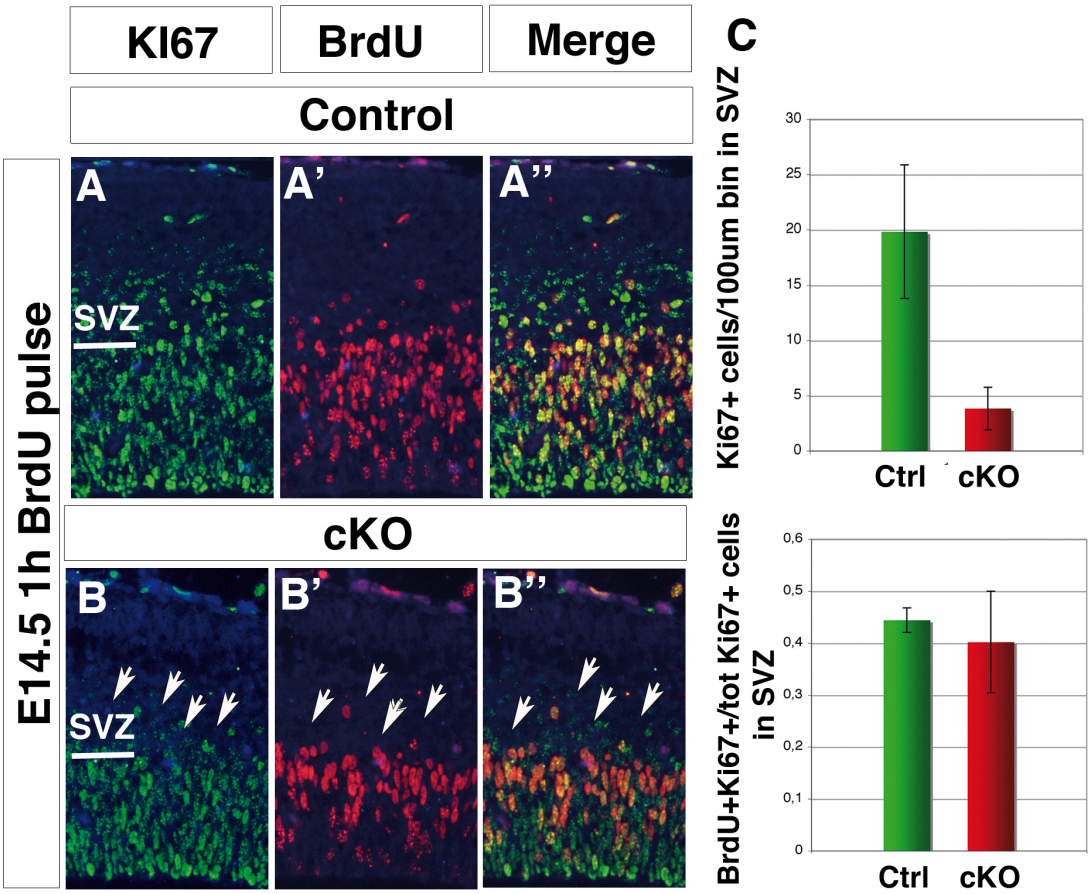

Figure 8: Cell cycle length is normal in *Arx* cKO SVZ precursors while (A-B'') E14.5 wild type and *Arx* cKO cortical sections were double labeled for KI67 and BrdU following a 1-hour BrdU pulse. (C) Quantifications of KI67+ cells in control and cKO SVZ and of Brdu+ Ki67+ double positive cells on the total of Ki67+.

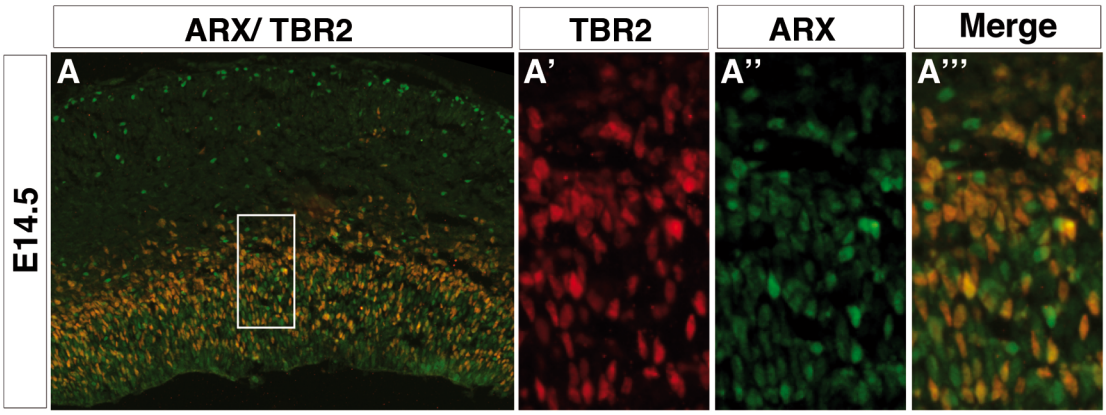

Figure 9: ARX is expressed in TBR2+ intermediate precursor cells. (A) E14.5 coronal sections of cortex and relative higher magnifications (A', A'', A''') of control brains labeled for TBR2 (A') and ARX (A''). (A''') Higher magnification showing the presence of ARX and TBR2 co-stained cells in both cortical VZ and SVZ.

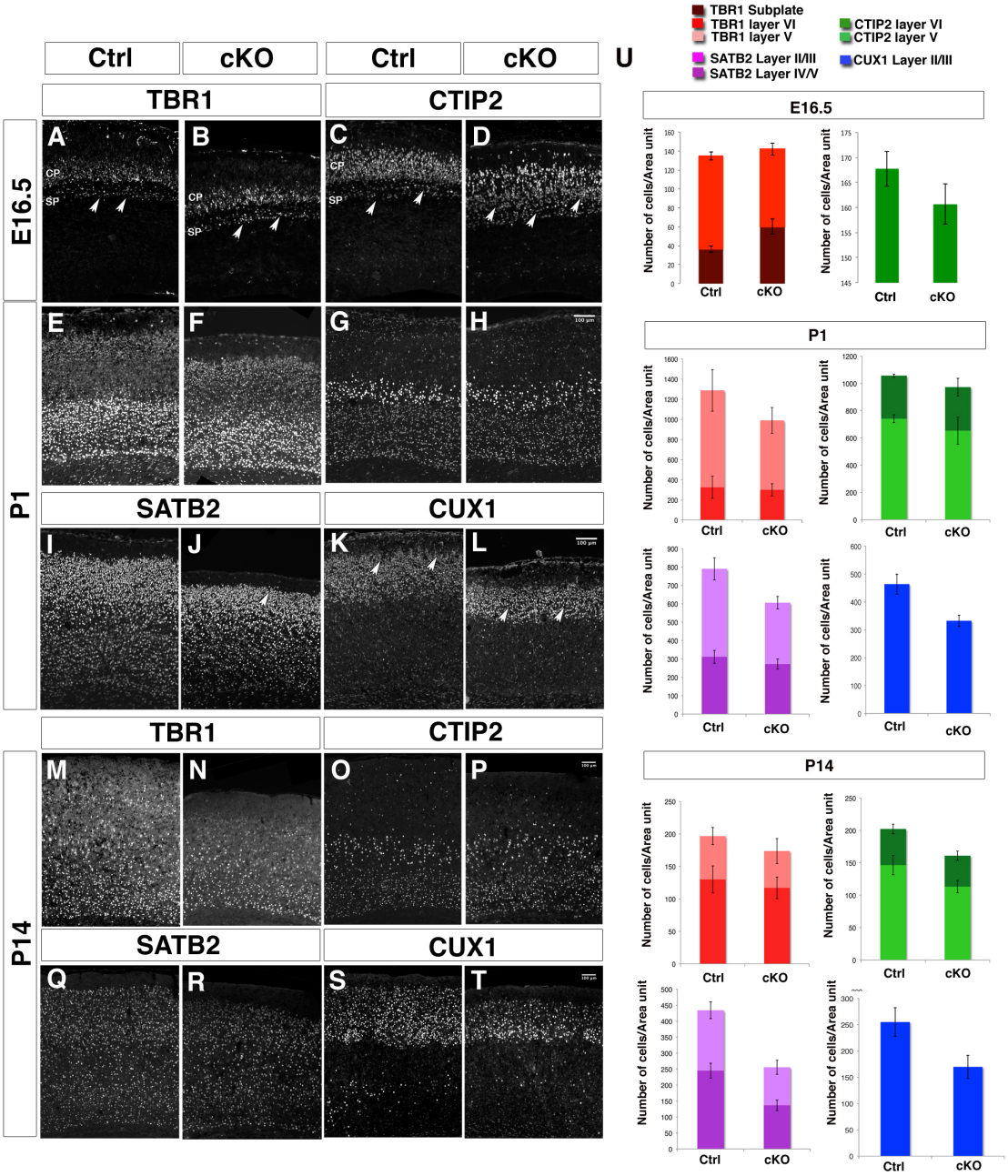

Figure 10: Cortical layering is altered in *Arx* cKO brains. Immunohistochemistry for molecular markers identifying deeper cortical layers at E16.5 and both deeper and upper cortical layers at P1 and P14, in control and *Arx* cKO cortices (A-T). (A, B) TBR1+ cells are slightly decreased in layer V-VI neurons and increased in subplate in E16.5 *Arx* cKO cortices with respect to the controls; (C, D) CTIP2 immunolabeling shows the same alterations observed with TBR1 although more prominantly. (E, F) At P1, similar numbers of TBR1+ cells in *Arx* cKO cortices with respect to control are detected as well as a similar number of CTIP2+ cells in both layer V and VI (G, H). (I, J) SATB2 is decreased in upper layer neurons (II, III) in the *Arx* cKO cortices with respect to the controls; (K, L) Similarly, staining for CUX1 (layers II-IV) shows a diminution of upper cortical layer neurons in *Arx* cKO cortices with respect to controls. (M-P) At P14, there are still similar numbers of TBR1+ and CTIP2+ cells in the Arx cKO cortices when

compared to controls but still a decrease in SATB2+ cells in layers II/III (Q, R). Similarly, there are also still fewer CUX1+ cells in the *Arx* cKO cortices (S, T). (U) Quantifications of TBR1+ and CTIP2+ cells in layer VI and V and of SATB2+ and CUX1+ at E16.5, P1 and P14 in both control and *Arx* cKO cortices. TBR1+ and CTIP2+ cells at P14. Cells positive for each molecular marker were counted 25% of the cortex in P1 and in a 200 μm bin in P14, both from the ventricular to the pial surface in both control and *Arx* cKO cortices.

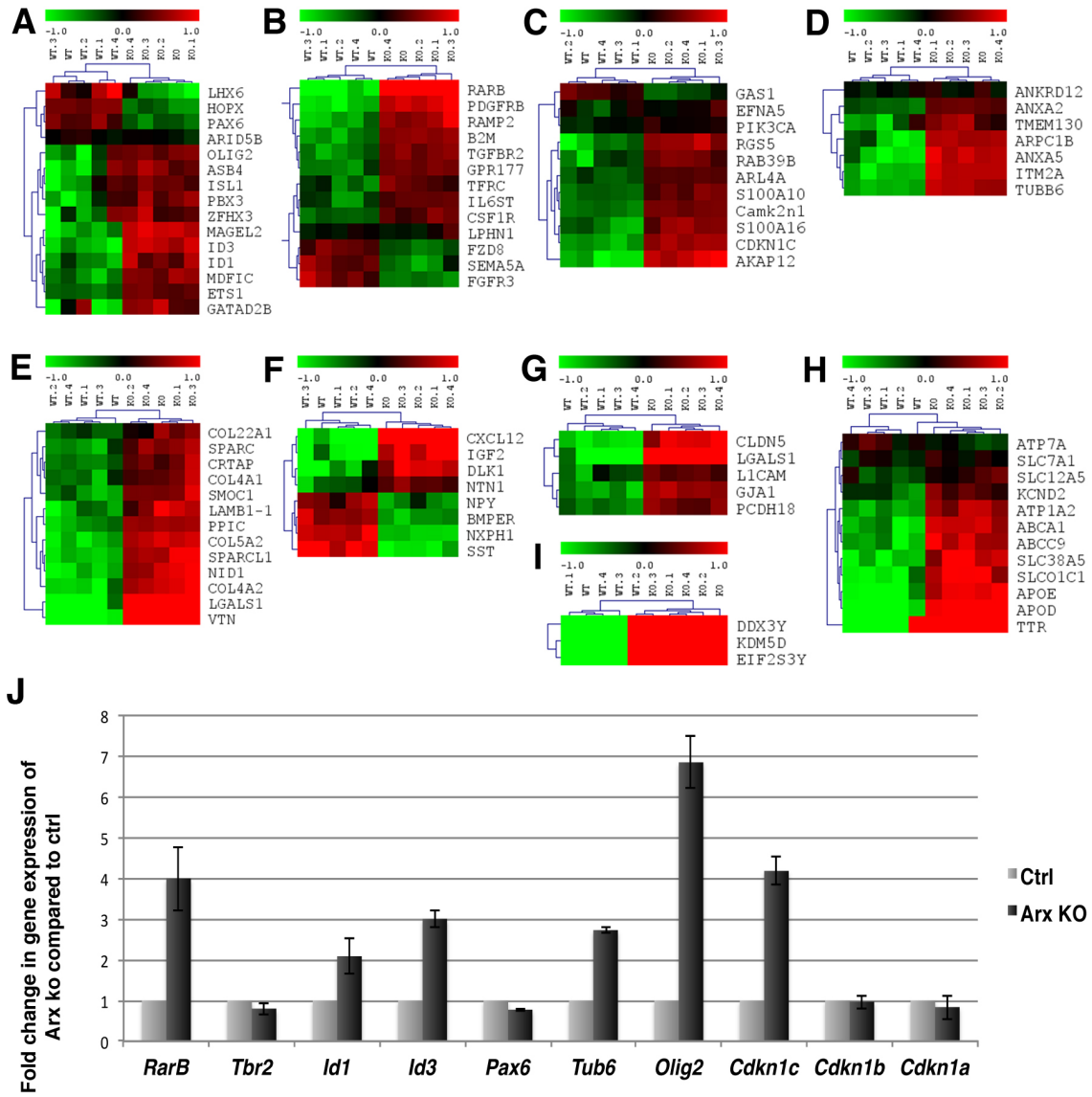

Figure 11: Outline of the gene expression profile analysis and hierarchical clustering of the transcripts found differentially expressed between control and *Arx* KO dorsal telencephalon. (A-I) The 86 genes found differentially expressed between control and *Arx* KO cerebral cortices were grouped according to the protein function they codify for, in: (A) transcription factors; (B) receptors; (C) intracellular regulatory proteins; (D) structural proteins; (E) extracellular matrix proteins; (F) extracellular regulatory proteins; (G) junctions and adhesion molecules; (H) carriers and transporters; (I) Y linked genes. (J) 7 genes found misregulated by microarray analysis were selected for quantitative real-time RT-PCRs (qPCRs) validation.

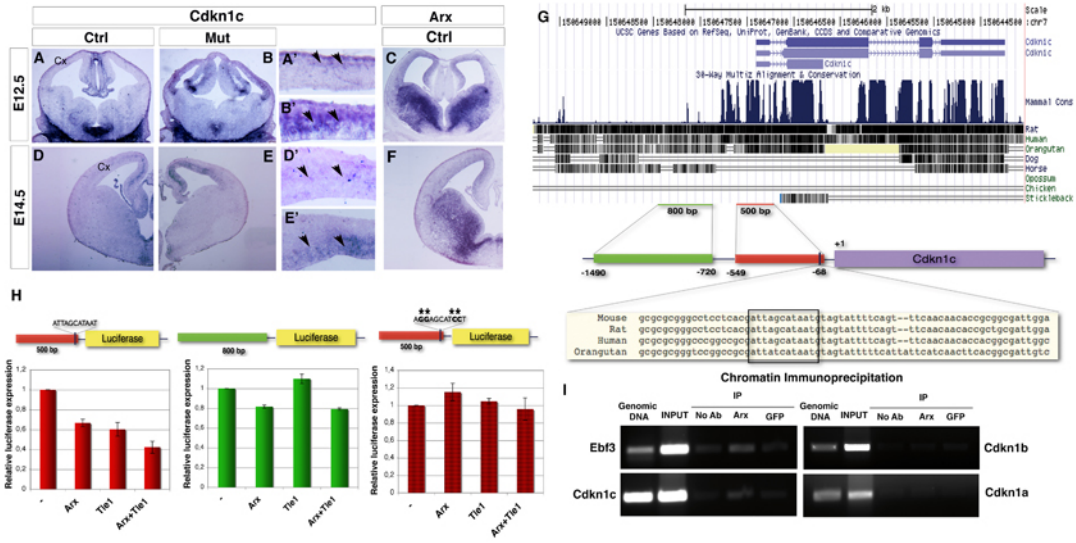

Figure 12: The cyclin dependent kinase inhibitor (CKi) *Cdkn1c* is ectopically expressed in *Arx* KO cortical VZ and SVZ and it is a direct transcriptional target of ARX. In situ hybridizations for *Cdkn1c* on telencephalic coronal sections at different embryonic stages (E12.5-E14.5) of control (left) and *Arx* KO (right) brain tissues; in situ hybridizations for *Arx* on control coronal sections at the corresponding developmental stages are also showed. (A-C) At E12.5 *Cdkn1c* transcript is detected in the neo-formed SVZ in control brains (arrowheads, A'); differently, in *Arx* KO, it is significantly upregulated in both VZ and SVZ (arrowheads, B'), where *Arx* is normally expressed at this stage (C). Similarly, *Cdkn1c* is found upregulated in *Arx* KO VZ and SVZ at E14.5 (arrowheads, E') whereas in the relative control sections it is still barely detected in the SVZ (arrowheads, D'). (G) A 5 kb genomic region upstream to the murine *Cdkn1c* gene locus was screened for the presence of paired homeodomain binding sites: a palyndromic sequence 5'-ATTAGCATAAT-3', highly conserved in mouse, rat, human and orangutan, was found between -71/-81 bp before the *Cdkn1c* transcription start site (+1). (H) A ~ 500 bp (-549/-68) genomic region containing the putative ARX binding site, a ~ 750 bp (-1490/-720) containing some TA rich repeats and the same 500 bp (-549/-68) genomic region with the binding site mutagenized 5'-AGGAGCATCCT-3' were separately cloned in a construct containing the *Luciferase* gene and tested in transcriptional activity assays in P19 cells. When the 500 bp(-549/-68)-Luc construct is cotransfected with pCAG-ArxIRESGFP a reduction in Luciferase expression compared control plasmid pCAG-IRESGFP cotransfection was appreciable (0.67±0.04; n=3, p<0.005,); similar reduction was observed when the corepressor TLE1 was cotransfected (0.60±0.07, n=3); finally, higher reduction was detected when both ARX and TLE1 were cotransfected (0.42±0.06, n=3). Differently, ARX cotransfected with the 750 bp(-1490/-720)-Luc induced only a slight reduction in the basal transcriptional activity (0.94± 0.01, n=3, p<0.05,), even in combination with TLE1. When the binding site 5'-ATTAGCATAAT-3' was mutagenized in 5'-AGGAGCATCCT-3', no significant reduction in Luciferase expression was appreciable in cotransfection experiments. (I) Immunoprecipitation of E14.5 telencephalic chromatin with anti-ARX, anti-GFP and IgG only. Primers spanning the 500 bp(-549/-68) genomic region upstream to the *Cdkn1c*, and *Ebf3*, *Cdkn1b* and *Cdkn1a* regulative regions were used for PCR analysis of the immunoprecipitated DNA. Enrichment of the PCR products in anti-ARX immunoprecipitated chromatin sample compared to the anti-GFP and IgG only samples was evaluated

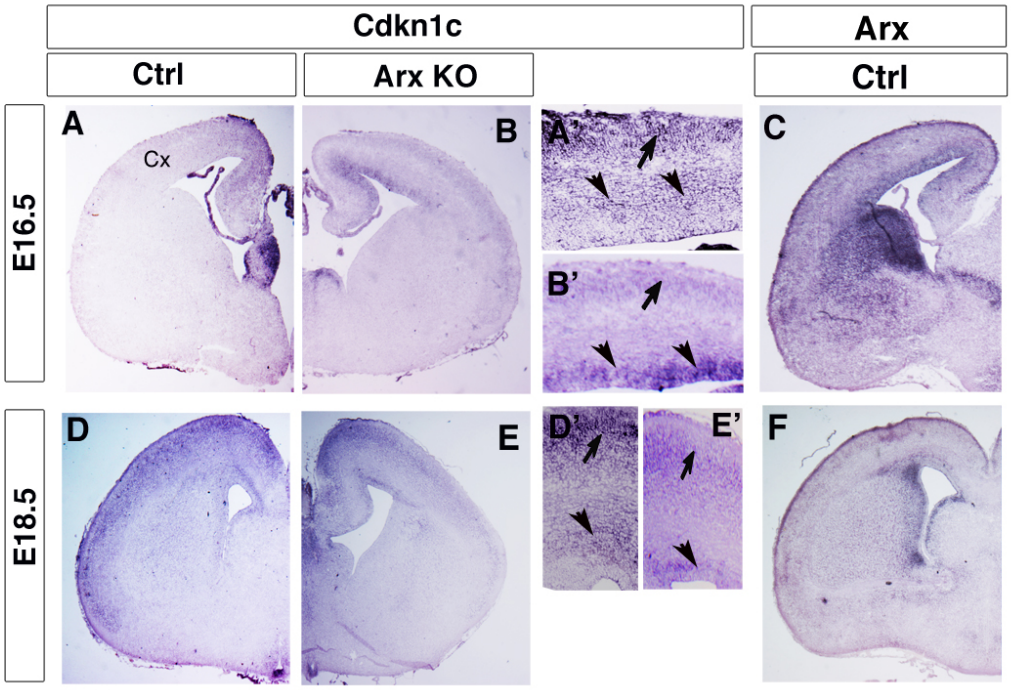

Figure 13: Expression of the cyclin dependent kinase inhibitor (CKi) *Cdkn1c* in *Arx* KO cortical VZ and SVZ, at later stages of development. In situ hybridizations for *Cdkn1c* on telencephalic coronal sections at late embryonic stages (E16.5-E18.5) of control (left) and *Arx* KO (right) brain tissues; in situ hybridizations for *Arx* on control coronal sections at the corresponding developmental stages are also showed. At E16.5, in control sections, *Cdkn1c* transcript is still detected in the SVZ (arrowheads, A') and it starts to accumulate also in the cortical plate cells (arrows, A'); in the corresponding *Arx* KO tissues, upregulation in the VZ (arrows, B, B') is still evident as well as the expression in the cortical plate (arrowheads, B, B'). Consistently, *Arx* transcript is still detected at E16.5 in control section VZ (C). At E18.5, only a slight up-regulation of *Cdkn1c* is still detectable in *Arx* KO VZ (E, E') in agreement with a reduced residual expression of *Arx* at this stage (F).

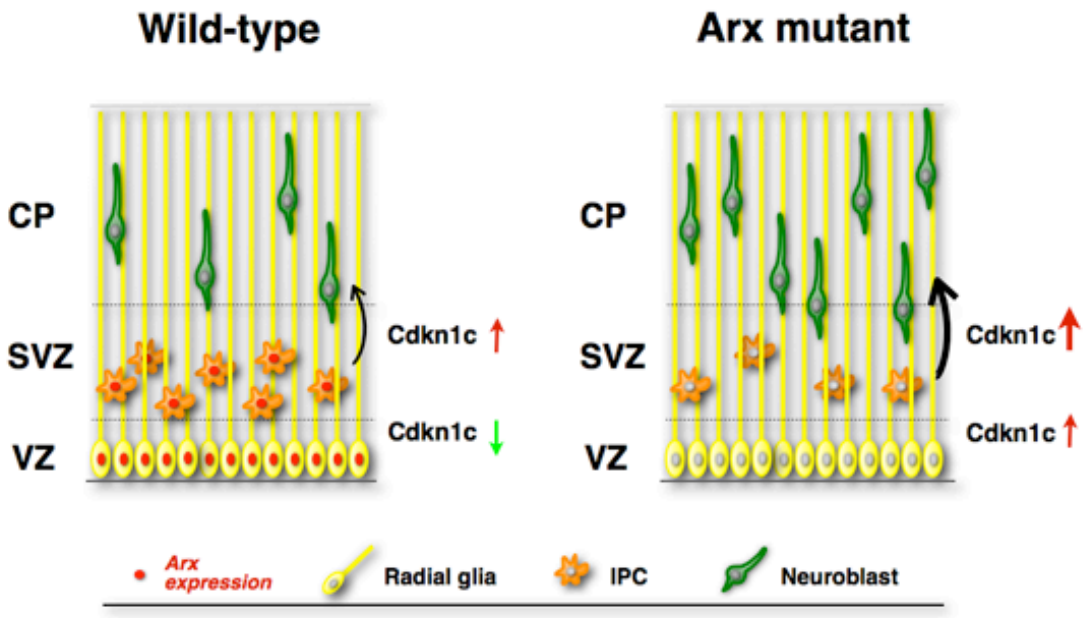

Figure 14: Schematization of the molecular mechanism through which ARX controls cortical progenitor expansion. ARX expression in the cortical VZ/SVZ normally represses CDKN1C expression allowing progenitor cell proliferation and expansion. Loss of *Arx* in the VZ/SVZ causes precocious CDKN1C upregulation in the cortical progenitors cells, which results in a mild decrease in proliferation of RGCs and a significant loss of IPC proliferation, with consequent cell cycle exit. This ultimately results in a loss of upper layer neurons in the adult cortex.

CHAPTER 3: Conditional loss of *Arx* from the developing dorsal telencephalon results in behavioral phenotypes resembling mild human *ARX* mutations

Introduction

Aristaless-Related Homeobox gene (*ARX*) is one of the more commonly mutated genes causing X-linked intellectual disability (XLID) (Lin CH et al. 2009; Shoubridge C et al. 2010). Over 44 distinct mutations have been found resulting in a spectrum of phenotypes (Shoubridge C et al. 2010). Mutations that lead to a deletion or truncation along with those that reside in the homeodomain cause primarily brain malformation phenotypes such as X-linked lissencephaly associated with ambiguous genitalia (XLAG), hydranencephaly, and Proud syndrome (agenesis of the corpus callosum) (Bonneau D et al. 1992). Point mutations outside the homeodomain, in non-conserved amino acids of the homeodomain, missense mutations, and poly-alanine track expansion mutations lead to various neurological phenotypes that are mainly characterized by intellectual disability, but frequently also include epilepsy (typically infantile spasms), autism, or dystonia but typically have no structural brain defects (Lafaucheur L et al. 1992; Turner G et al. 2002). The only phenotype consistently observed in patients with all *ARX* mutations is intellectual disability.

Mice with a germline loss of *Arx* have a thin disorganized cortex, malformed thalamus, major white matter tract defects (corpus callosum and thalamo-cortical), and mislocalization and loss of interneurons in the cortex and striatum (Kitamura K et al. 2002). Unfortunately these mice die shortly after birth precluding behavioral or EEG phenotyping. In the developing telencephalon *Arx* is expressed in pallial progenitor cells

located in the ventricular zone (VZ) and in subpallial sub-ventricular zone (SVZ) cells, which generate interneurons that populate the cortex, striatum, and hippocampus. The selective removal of *Arx* from interneurons results in no brain malformations, but similar to the knockout mouse they have fewer interneurons in the cerebral cortex and hippocampus (Marsh E et al. 2009). They also have a severe epilepsy phenotype with features overlapping those observed in some patients with *ARX* mutations (Marsh E et al. 2009). Hence, it appears that perturbation of the developing interneurons is sufficient to produce an epileptic phenotype that recapitulates the seizures found in patients with *ARX* mutations. Selective removal of *Arx* from the pallial progenitor cells using an shRNA against *Arx* at e13.5 causes the progenitors cells to prematurely exit the cell cycle and the VZ, however because this was just a partial knock down it is unclear what affect this has on later development of the cortex (Friocourt G et al. 2008).

In contrast to mice with a germline loss of *Arx* (Kitamura K et al. 2002), mice deficient for *Arx* in cortical interneurons ($Arx^{-/Y}$ $Dlx5/6^{Cre}$ mice) have a normal cortical thickness, indicating an interneuron independent function of *Arx* on cortical thickness (Marsh E et al. 2009). To examine the role of *Arx* in cortical development, we mated $Arx^{F/X}$ mice to $Emx1^{Cre}$ mice, which selectively deletes *Arx* from the dorsal telencephalon (pallium). These mice have a thin cerebral cortex, similar to the *Arx* knockout, and are predominantly missing superficial layer neurons, sparing deeper layer neurons, due to a loss of proliferating intermediate progenitor cells (Colasante G et al. 2013). Since loss of *Arx* in interneurons appears to cause the epilepsy phenotype we sought to determine which characteristics of the human *ARX* patient phenotype might be explained by loss of *Arx* in cortical progenitor cells. Thus, we performed a detailed behavioral and anatomic

analysis of the $Arx^{-/Y}$ $Emx1^{Cre}$ mice to determine the functional consequences of *Arx* loss in cortical progenitors and whether this loss may model specific phenotypic aspects of human *ARX* patients.

Materials and Methods:

Mice

Arx conditional mutant mice ($Arx^{F/X}$) (Fulp CT et al. 2008) were maintained on a C57Bl/6 background. To inactivate *Arx* in the dorsal telencephalon specifically during development $Arx^{F/X}$ heterozygous female mice were crossed with homozygous male $Emx1^{Cre/Cre}$ animals also on a C57Bl/6 background (Jax Mouse Strain 005628). Genotyping to distinguish wild type, floxed, and cre positive alleles was performed as described (Jin XL et al. 2000; Fulp CT et al. 2008). Mice were maintained at the Children's Hospital of Philadelphia animal facility on a 12:12 hours light-dark cycle (lights on 0600-1800 hours) and *ad libitum Lab Diet mouse food 5LG4*. All experiments were approved by the Institutional Animal Care and Use Committee of the Children's Hospital of Philadelphia.

EEG Recordings and Analysis

All electrophysiologic studies were conducted as previously described (Marsh E et al. 2009). Adult animals at least 3 months old were used for all EEG recordings. Briefly, under isoflorane anesthesia, 4 electrodes were stereotaxically implanted (3 cortical-left and right frontal, right parietal and a hippocampal depth) using the

coordinates in our previous publication (Marsh E et al. 2009). The animals recovered in their home cage for 48 hours prior to recordings and then were transferred to the recording cage and recorded with a Triangle Biosystems preamplifer and a Stellate EEG recording system (Natus Technologies) for 48 to 96 hours.

The EEG and video were reviewed manually for the presence of seizures. Background EEG was quantified as previously published (Marsh E et al. 2009). Briefly ten 10-second segments of awake and asleep EEG were randomly selected, but checked for artifact and behavioral state. The awake state was defined as the period when the mouse was moving with hippocampal theta present. In contrast, when the animal was still, head down, and delta dominated the EEG it was considered asleep. A Fast Fourier Transform (FFT) was calculated for each segment (MATLAB 2010b, Mathworks, Inc., Natick, MA) and the resultant spectrums were quantified by calculating the power in selected bandwidths (Delta 0.1-3.5Hz, Theta 3.5-8.5Hz, Alpha 8.5-13Hz, Beta 13-25Hz, and Gamma 25-100Hz) and dividing by total FFT power. The percent power in each bin was averaged across genotype and compared using a Student's t-test in Excel (version 12.2.7, Mircosoft). To correct for the 10 comparisons, a difference was considered significant if the p value was less than 0.005 (the Bonferoni correction). Eight mutant mice and six wild type mice were recorded for 3 days each, but only 4 wild type and 4 mutant mice were analyzed using the FFT.

Behavioral Studies

Behavioral testing was conducted during the light phase between 1000 and 1800 hours (h), starting at 8 weeks of age and each individual paradigm was separated by at

least 2 days. Mice were handled for 5 minutes each day for 3 days prior to the beginning of testing. Six cohorts of mice were used for behavior testing. Each cohort consisted of at least two different litters of mice. See Chapter 3; Table 1 for a list of the tasks each cohort of mice performed. The numbers of mice tested for each task are listed below. Only male mice were tested and all cohorts were a mix of mutant mice ($Arx^{F/Y}$ $Emx1^{Cre/Cre}$) and wild type littermates ($Arx^{X/Y}$ $Emx1^{Cre/Cre}$). Cleaning wipes (PDI Sani-Cloth Plus germicidal disposable cloth) were used to clean equipment between mice. With the exception of grip strength and rota-rod, all paradigms were video recorded and automatically scored using ANY-maze software (Stoelting Co., Wood Dale, IL).

Grip Strength

The grip strength of the mice was tested using a grip strength meter (080312-3 Columbus Instruments, Columbus, Ohio). Each mouse was tested in 6 consecutive trials; the first 3 were for forelimbs, and then 3 more for hindlimbs. The value from each trial was recorded and the forelimb and hindlimb trials were each averaged and taken as the result for that mouse. (Golub MS and SL Germann 2001; Fowler SC et al. 2002; Munn E et al. 2011) The results for all mutant mice and their wild type littermates were compared using a two-tailed unpaired Student's t-test in Excel; WT=13 and Mut=14.

Rota-rod

Mice were tested on a rota-rod from Ugo Basile (Model 47600, Comerio, Italy). The mice were tested in groups, 5 at a time for 6 minute trials with 5 trials per day for 4 days. The rota-rod was used in acceleration mode, accelerating every 6 seconds up to 60 rpm. The latency until falling for each mouse was recorded. Between trials the mice

were placed back into their home cages. (Crawley JN 2007; Miwa JM and A Walz 2012; Heyser CJ et al. 2013) Each day, the trials were averaged and the genotypes were compared across the four days using a repeated measure ANOVA in Prism (version 5.0, GraphPad, San Diego, CA); WT=13 and Mut=14.

Home Cage Activity

Mice were placed in plastic EEG recording boxes (Marsh E et al. 2009) with their normal bedding and food and were allowed to acclimate for 2 days before being video recorded for 3 days. The video was analyzed using an in-house program written in MATLAB that detects movement by subtracting pixels between each video. The pixel counts were averaged over the 3 days of recordings for each genotype. The genotypes were compared using a Student's t-test in Excel; WT=8 and Mut=8.

Open Field

A 53 x 53 cm plastic box with 22cm high walls and no top was used in a well-lit room (450 lumens/meter^2). The mice were placed in the center of the box and allowed to roam freely in the box for 15 minutes. The mice were video recorded and scored using ANY-maze software. ANY-maze scored a mouse to be in the periphery if it was within 13cm of the wall of the box. Otherwise they were considered to be in the center of the box. (Crawley JN 2007; Buschert J et al. 2013; Han Q et al. 2013) The ratio of time in the center to time in the periphery was calculated and averaged. The distance traveled during the test and the number of crossings between the center of the box and the periphery were also calculated and averaged using the ANY-maze software. Genotypes

were compared using a two-tailed unpaired Student's t-test in Microsoft Excel version 12.2.7; WT=20 and Mut=21.

Light/Dark Box

A 55 x 28cm plastic box with 22cm tall walls and divided in half was used. Both sides of the box were accessible by a 7.5 x 7.5cm door in the middle. One half of the box was clear with no top and the other half was black plastic with a covered top. The mice were placed in the box on the light side and allowed to roam freely for 15 minutes. The tests were video recorded and scored using ANY-maze software. (Bale TL et al. 2000; Bourin M and M Hascoet 2003; Crawley JN 2007) The ratio of time in the light side of the box to time in the dark side was calculated and averaged for each genotype and compared using a two-tailed unpaired Student's t-test in Excel. The linear distance the animal traveled during the test and the number of crossings between the two sides was also calculated and analyzed the same way; WT=17 and Mut=14.

Marble Burying

A clear plastic cage, 32 x 43cm, with 19cm high walls was filled with 5cm deep corncob bedding evenly covering the bottom. Twenty-four marbles, spaced 6cm apart, were placed evenly on top of the bedding. The mice were placed in the box and allowed to roam freely and bury marbles for 30 minutes. After 30 minutes, the number of marbles buried at least two thirds of the marble's depth with bedding was recorded. (Deacon RM 2006; Krass M et al. 2010; Chioca LR et al. 2013) The tests were video recorded and scored for distance traveled using ANY-maze software. The number of marbles buried,

and the distance traveled was calculated and averaged for each genotype and compared using a two-tailed unpaired Student's t-test in Excel; WT=8 and Mut=8.

Morris Water Maze

The Morris water maze consists of a 128cm diameter round plastic tub filled with 21°C water to within 15cm of the top of the tub and a 0.5 cm above a square clear plastic platform. White tempera paint was mixed into the water until it was opaque enough that the edge of the platform could not be seen from the side. Spatial cues were placed around the tub and were not moved for the duration of the experiments. The mice were tested using 4 trials per day for 5 days. The mice were placed in the tank in a different location for each trial and the order of locations was changed each day (see (Vorhees CV and MT Williams 2006) and Chapter 3;Table 1). In each trial mice were allowed to swim for up to 60 seconds before being led to the platform. Once on the platform, the mice were allowed 10 seconds of observation time. The latency to find the platform (up to 60 seconds) for each trial was recorded and averaged for each day. The genotypes were compared using a repeated measures ANOVA in Prism. On the 6^{th} day a probe trial was performed to test the memory of the location of the platform. In this trial, the platform was removed and the mice swam around the tub, searching for the missing platform for 60 seconds. The time spent in the quadrant of the tub where the platform had been and in the opposite quadrant was recorded and compared using an unpaired Students t-test. A reversal test was then performed for 5 days following the probe trial. During this test, the platform was placed on the opposite side of the tub and the mice were re-trained, with the same protocol of 4 trials a day for 5 days. A reversal probe trial was performed on the 6^{th}

day in the same fashion as the first probe trial. (Crawley JN 2007; Harris L et al. 2013) The same statistical analysis was performed for the reversal trials as for the learning test; WT=20 and Mut=21.

Contextual Fear Conditioning

Each mouse was placed in a modular test chamber (Model ENV-307W, Med Associates, Inc., Georgia, VT) and allowed to explore the box for 2 ½ minutes before a 2 second foot shock of 1.12 mA was given with a SA shock scrambler (ENV-4145), a digital timer (SG-592), and a 1 Amp power supply (SG-501 Med Asoociates, Inc., Georgia, VT). The mouse was then left in the box for another 28 seconds before being removed to its home cage. Twenty-four hours later the mouse was placed in the same modular test chamber and was video recorded for 5 minutes using ANY-Maze software, which quantified time spent not moving (freezing). (Wood MA et al. 2005; Crawley JN 2007; Cole JT et al. 2010) The amount of time spent freezing was compared across genotypes using an unpaired Student's t-test; WT=17 and Mut=14.

Social Choice Test

A social choice apparatus was constructed from the description by Sankoorikal (Sankoorikal GM et al. 2006). The bottom of the chamber was covered with bedding and that bedding was changed for each mouse tested. The protocol used to test the mice was the same as the one used in Fairless et al. 2008. Briefly, the mice were first acclimated to the chamber for 10 minutes. Then a novel object was added to one tube and a gonadectomized male mouse to the other tube and the behavior of the test mouse was recorded for 5 minutes. The tubes were then removed and the behavior of the test mouse

while interacting with the gonadectomized mouse was observed for another 5 minutes, unless the mouse was aggressive in which case both mice were removed immediately. The test mouse was then returned to its home cage. A single novel object was used for all tests and was cleaned, along with the apparatus before each test. Each gonadectomized male was used only once per day. The side of the chamber that had the mouse or the object was alternated between tests. (Nadler JJ et al. 2004; Crawley JN 2007) The tests were video recorded and scored using ANY-maze software. The time spent in the social section, the center, and the non-social section was compared using a Two-way ANOVA in Prism. The ratio of the amount of time spent within 3cm of the tube with the mouse (sniffing social tube) verses the time spent within 3cm of the tube with the object (sniffing object tube) was calculated and averaged for each genotype and compared using a Student's t-test in Excel. The number of entries to either the social section of the box (mouse) or the non-social section of the box (object) was also calculated and compared across genotypes; WT=15 and Mut=18.

Buried Food Test of Olfaction

For 2 days prior to the test each mouse was given a Froot Loop (Kellogg's® *Froot Loops*® Cereal) in its cage and the next day the cage was checked to make sure they ate the Froot Loop. Mice were then deprived of food for 24 hours. The next day a Froot Loop was buried in 1.5 cm deep bedding in a clean normal mouse cage with nothing else but the top of the cage. A mouse was placed in the cage and the time to dig up the piece of food documented, up to 10 minutes. (Moy SS et al. 2004; Crawley JN 2007; Yang M

and JN Crawley 2009) The average time for each genotype was compared using an unpaired Student's t-test; WT=8 and Mut=8.

In Situ Hybridization

P21 and P30 mice were perfused transcardially with phosphate buffered saline (PBS) followed by 4% paraformaldehyde (PFA). The brains were removed and post fixed in 4% PFA overnight at 4°C. Fixed brains were cryoprotected in 30% sucrose and coronally sectioned at 10um. All slides were baked at 65°C for 20 minutes, post-fixed in 4% PFA for 10 min, washed in phosphate buffered saline with 0.1% Tween-20 (PBT). The slides were then acetylated for 10 min in 0.1 M TEA (1.86% triethanolamine, 0.4% 10N NaOH, 0.5% acetic anhydride, and water) and washed in PBT. The Glutamate decarboxylase 67 (GAD67) probe (courtesy of Dr. N. Tillakaratne (Erlander MG et al. 1991)) was added at 1:1000 in pre-warmed hybe solution (50% formamide, 5x SSC, 2% blocking reagent (Roche, Mannheim, Germany; 11096176001), 0.1% Triton, 0.15 CHAPS, 1mg/ml tRNA from yeast, 5mM EDTA, 50ug/ml heparin) and incubated overnight at 65°C. Slides were washed with 5x SSC, then incubated with 1xSSC/ 50% formamide 30 minutes at 65°C, then TNE (10mM Tris pH 7.5, 500nM NaCl, 1mM EDTA, and water) for 10 minutes at 37°C, then RNaseA for 30 min at 37°C and washed with TNE and then at 65°C with 2x SSC and 0.2x SSC for 20 min, each. Then the slides were incubated in MABT pH 7.5 (100mM maleic acid, 150mM NaCl, 0.1%tween-20, and water) and blocked in MABT with 2% blocking reagent (Roche) and 20% goat serum for 1 hour at room temperature. Slides were incubated overnight at 4°C in MABT with 2% blocking reagent and 5% goat serum and anti-DIG antibody 1:2500 (Roche,

11093274910). The slides were then washed with MABT and then NTM. The slides were then incubated with 1ml BM Purple (Roche, 11442074001) in the dark, overnight at room temperature. The slides were then washed with NTM and PBS, fixed in PFA, dehydrated to 100% ethanol, and mounted with Permount (SP15-500, Fisher Scientific).

Immunohistochemistry

P21 mice were processed as described in *in-situ* section above. The brains were cryoprotected in 30% sucrose and cryosectioned coronally at 10um or 16um. All slides were baked at 37°C for 30 minutes. Two antibodies, Somatostatin (SST; Rabbit 3387-1, Epitomics, Burlingame, CA; 1:50) and Parvalbumin (Parv; Mouse MAB1572, Millipore, Billerica, CA; 1:100) were used to assess for changes in interneuron subtypes. For the *Sst* antibody, antigen retrieval was performed in citric acid-based Antigen Unmasking Solution (H-3300, Vector Laboratories, Burlingame, CA) autoclaved at 105°C for 20 minutes. For the *Parv* antibody the MOM blocking reagent (FMK-2201, Vector Laboratories) was used for 30 minutes followed by blocking for 30 minutes with 10% normal goat serum (Sigma) in TBST (TBS with 0.5% triton) all at room temperature. After antigen retrieval, SST sections were blocked for 30 minutes at room temperature with 0.5% normal goat serum (Sigma) in TBST. Anti *Parv* primary was diluted in 1% normal goat serum in TBST and Anti-*Sst* was diluted in 0.5% normal goat serum in TBST and incubated on slides overnight at 4°C. The secondary antibodies used were a biotinylated goat anti-mouse (BA-9200, Vector Laboratories, 1:300) and biotinylated goat anti-rabbit (BA-1000, Vector Laboratories, 1:300), diluted in TBST and placed on slides for 30 minutes at room temperature. The biotinylated secondary antibodies were

subsequently incubated with ABC kit mix (PK-6100, Vector Laboratories) in PBS for 30 minutes and then ImmPACT DAB for 2 minutes (SK-4105, Vector Laboratories). Slides were counterstained with hematoxylin, dehydrated, and mounted with Permount. Stained sections were viewed on a Leica DM6000B equipped with a Leica DFC360FX digital camera. 10X images were taken of the entire cortex for each section and then stitched together using Fiji version ImageJ 1.45b.

Nissl Staining

Cresyl Violet acetate (C5042, Sigma-Aldrich) (0.1g) was mixed with 100 mL distilled water. To each 10ml of Cresyl Violet acetate solution 50μL of 15% glacial acetic acid was added and the solution was filtered to make Nissl stain. Cryosections were covered in Nissl stain for 10 minutes and then washed 2 times with distilled water. The sections were destained by dipping them once in acid alcohol (50% ethanol/50% distilled water with 0.1% HCl). Slides were mounted with Flouromount-G (0100-01, SouthernBiotech) and imaged the same as the immunohistochemistry sections.

Cell Counting

For the GAD67 counts a 1mm area of the cortex from the pial surface to the white matter directly above the hippocampus (2mm posterior to Bregma) and 2mm from the medial edge of the cortex was counted. For the basolateral amygdala counts all of the Nissl stained neurons in the basolateral amygdala (2.1mm posterior to Bregma) were counted. Cell counts were averaged for each genotype and compared using an unpaired Student's t-test.

MRI

Adult mice brains were processed as described above, and then post-fixed in 4% PFA for 2 weeks. Prior to MRI the samples were transferred to a PBS 1X solution containing 0.2mM Gd-DTPA (Gadopentetic acid)(J140 Omniscan GE Healthcare). At the time of scanning the samples were removed from the PBS/Gd-DTPA solution, rinsed with pure PBS and introduced in a short 11 mm glass tube containing Fomblin (317993 Sigma-Aldrich) to provide a susceptibility match and a black background for the images. Bubbles were carefully removed by tapping gently on the tube. An inverted Pasteur pipette was inserted on top of the brain to maintain the tissue immersed in the Fomblin. MRI was performed at 9.4T in a vertical bore magnet (Avance III Bruker-Biospin Inc) using the micro 2.5 self-shielded gradients (2.5G/cm/A) and a 15 mm RF coil. The image acquisition and reconstruction was performed with the Paravision software 5.1 (Bruker Biospin Inc.). The temperature of the sample was maintained at 37C. Diffusion tensor images and T2 weighted 3D images of the brain tissue were obtained sequentially with the DTIEpi 30 directions and the 3D turboRARE Bruker protocols respectively. The following conditions were used: for the DTI, field of view (FOV) 20 x 12.8 x 10 mm, data size (SI) 128x80x64, which results in a resolution of 160 m^3, number of averages (NEX) 2, repetition time (TR) 1250 ms, echo spacing (Te) 26 ms, 8 segments, bandwidth 300kHz, diffusion gradients 3ms, diffusion gradient separation 7.53ms, 30 directions, 5 A0 images and a B value of 1500 $s.mm^2$. The duration of the acquisition was 12h 26 min. For the 3D rare the parameters were FOV 19.2 x 12.8 x 9.6 mm, SI

256x176x128, giving a resolution of 75 m^3, 5 NEX, TR 1500 ms, Te 13 ms, echo train 8 which results in an average echo time of 39 ms and a 5h long experiment. To analyze the T2 weight images for volume data on specific brain regions. We used a registration-based segmentation method to extract various structures in T2-weight MR images of mouse brains. A mouse brain atlas with accompanying labels of structures of interest was registered to the target image. We adapted the mouse atlas from Johns Hopkins University, which is available to the public (http://cmrm.med.jhmi.edu/). Registration was aligned followed by non-rigid diffeomorphic warping using Advanced Normalization Tools (ANTs), which is an open-source software freely available online. The labels were also transformed to the target space by the same warping and thus completed the segmentation.

Results:

Arx$^{-/Y}$ *Emx1*^{Cre} mutant mice have normal numbers of interneurons

We previously found that *Arx*$^{-/Y}$ *Emx1*^{Cre} mice have reduced numbers of upper cortical layer neurons with relative sparing of neurons in the deeper layers (Colasante G et al. 2013). *Arx* expression was preserved in the developing ventral telencephalon and in the interneurons migrating from the ganglionic eminence to the cortex (Colasante G et al. 2013). Several studies have found that changes in the development of cortical excitatory neurons can affect interneuron migration into the cortex (Sessa A et al. 2010; Lodato S et al. 2011). Therefore, to confirm that cortical interneurons were not adversely affected by the loss of upper layer neurons we first assessed the total number of interneurons using a

GAD67 *in situ* hybridization probe on sections from brains of P21 $Arx^{-/Y}$ $Emx1^{Cre}$ (mutant) mice and their wild type littermates ($Arx^{X/Y}$ $Emx1^{Cre}$). Similar numbers of interneurons were found in the mutant brains when compared to wild type brains (Chapter 3;Fig. 1B,C; WT= 137.3±5.84 and Mut=124±2.65; n=3 for each; p=0.1359).

We next sought to exclude the possibility that while the total number of interneurons was unchanged, subtypes of interneurons were disproportionately represented (Azim E et al. 2009). Labeling for two interneuron subtypes, parvalbumin and somatostatin, which together mark 50-70% of all cortical interneurons (Xu X et al. 2010; Rudy B et al. 2011), revealed both types to be similarly represented (parvalbumin WT=50±5 and Mut=53±2; n=3 for each; p=0.6575; somatostatin WT=37±7.23 and Mut=29±2.89; n=3 for each; p=0.3897)(Chapter 3;Fig. 1C). Thus, both the total number and representative subtypes of interneurons were unaltered by the loss of *Arx* from the dorsal telencephalon.

$Arx^{-/Y}$ $Emx1^{Cre}$ mice do not have seizures

Patients and mice with *ARX/Arx* mutations have seizures as a principle feature. The conditional loss of *Arx* from developing interneurons in the ventral telencephalon ($Arx^{-/Y}$ $Dlx5/6^{Cre}$) results in a severe seizure phenotype (Marsh E et al. 2009). Furthermore, mice with a polyalanine track expansion mutation or with a point mutation in the homeobox also have seizures (Kitamura K et al. 2009; Price MG et al. 2009). To determine if the loss of *Arx* from the cortical projection neuron progenitor pools ($Arx^{-/Y}$ $Emx1^{Cre}$ mice) is also associated with seizures, video-EEGs were recorded for up to 96 hours following our previously published protocol (Marsh E et al. 2009). Review of up

to 96 hours of EEG and video recordings from 8 mutant mice and 6 control animals revealed no seizures in the either the mutant or control mice. However, there were differences that were observed in the EEG (Chapter 3;Fig. 1A). Qualitatively, the EEG appeared to be slower in the $Arx^{-/Y}$ $Emx1^{Cre}$ mice than the wild type mice (Chapter 3;Fig. 1A). To confirm our visual interpretation, we performed a Fast Fourier Transforms (FFTs) on randomly selected awake and sleep EEG segments in the cortex from 6 control and 4 mutant mice. An increase in Delta (Awake: WT=23.50±4.34 and Mut=29.69±4.85 p=0.0036, Sleep: WT=22.19±3.84 and Mut=31.77±3.84 $p=2.3x10^{-8}$) and decrease in Alpha or Beta (Awake; Alpha: WT=9.28±0.77 and Mut=11.06±1.53 p=0.0017; Sleep; Beta: WT=16.88±1.00 and Mut=14.20±1.24 $p=9.2x10^{-7}$) and Gamma (Awake: WT=32.08±3.92 and Mut=24.83±2.89 $p=9.1x10^{-6}$; Sleep: WT=30.96±3.11 and Mut=24.16±2.46 $p=4.7x10^{-6}$; WT n=6 and Mut n=4) power was present during both sleep and awake states (Chapter 3;Fig. 1B). Similar, results were seen in the FFTs for the hippocampal recordings (Chapter 3;Fig2A,B). Interestingly, this change in EEG frequency content is the opposite from the $Arx^{-/Y}$ $Dlx5/6^{Cre}$ mice, which had an increase in faster (Beta and Gamma) activity (Marsh E et al. 2009).

$Arx^{-/Y}$ $Emx1^{Cre}$ mutant mice have normal spatial learning and memory

An invariant feature among males with an *ARX* mutation is a severe intellectual disability (Shoubridge C et al. 2010). To investigate whether the $Arx^{-/Y}$ $Emx1^{Cre}$ mice had intellectual disabilities we performed several learning and memory tests. Prior to performing these tasks, physical strength and coordination defects were evaluated and excluded. Grip strength and rota-rod testing revealed no differences between the $Arx^{-/Y}$

Emx1^{Cre} mice and their wild type littermates (Chapter 3;Fig. 3A,B Grip strength: Forelimb: WT= 0.042±0.0033, n=13 and Mut=0.052±0.0053, n=12; p=0.1030; Hindlimb: WT= 0.079±0.0055, n=13 and Mut=0.082±0.0044, n=12; p=0.3447; Rota-rod: WT n=13 and Mut n=12; p=0.0801). Thus, no motor deficits were uncovered suggesting the mutant mice should have normal physical capabilities.

Once a motor abnormality was excluded, the Morris water maze test was performed to assess spatial learning and memory. The mice were first trained with spatial cues around the tank and the platform hidden. There was no difference in learning the task as both mutant mice and wild type littermates located the platform in similar times each day of training (Chapter 3;Fig. 4A; WT n=20 and Mut n=21; p=0.0669). Next, memory for the platform location was probed by recording the time spent in the original quadrant of the platform after the platform was removed (Chapter 3;Fig. 4B). Again, there was no difference found between the mutant and wild type mice (Chapter 3;Fig. 4B: Time (secs) in platform quadrant: WT=22.8±1.47 and Mut=25.6±1.97; p=0.271; Time in opposite quadrant: WT=9.61±1.07, n=20 and Mut=7.7±1.28, n=21; p=0.256). Finally, reversal learning and memory testing, which is a more sensitive indicator to changes in cortical function, was tested by relocating the platform to the opposite side of the tank. No differences were noted in this measure of cortically-mediated learning (Chapter 3;Fig. 4C; WT n=20 and Mut n=21; p=0.1545) or memory (Chapter 3;Fig. 4D: Time (secs) in platform quadrant: WT=19.5±0.87 and Mut=19.9±1.33; p=0.762; Time in opposite quadrant: WT= 11.7±0.85, n=20 and Mut=11.7±1.02, n=21; p=0.997). Thus, by the highly-standardized and accepted Morris water maze paradigm the *Arx*$^{-/Y}$ *Emx1*^{Cre} mice exhibit normal spatial learning, memory, and reversal learning.

Arx$^{-/Y}$ *Emx1*^{Cre} mutant mice have normal fear memory, but are hyperactive

In some mutant mouse strains hippocampal based spatial learning and memory can be normal despite alterations in other forms of learning such as fear conditioning learning because the hippocampus is not as involved in this type of learning (Angelo M et al. 2003; d'Isa R et al. 2011; Albarran-Zeckler RG et al. 2012). To test whether the *Arx*$^{-/Y}$ *Emx1*^{Cre} mutant mice had a learning and memory deficit independent of spatial learning, we tested the animals in a conditioned fear-learning task. The mutant mice spent significantly less time freezing than their wild type littermates did both during the training session and during the testing session (Chapter 3;Fig. 4E: percentage of time spent freezing training: WT=10.5±1.06, n=17 and Mut=5.57±0.82, n=14; p=0.00099; percentage of time spent freezing testing: WT=52.1±3.65, n=17 and Mut=34.4±4.99, n=14; p=0.0086). This suggests that the mutant mice are hyperactive; a finding confirmed by the longer distances travelled by the mutant mice than their wild type littermates during the testing session (Chapter 3;Figure 5A: distance traveled: WT=2.43±0.42, n=17 and Mut=4.00±0.49, n=14; p=0.0217). The ratio of the percentage of time spent freezing during the training session verses the testing session indicated that the mutant mice learn the contextual fear conditioning just as well as their wild type littermates (Chapter 3;Figure 5B: ratio of percentage of time spent freezing traing/testing: WT=5.36±0.43, n=17 and Mut=6.80±1.31, n=14; p=0.3097).

$Arx^{-/Y}$ $Emx1^{Cre}$ mutant mice are anxiolytic, more exploratory, and more active than wild type mice.

Surprisingly, no learning deficit was uncovered but there was a suggestion of a more active state, therefore we further examined the mutants exploratory and anxiety behaviors. To evaluate the anxiety level of the $Arx^{-/Y}$ $Emx1^{Cre}$ mutant mice open field and light/dark box tests were used. For the open field test, mice with a higher ratio of the time spent in the center to time spent in the periphery of the chamber are considered to have a low anxiety-like or anxiolytic phenotype. Mutant mice appeared anxiolytic as they spent significantly more time in the center of the box compared to their wild type littermates (Chapter 3;Fig 6A: WT= 0.170±0.019, n=20 and Mut=0.229±0.020, n=21; p=0.0405). For the light/dark box, testing the ratio of time spent on the light side of the box compared to the time on the dark side of the box was used as a measure of anxiety. Again, the mutant mice spent significantly more time on the light side when compared to their wild type littermates suggesting a reduced anxiety-like phenotype (Chapter 3;Fig 6C: WT= 0.891±0.118, n=17 and Mut=1.61±0.202, n=14; p=0.00204).

Both the open field and light/dark box tests can also be used to quantify the activity level of mutant mice. In both, the mutant mice travelled further than their wild type littermates indicating a higher activity level in the mutant mice (Chapter 3;Fig. 6B,D: Open field: WT= 65.9±3.02 cm, n=20 and Mut=77.6±3.79 cm, n=21; p=0.0201; Light/dark box: WT= 12.2±0.867 cm, n=17 and Mut=20.2±1.13 cm, n=14; p=0.000007). Similarly, the mutant mice crossed between the light and dark side of the box and between the center and the periphery of the open field, which also indicates higher

activity (Chapter 3;Fig. 7A,B: Open field: WT=117±6, n=20 and Mut=158±8, n=21; p=0.0000863; Light/dark box: WT= 28±1, n=17 and Mut=40±4, n=14; p=0.00143). However, the mutant mice displayed normal activity levels in home cage recordings so they appear to be more active only in novel environments (Chapter 3;Fig 3C: WT=13.75±1.73 Δ pixels/frame, n=8 and Mut=12.59±1.84, n=8; p=0.5191).

Since our data suggests that the *Arx*$^{-/Y}$ *Emx1*^{Cre} mice are both anxiolytic and more active in both the open field and the light/dark box tests, we wanted to determine whether the increased activity was confounding our anxiety test results. Therefore, we performed a marble burying test, another anxiety test, but one in which less activity constitutes lower anxiety (Thomas A et al. 2009). We found that the mutant mice buried significantly fewer marbles then the wild type animals (Chapter 3;Fig. 6E: WT= 6.13±1.25, n=8 and Mut=0±0, n=8; p=0.00759) yet they were still hyperactive based on distance traveled in the novel cage (Chapter 3;Fig. 6F: WT= 85.34±2.10cm, n=8 and Mut=93.42±5.94cm, n=8; p=0.2322), similar to the open field and light dark box. This indicates that although still hyperactive in a novel environment, they were less anxious than their wild type littermates. Together, the data suggests that the anxiety and hyperactivity phenotypes are separable and the *Arx*$^{-/Y}$ *Emx1*^{Cre} mice are both less anxious and hyperactive when compared to their wild type littermates.

Arx$^{-/Y}$ *Emx1*^{Cre} mutant mice have social deficits

One of the core symptoms of autism is abnormal social interactions (Crawley JN 2007; Silverman JL et al. 2010). To test for the mice for "social" deficits we performed the social choice task (Crawley JN 2007; Silverman JL et al. 2010). In the social choice

task the test mouse is given a choice between a novel object and novel mouse. As mice are normally social animals they should typically spend more time exploring a novel mouse then a novel object. Therefore, we compared the time spent in the area of the novel mouse (social), the time spent in the center, and the time in the section with the novel object (nonsocial) (Sankoorikal GM et al. 2006; Fairless AH et al. 2008). The *Arx*$^{-/Y}$ *Emx1*^{Cre} mutant mice appear to have a socialization deficit as they spent significantly less time in the social section of the box (Chapter 3;Fig. 8A; Time spent in social section: WT= 142.07±8.54, n=15 and Mut=111.37±4.28, n=18; $p<0.001$). In addition, the mutant mice entered the social section of the box significantly fewer times as compared to the wild type mice (Chapter 3;Fig. 8B; WT= 2.97±0.50, n=15 and Mut=1.44±0.14, n=18; p=0.00952). Similarly mutant mice spent significantly less time sniffing around the novel mouse verse the novel object than their wild type littermates did (Chapter 3;Fig. 8B; WT= 4.53±0.80, n=15 and Mut=2.15±0.18, n=18; p=0.01379).

The olfactory ability of the mice was tested using the buried food test in order to rule out the possibility that reduced olfactory ability was confounding the social choice test. Both the mutant mice and their wild type littermates found the buried Froot Loop in similar amounts of time showing that the mutants have normal olfactory skills (Chapter 3;Fig 8C; WT=143.38±34.86 and Mut=242.13±79.60, n=8 for each; p=0.2834).

Arx$^{-/Y}$ _Emx1_^{Cre} mutant mice have smaller cerebral cortices, amygdalas, and white matter tracts

In addition to the neurocognitive and behavioral deficits patients with various *ARX* mutations exhibit, structural defects such as lissencephaly, agenesis of the corpus

callosum and microcephaly are present in many patients (Suri M 2005; Friocourt G et al. 2006; Gecz J et al. 2006). In an effort to begin linking the structural defects with the neurocognitive deficits we examined regional size variation and connectivity. Using structural MRI in fixed *Arx*$^{-/Y}$ *Emx1*^{Cre} and wild type mouse brains the volume of various brain structures was calculated (Chapter 3;Fig. 9). As observed in Nissl stained sections the cerebral cortical volume was significantly smaller in the mutant mouse (Colasante G et al. 2013)(Chapter 3;Fig. 9A,C,E). The MRIs also revealed the corpus callosum and anterior commissure to be significantly reduced in volume, as is also found in patients with various *ARX* mutations (Proud VK et al. 1992; Bonneau D et al. 2002; Marsh E et al. 2009)(Chapter 3;Fig. 9A,C,D,E). However, analysis of the MRIs also reveled that the amygdala volume was significantly smaller in the mutant mice (Chapter 3;Fig. 9E). It is possible that there are changes to the amygdala in the *Arx*$^{-/Y}$ *Emx1*^{Cre} mice since both *Arx* and *Emx1* are expressed in the amygdala (Puelles L et al. 2000; Medina L et al. 2004; Poirier K et al. 2004; Remedios R et al. 2007). To confirm this finding, we counted neurons in the basolateral amygdala in Nissl stained sections and found that the number of neurons was reduced (Chapter 3;Fig. 10C; WT=1118±124 and Mut=891±152, n=3 for each; p=0.01952). Interestingly, the behavioral phenotypes of decreased anxiety and loss of fear memory have been hypothesized to represent amygdala dysfunction (Phillips RG and JE LeDoux 1992; Grillon C et al. 1996; Tottenham N et al. 2010; Schienle A et al. 2011). Combining the MRI volume changes with the loss of cells in the basolateral amygdala suggest that amygdala dysfunction could explain at least part of the *Arx*$^{-/Y}$ *Emx1*^{Cre} behavioral phenotype. Over all, the MRI data are consistent with the hypothesis that the *Arx*$^{-/Y}$ *Emx1*^{Cre} mutant mice have a long-range connectivity defect. Unexpectedly

the thalamus was also significantly smaller in the mutant mice even though the *Cre* is not expressed in the diencephalon, suggesting a possible corticothalamic connectivity defect (Chapter 3;Fig. 9E) that could contribute to the abnormal behaviors found in these mice.

Discussion:

Loss of *Arx* in dorsal progenitors resulted in structural, functional and behavioral deficits in the $Arx^{-/Y}Emx1^{Cre}$ mice. Specifically, we demonstrated that disruption of both local superficial cortical connections, long-range connections between hemispheres and within limbic regions results in a hyperactive and anxiolytic mouse that socializes poorly. Of note, these behaviors all occur in the absence of ongoing epilepsy as a confounding variable. By comparing the deficits in the $Arx^{-/Y}Emx1^{Cre}$ mice to those of the previous *Arx* mutant mice and the clinical phenotype of *ARX* patients we can begin to shed some insight into the possible function of different cortical regions, connections, and the lack of a role for seizures in generating the behaviors found in the *Arx/ARX* mice and patients.

The complete *Arx* knockout mouse created by the Kitamura lab had a thin cortex due to decreased cortical progenitor proliferation during development (Kitamura K et al. 2002). Loss of *Arx* expression in the cortical VZ at e13.5 causes cortical progenitor cells to exit the cell cycle and the VZ prematurely (Friocourt G et al. 2008). Our lab recently determined that $Arx^{-/Y}Emx1^{Cre}$ mice have thinner and smaller cortices and are specifically missing superficial layer neurons and not deeper layer neurons (Colasante G et al. 2013). A loss of proliferative intermediate progenitor cells was found to be the cause of the thinner cortex (Colasante G et al. 2013). Unlike most other *Arx* mutant mice, these mice

do not die at a young age, likely because they do not develop seizures (Chapter 3;Fig. 1A) and have intact olfaction allowing for normal feeding behaviors. Consistent with a lack of seizures, $Arx^{-/Y}Emx1^{Cre}$ mice have normal numbers of interneurons in their cortices (Chapter 3;Fig. 1B). Therefore, we wanted to examine the behavioral phenotype of these mice to determine the impact on cognitive functioning of isolated loss of upper layer neurons, without the complicating factors of interneuron loss and seizures as found in all other *Arx* mutant mice models.

Intellectual disability is the common feature of all human *ARX* mutations. To determine what aspects of the human condition the $Arx^{-/Y}Emx1^{Cre}$ mice recapitulate, we tested learning and memory. Somewhat surprisingly, the Morris water maze test did not reveal any abnormalities in spatial learning and memory and the contextual fear conditioning test did not reveal any abnormalities in fear learning and memory (Chapter 3;Fig. 4A-E). This contrasts to the $Arx^{(GCG)7/Y}$ mice and the $Arx^{PL/Y}$ mice which showed impaired spatial learning in the win-shift task of the eight-arm radial maze and impaired passive avoidance learning (Kitamura K et al. 2009). The $Arx^{(GCG)7/Y}$ mice also showed impaired procedural learning in the win-stay task (Kitamura K et al. 2009). Another $Arx^{(GCG)10+7}$ mouse also showed impaired learning of the fear conditioning task (Price MG et al. 2009). These data indicate that the learning deficits seen in the other *Arx* mutant mice might be due to, either individually or in combination, the of loss of interneurons in the cortex and the hippocampus or the seizure activity they exhibit.

The $Arx^{-/Y}Emx1^{Cre}$ mice registered less anxiety-like behavior and increased exploration as evidenced by their spending significantly more time in the center of the

open field and in the light part of the light/dark box than their wild type littermates (Chapter 3;Fig. 6A and B). In addition, the mice were hyperactive, having travelled a further distance during both tests (Chapter 3;Fig. 6B and D). These findings are similar to the $Arx^{(GCG)10+7}$ mice that also were reported to have a low anxiety and hyperactivity phenotype (Price MG et al. 2009). However, other *Arx* mutant mice ($Arx^{(GCG)7/Y}$ and $Arx^{PL/Y}$ mice) were more anxious in the same tests (Kitamura K et al. 2009). Based upon these varying results, no conclusions can be made regarding the relationship of these behavioral phenotypes to alterations in excitatory or inhibitory interneurons of the cortex or seizure burden. These changes in anxiety in *Arx* mutant mice could also be explained by changes in the amygdala, which was not investigated in any of the other *Arx* mutant mice, but do exist in the $Arx^{-/Y}\,Emx1^{Cre}$ mutant mouse.

Autistic features, including social deficits and stereotypies, have been described in patients with *ARX* mutations (Turner G et al. 2002; Shoubridge C et al. 2010). The $Arx^{-/Y}\,Emx1^{Cre}$ mice appear to have social deficits in the social choice test (Chapter 3;Fig. 8A). This is similar to the $Arx^{(GCG)10+7}$ mice for which there was a reported deficit in the tube test for social dominance (Price MG et al. 2009). This suggests that the autistic phenotypes of these mice could be due either to changes in the excitatory neurons of the cortex, amygdala or the connections between the two.

$Arx^{-/Y}\,Emx1^{Cre}$ mice have decreased cerebral cortical and amygdala volumes, which can be correlated with the behavioral phenotypes of decreased anxiety-like behavior, hyperactivity, and social deficits. The cortical defect described in these mice (Colasante G et al. 2013) is one explanation for these behavioral findings. Another

possible rationale for these behavioral deficits is defects in the amygdala structure as indicated by the volume and neuron number changes. The combined or separate roles of these two brain structures in mediating these behavioral functions requires further investigation. The white matter tract abnormalities (including the corpus callosum, the anterior commissure, and possibly the cortico-thalamic tract) suggest a loss of long-range connectivity between different brain regions in these mutant mice. Agenesis of the corpus callosum was reported in the Arx knockout mice, but not in the $Arx^{(GCG)10+7}$, $Arx^{(GCG)7/Y}$, $Arx^{PL/Y}$, or $Arx^{PR/Y}$ mice (Kitamura K et al. 2002; Kitamura K et al. 2009; Price MG et al. 2009). It has also been documented in some *ARX* patients with XLAG or Proud syndrome and heterozygous females from families with these syndromes (Proud VK et al. 1992; Bonneau D et al. 2002; Marsh E et al. 2009). In contrast, corpus callosum agenesis has been seen in both severely affected males and in unaffected carrier females making it unlikely for corpus callosal defects alone to be the primary mechanism of the behavioral deficits seen in mice and patients.

The differences in the frequency composition of the EEG between the $Arx^{-/Y}$ $Emx1^{Cre}$ and wild type mice were reminiscent of the slow background and increase in Delta activity that is present in most children with a diffuse encephalopathy, including children with *ARX* mutations. Though nonspecific, a slow EEG background suggests diffuse brain dysfunction as might be expected in a cortical layer defect (Pedley TA 1980). Interestingly, the composition of the EEG in the $Arx^{-/Y}$ $Emx1^{Cre}$ and $Arx^{-/Y}$ $Dlx5/6^{Cre}$ are different, with the interneuron specific mouse ($Arx^{-/Y}$ $Dlx5/6^{Cre}$) gaining faster frequency activity and the excitatory neuron specific mouse ($Arx^{-/Y}$ $Emx1^{Cre}$) gaining slower activity (Marsh E et al. 2009). This difference supports the notion that

interneurons and subcortical structures are necessary for the generation of Theta and Gamma oscillations, and local cortical networks are not (Bragin A et al. 1995; Whittington MA et al. 2011).

The absence of seizures in the *Arx*$^{-/Y}$ *Emx1*^{Cre} mice provided a unique opportunity to separate out the basic structural and cellular deficits from the resulting seizures on a variety of behavioral phenotypes. Neurologists question the ultimate role of seizures in generating the cognitive deficits in their patients (Shinnar S and WA Hauser 2002; Hamiwka LD and EC Wirrell 2009; Hermann BP et al. 2009). These studies demonstrate that for *ARX* related disorders, alterations in anxiety, hyperactivity, social deficits, and repetitive behaviors could be unrelated to the epilepsy. Indeed, the absence of epilepsy, altered anxiety, hyperactivity, and social deficits observed in these *Arx* mutant mice are reminiscent of patients with mild *ARX* phenotypes. Other phenotypes, like the small amygdala, have not been studied in this relatively small patient population. It remains possible that a more thorough brain imaging and behavioral analysis of these patients might reveal even more similarities between the *Arx*$^{-/Y}$ *Emx1*^{Cre} mice and patients with *ARX* mutations.

Overall, the *Arx*$^{-/Y}$ *Emx1*^{Cre} mouse line, with the other conditional and mutant *Arx* mice that have been generated offer an opportunity to dissect apart a complex circuit to look for local circuit or regional connections that are necessary or sufficient for the generation of complex behaviors. We acknowledge at the onset that this is a difficult endeavor as any one change in a developing system alters the others and that both cognitive and social behaviors are complex tasks that involve the function of networks,

not just cortical regions and layers. With those caveats in mind, our findings suggest an important role for superficial cortical regions and the amygdala, in the generation of a hyperactive, anxiolytic, anti-social phenotype.

Table 1: Cohorts of mice used in behavior experiments and order of behavior tests.

Cohort	Number of Mice	Order of Behavior Tests
1	WT=3 Mut=4	Grip Strength, Rota-rod, Open Field, Water Maze
2	WT=10 Mut=8	Grip Strength, Rota-rod, Open Field, Water Maze
3	WT=13 Mut=9	Light/Dark Box, Open Field, Water Maze, Fear Conditioning
4	WT=4 Mut=5	Light/Dark Box, Buried Food, Social Choice, Fear Conditioning
5	WT=11 Mut=13	Buried Food, Social Choice
6	WT=8 Mut=8	Buried Food

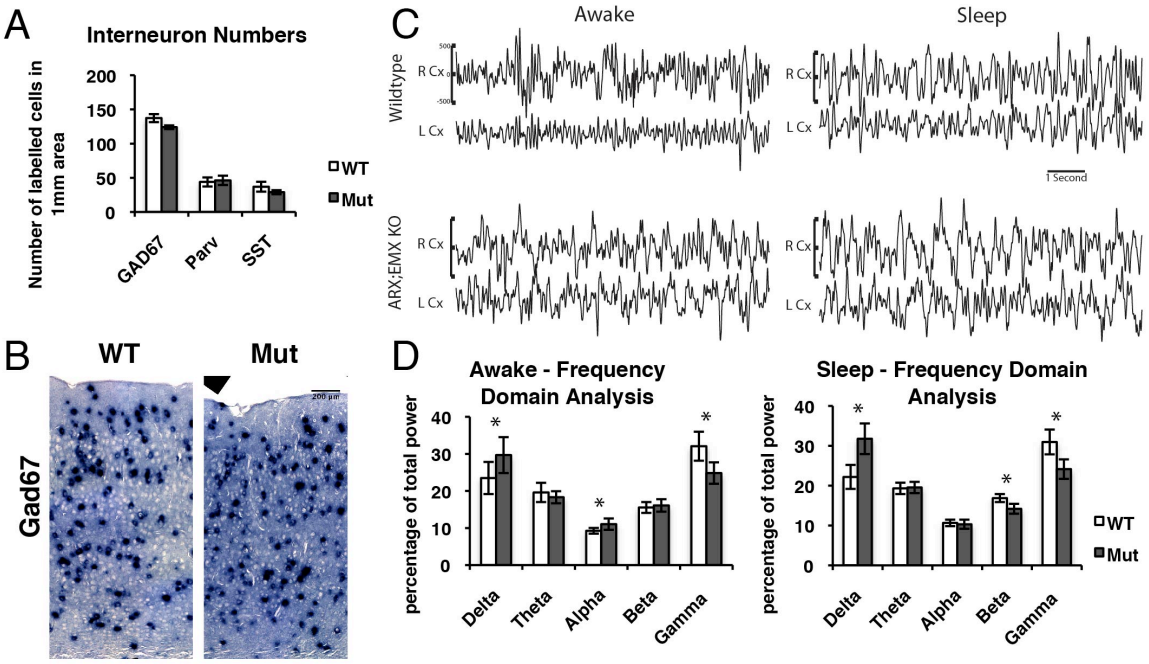

Figure 1: *Arx*$^{-/Y}$ *Emx1-Cre* mice do not have seizures and have normal interneuron numbers. A) Samples of cortex recordings for *Arx*$^{-/Y}$ *Emx1-Cre* mice (Mut) and their control wild type littermates (*Arx*$^{X/Y}$ *Emx1-Cre*), which showed no seizure activity. B) Quantifications of EEGs of the cortex by Fast Fourier Transform (FFT) on both Awake and Sleep segments for wild type and mutant mice (Awake; Delta: WT=23.50±4.34 and Mut=29.69±4.85 p=0.0036, Theta: WT=19.61±2.60 and Mut=18.32±1.63 p=0.1894, Alpha: WT=9.28±0.77 and Mut=11.06±1.53 p=0.0017, Beta: WT=15.54±1.46 and Mut=16.11±1.68 p=0.4199, Gamma: WT=32.08±3.92 and Mut=24.83±2.89 p=9.1x10^{-6}; Sleep; Delta: WT=22.19±3.84 and Mut=31.77±3.84 p=2.3x10^{-8}, Theta: WT=19.32±1.42 and Mut=19.55±1.41 p=0.7178, Alpha: WT=10.65±0.83 and Mut=10.32±1.13 p=0.4597, Beta: WT=16.88±1.00 and Mut=14.20±1.24 p=9.2x10^{-7}, Gamma: WT=30.96±3.11 and Mut=24.16±2.46 p=4.7x10^{-7}; WT n=6 and Mut n=4). C) Quantifications of interneurons in a 1mm bin of cortex from ventricular to pial surface from in situ hybridizations of GAD67 and immunofluorescence staining of parvalbumin and somatostatin on adult brain sections showing no difference in total number of interneurons (GAD67; WT= 137.3±5.84 and Mut=24±2.65; n=3 for each; p=0.1359) and no change in the number of interneurons of two subtypes (Parv; WT=50±5 and Mut=53±2; n=3 for each; p=0.6575; and SST; WT=37±7.23 and Mut=29±2.89; n=3 for each; p=0.3897). Error bars correspond to S.E. D) GAD67 *in situ* hybridizations on cryosections of P21 brains of wild type (Arx$^{X/Y}$ Emx1-Cre) and mutant (Arx$^{F/Y}$ Emx1-Cre) brains. Section of the cortex just above the hippocampus from pial surface (top) to white matter (bottom). Error bars are S.E.

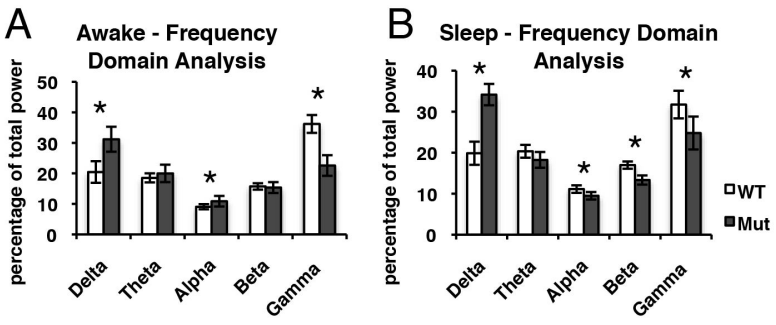

Figure 2: *Arx*$^{-/Y}$ *Emx1*^{Cre} mice have increased lower frequencies in their EEGs and decreased higher frequencies. A and B) Quantifications of EEGs of the hippocampus by Fast Fourier Transform (FFT) on both Awake (A) and Sleep (B) segments for wild type and mutant mice (Awake; Delta: WT=20.45±3.55 and Mut=31.18±4.08 $p=1.4x10^{-8}$, Theta: WT=18.53±1.47 and Mut=20.00±2.84 p=0.1531, Alpha: WT=9.08±0.84 and Mut=10.86±1.73 p=0.0049, Beta: WT=15.74±1.04 and Mut=15.37±1.77 p=0.5723, Gamma: WT=36.21±2.93 and Mut=22.58±3.39 $p=2.9x10^{-15}$; Sleep; Delta: WT=19.85±2.83 and Mut=34.15±2.61 $p=3.5x10^{-20}$, Theta: WT=20.34±1.56 and Mut=18.24±1.91 p=0.0087, Alpha: WT=11.12±0.92 and Mut=9.49±0.92 p=0.00017, Beta: WT=16.97±0.88 and Mut=13.33±1.13 $p=7.1x10^{-12}$, Gamma: WT=31.73±3.37 and Mut=24.78±4.00 p=0.000070; WT n=6 and Mut n=4). Error bars are S.E.

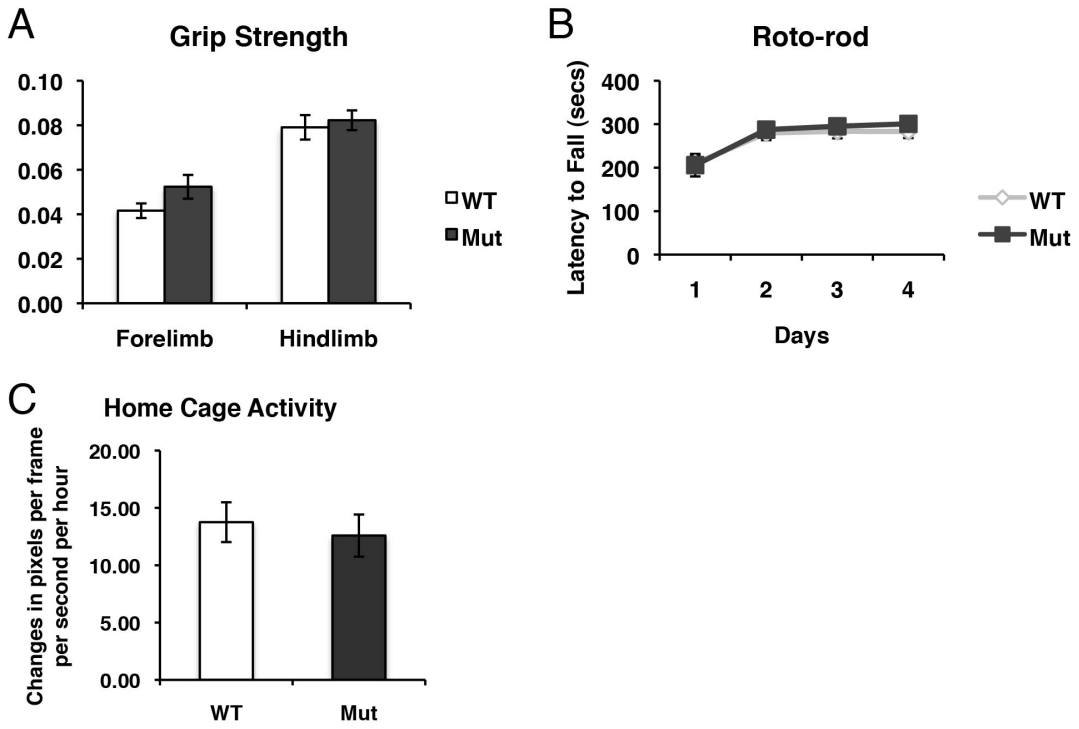

Figure 3: *Arx*$^{-/Y}$ *Emx1*^{Cre} mice have normal motor strength and coordination. A) The grip strength test was used as measure of motor strength in the wildtype and mutant mice. Grip strength for both fore and hind limbs was similar for the mutant and wildtype mice (Forelimb: WT= 0.042±0.0033, n=13 and Mut=0.052±0.0053, n=12; p=0.1030; Hindlimb: WT= 0.079±0.0055, n=13 and Mut=0.082±0.0044, n=12; p=0.3447). B) The rotarod test was used as measure of motor coordination. The mutant mice performed just as well in the rotarod test and learned to stay on the rotarod just as quickly as their wildtype littermates (WT n=13 and Mut n=12; p=0.0801). C) Home cage activity was similar for mutant mice and their wild type littermates (WT=13.75±1.73, n=8 and Mut=12.59±1.84, n=8; p=0.5191). Error bars are S.E.

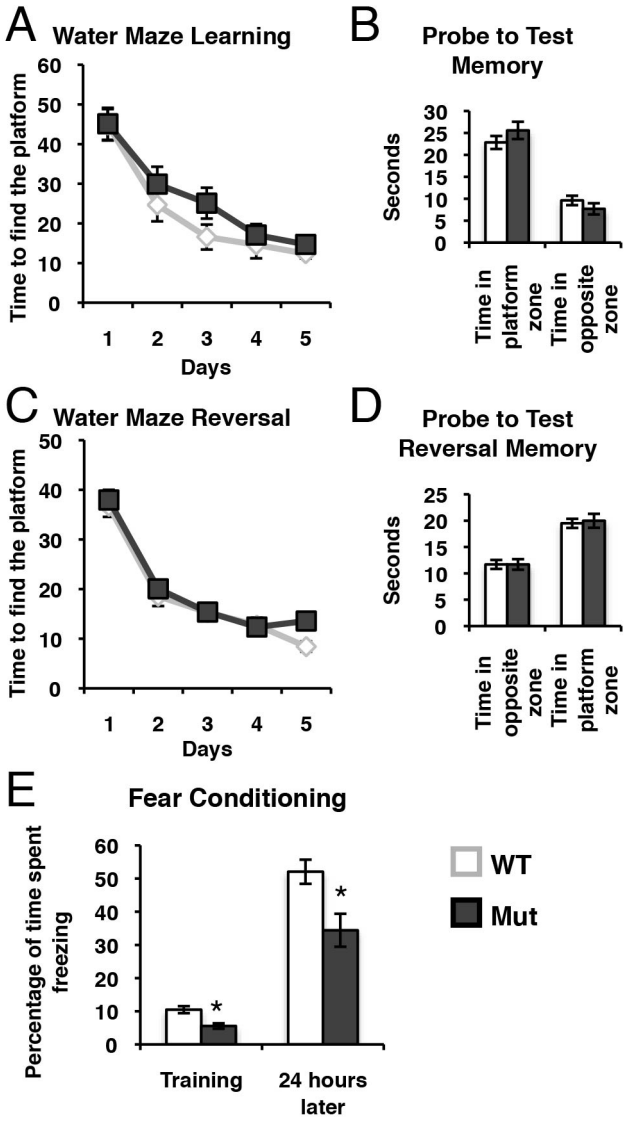

Figure 4: *Arx*$^{-/Y}$ *Emx1-Cre* mice have normal spatial learning and memory but impaired fear-based memory. A) Mutant mice and wild type littermates were trained in the Morris water maze for 5 days and the mutants learned how to reach the platform just as quickly as their wild type littermates (WT n=20 and Mut n=21; p=0.0669). B) On day 6 with the platform removed the mutant mice spent just as much time as their wild type littermates in the correct quadrant showing that they remembered where the platform was located (time in platform quadrant in seconds: WT=22.8±1.47 and Mut=25.6±1.97; p=0.271; time in opposite quadrant in seconds: WT=9.61±1.07, n=20 and Mut=7.7±1.28, n=21; p=0.256). C) The reversal learning of the mice was then tested by retraining them for another 5 days with the platform on the opposite quadrant of the tank. The mutant mice relearned the task just as well as their wild type littermates (WT n=20 and Mut n=21; p=0.1545). D) On day 12 the platform was again removed and the time the mice spent in each quadrant was recorded. The mutant mice spent just as much time in the new platform quadrant as their wild type littermates (time in platform quadrant in seconds: WT=19.5±0.87 and Mut=19.9±1.33; p=0.762; time in opposite quadrant in seconds: WT= 11.7±0.85, n=20 and Mut=11.7±1.02, n=21; p=0.997). E) Contextual fear conditioning was used

to evaluate fear learning in wild type and mutant mice. During a 3 min training period the mice were given a foot shock and the amount of time spent freezing was recorded. Twenty-four hours later the mice were re-exposed to the context where they were given the foot shock and the amount of time they spent freezing over a 5 min period was recorded. Mutant mice spent significantly less time freezing as compared to their wild type littermates both in the training period and during testing so therefore they did learn this task (percentage of time spent freezing training: WT=10.5±1.06, n=17 and Mut=5.57±0.82, n=14; p=0.00099; percentage of time spent freezing testing: WT=52.1±3.65, n=17 and Mut=34.4±4.99, n=14; p=0.0086). Error bars are S.E.

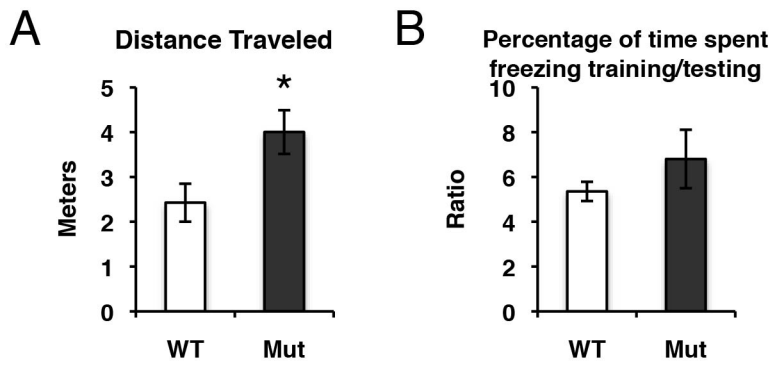

Figure 5: *Arx*$^{-/Y}$ *Emx1*^{Cre} mice are more active than their wild type littermates, but they do learn the contextual fear conditioning task. A) The mutant mice traveled a larger distance during the testing session of the fear conditioning task than their wild type littermates did (WT=2.43±0.42, n=17 and Mut=4.00±0.49, n=14; p=0.0217) indicating they are more active during the test. B) Therefore even though the mutant mice froze significantly less than their wild type littermates they did so during both parts of the task so the ratio of freezing during training to freezing during testing is not different between the two genotypes (WT=5.36±0.43, n=17 and Mut=6.80±1.31, n=14; p=0.3097). Error bars are S.E.

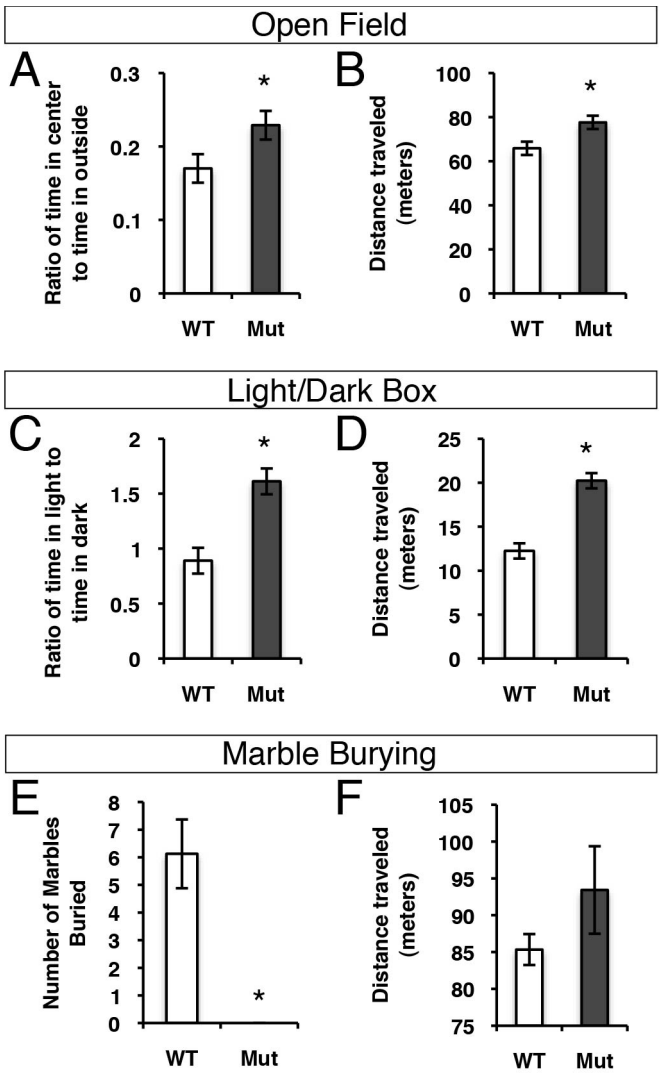

Figure 6: *Arx*$^{-/Y}$ *Emx1-Cre* mice are less anxious and more active than wild type mice. A) In the Open Field test the ratio of time spent in the center to time spent in the outside area of the box was used as a measure of anxiety. The mutant mice spent more time in the center of the box than their wild type littermates indicating they are less anxious (WT= 0.170±0.019, n=20 and Mut=0.229±0.020, n=21; p=0.0405). B) The linear distance traveled by the mice during their fifteen minute testing period was calculated as a measure of their activity level. The mutant mice traveled further than their wild type littermates during the open field test indicating that they are hyperactive (WT= 65.9±3.02, n=20 and Mut=77.6±3.79, n=21; p=0.0201). C) For the Light/Dark Box assay the ratio of time spent in the light side of the box to time spent in the dark side of the box was used as a measure of anxiety. The mutant mice spent more time in the light side of the box than their wild type littermates indicating that they are less anxious (WT= 0.891±0.118, n=20 and Mut=1.61±0.202, n=21; p=0.00204). D) The linear distance traveled by the mice during their ten minute testing period was calculated as a measure of their activity level. The mutant mice traveled further than their wild type littermates during the light/dark box test again indicating that they are hyperactive (WT= 12.2±0.867, n=20 and Mut=20.2±1.13, n=21; p=0.000007). E) The number of marbles buried in the Marble Burying assay was used as a measure of anxiety with

increased burying meaning increased anxiety (WT= 6.13±1.25, n=8 and Mut=0±0, n=8; p=0.00759). F) The amount of distance traveled by the mice during the thirty minute testing period was used as a measure of activity level (WT= 85.34±2.10, n=8 and Mut=93.42±5.94, n=8; p=0.2322). Error bars are S.E.

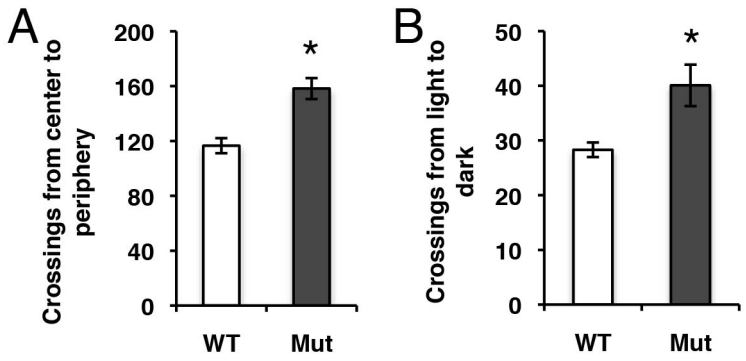

Figure 7: *Arx*$^{-/Y}$ *Emx1*^{Cre} mice are more active and have more crossings in the open field and light/dark box tests. A) The mutant mice crossed from the center to the periphery in the open field test more often than the wild type mice did (WT=117±6, n=20 and Mut=158±8, n=21; p=0.0000863) indicating they are more active during the test. B) Similarly, the mutant mice crossed from the light side to the dark side of the box in the light/dark box test more than the wild type mice did (WT= 28±1, n=17 and Mut=40±4, n=14; p=0.00143). Error bars are S.E.

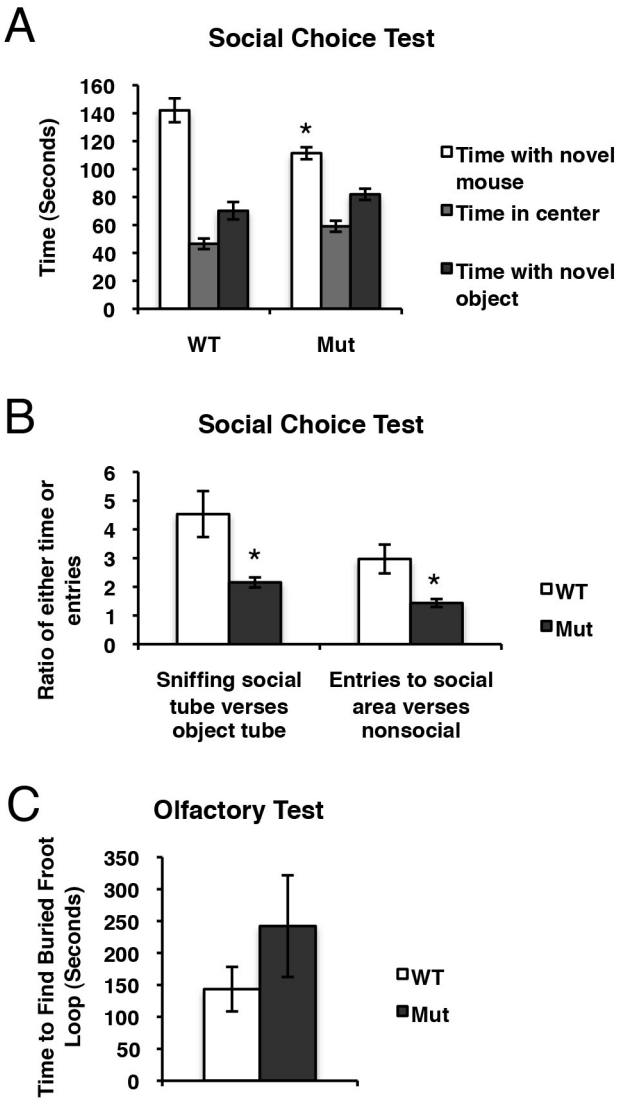

Figure 8: *Arx*$^{-/Y}$ *Emx1-Cre* mice have social deficits. A) The social abilities of mutant and wild type mice were assessed using the social choice test, the time spent in the novel mouse section (social), the center of the box, and the novel object section (nonsocial) was compared using a Two-way ANOVA. The mutant mice spent significantly less time in the social section of the box than their wild type littermates did (Time spent in social section: WT= 142.07±8.54, n=15 and Mut=111.37±4.28, n=18; $p<0.001$). B) The mutant mice spent significantly less time sniffing the novel mouse tube than their wild type littermates did as compared to the object tube (Sniffing: WT= 4.53±0.80, n=15 and Mut=2.15±0.18, n=18; p=0.01379). The mutant mice also entered the social section of the box few times as compared to the non-social section than their wild type littermates did (Entries: WT= 2.97±0.50, n=15 and Mut=1.44±0.14, n=18; p=0.00952). C) To assess the olfactory ability of the mice the buried food test was used. If the mice have normal olfactory abilities they should be able to find the Froot Loop buried in the bedding. Both the mutant mice and their wild type littermates were equally capable of finding the Froot Loop. (WT=143.38±34.86 and Mut=242.13±79.60, n=8 for each; p=0.2834). Error bars are S.E.

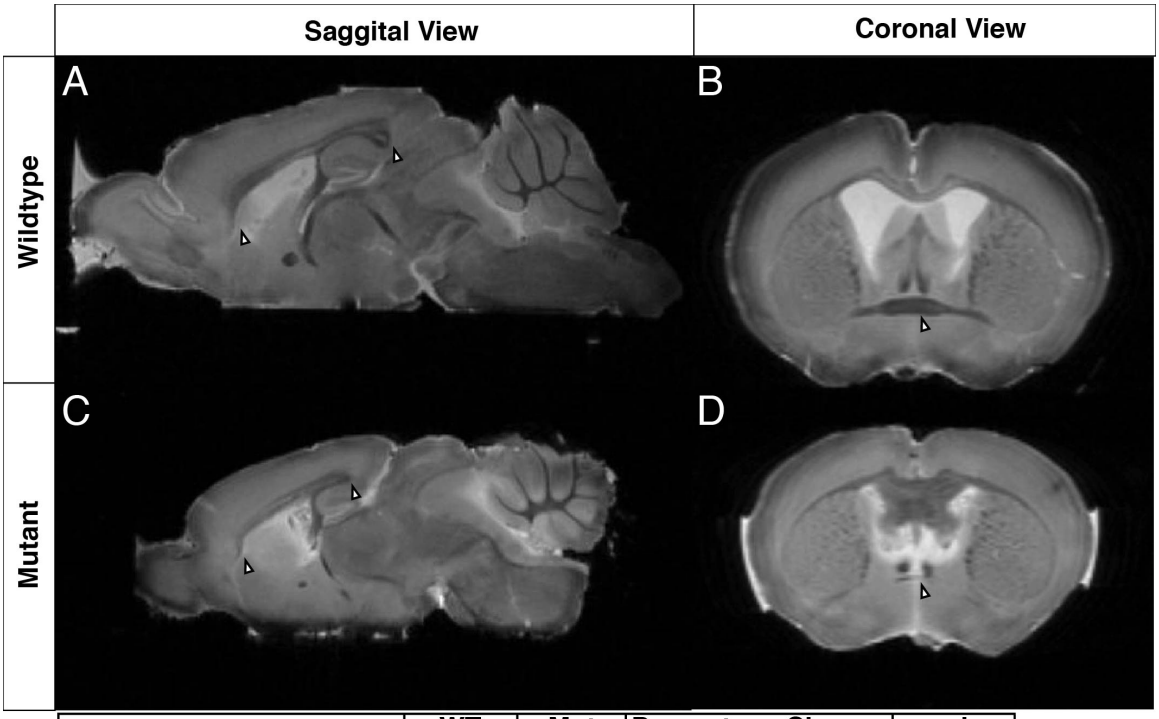

E

	WT	Mut	Percentage Change	p-value
Cortex volume	122.77	86.88	29.23	0.00616
Hippocampus volume	27.53	20.64	25.05	0.07666
Amygdala volume	8.39	5.42	35.4	0.00728
Thalamus volume	20.59	15.86	22.96	0.029
Basal ganglia volume	19.52	15.28	21.71	0.1243
Corpus callosum volume	10.57	8.28	21.69	0.04382

Figure 9: *Arx*$^{-/Y}$ *Emx1-Cre* mice have hypoplastic corpus callosums and anterior commissures. MRIs were made of three brains from mutant mice and three brains from their wild type littermates. A) A midsagittal section from an MRI of a wild type brain. The white arrows mark the rostral and caudal ends of a normal corpus callosum. C) A midsagittal section from an MRI of a mutant brain. The white arrows again mark the ends of the corpus callosum showing that the corpus callosum is both shorter and thinner in the mutant mice. B) A rostral coronal section from an MRI of a wild type brain. The white arrow marks the middle of the anterior commissure. D) A rostral coronal section from an MRI of a mutant brain. The white arrow marks the middle of the anterior commissure showing that in the mutant it is much thinner. E) Table of volumes (mm^3) of brain regions of wild type and mutant mice from T2W MRI data and comparisons between the wild type and mutant volumes for each region.

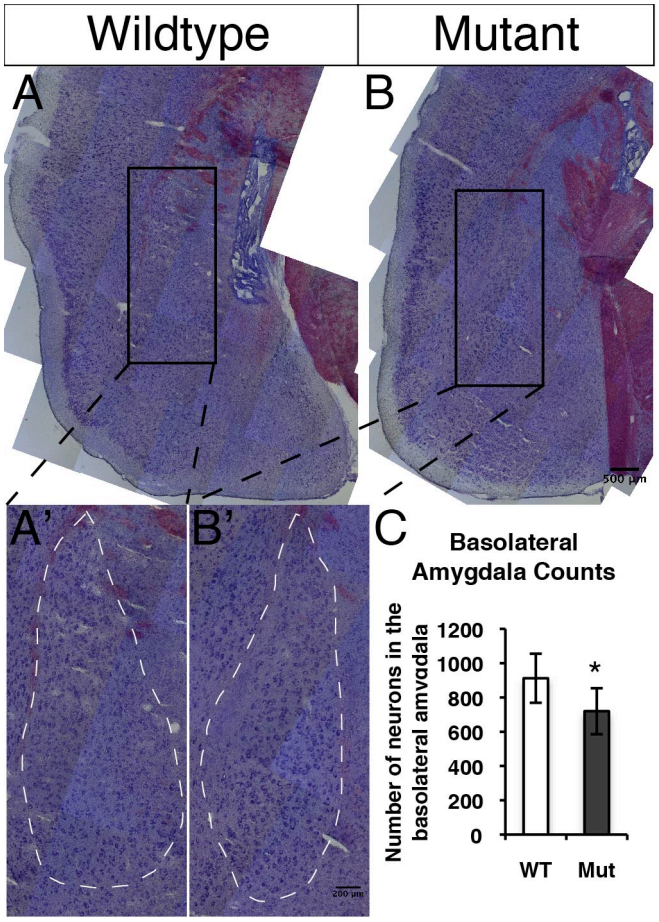

Figure 10: *Arx*$^{-/Y}$ *Emx1-Cre* mice have a loss of neurons in the basolateral amygdala. A and B) Coronal brain sections of adult mutant mice and their wild type littermates were stained with Nissl, which labels all neurons. A' and B') Enlarged sections showing the basolateral amygdala region (dotted white outline) which was counted. C) Quantification of number of neurons counted in the basolateral amygdala of the *Arx*$^{-/Y}$ *Emx1-Cre* mice and their wild type littermates showing that the mutant mice have fewer neurons in the basolateral amygdala as compared to wild type littermates (WT=1118±124 and Mut=891±152, n=3 for each; p=0.01952). Error bars are S.E.

CHAPTER 4: Discussion

The work presented herein, expands the data on the role of Arx into its function in dorsal progenitors. Mutations in ARX produce a spectrum of intellectual disability and epilepsy phenotypes in human patients (Shoubridge C et al. 2010). *Arx* is expressed in progenitor cells that produced both the excitatory and inhibitory neurons of the cerebral cortex during development (Colombo E et al. 2004). However, *Arx* studies have focused primarily on its role in interneurons during cortex development, as this was predicted to be the cause of the severe epilepsy found in patients with *ARX* mutations. The original report of *Arx* dysfunction in the mouse, however, found deficits in the proliferation and thickness of the cerebral cortex as well as in interneuron migration (Kitamura K et al. 2002). The decreased proliferation in the pallial (the dorsal part of the developing telencephalon) progenitor zone along with the expression of *Arx* in this region clearly pointed to a role for *Arx* in cortical progenitor cell development (Kitamura K et al. 2002; Colombo E et al. 2004).

To address the function of *Arx* in pallial progenitor cells, *in utero* electroporation was performed with an shRNA construct, to decrease *Arx* expression, and an overexpression construct, to observe changes with increased Arx function (Friocourt G et al. 2008). Knockdown of *Arx* in the cortical progenitors was found to cause premature cell cycle exit while *Arx* overexpression in the same population resulted in a lengthening of the cell cycle (Friocourt G et al. 2008). However, the methodology used in these experiments limits a full interpretation of the role of *Arx* in cortical progenitor cells, but confirmed that *Arx* has a role in normal cortical progenitor cell proliferation and

differentiation. Thus, we sought to more thoroughly investigate the role of *Arx* in the regulation of proliferation and differentiation of pallial progenitor cells during cortex development. Employing conditional genetic methodologies we eliminated *Arx* from the cortical proliferative zones by crossing the $Emx1^{Cre}$ driver mouse with the floxed *Arx* mouse (Fulp CT et al. 2008). The result of this cross was to effectively abrogate *Arx* specifically from the dorsal telencephalon cortical progenitor cells starting at embryonic day 9.5 (E9.5). This removed *Arx* from those cells that will give rise to all cortical excitatory neurons and glia, at the time of their birth and persisting through development.

Arx controls cortical progenitor cell number through repression of _Cdkn1c_

The $Arx^{-/Y}$ $Emx1^{Cre}$ mice were found to have smaller, thinner and somewhat disorganized cortices along with agenesis of the corpus callosum, mimicking the morphological abnormalities seen in $Arx^{-/Y}$ mice. The $Arx^{-/Y}$ mouse recapitulated some of the structural abnormalities found in X-linked lissencephaly with ambiguous genitalia patients (XLAG) with severe *ARX* mutations. This indicates that these abnormalities are due to a loss of *Arx* in cortical progenitor cells rather than other cell types in the cortex.

These $Arx^{-/Y}$ $Emx1^{Cre}$ mice have fewer radial glia progenitor cells (RGCs) and intermediate progenitor cells (IPCs) in their cortices during development (Chapter 2: Fig. 3). With decreased proliferation of the IPCs and increased cell cycle exit of the RGCs, but normal cell cycle length for both types of progenitors (Chapter 2: Figs. 3, 5, and 7). To uncover the transcriptional pathways mediating this loss of proliferation and premature cell cycle exit we compared transcript profiles between *Arx* KO cortices and wild type cortices. Eighty-three genes were found to be differentially expressed in the

Arx KO cortices as compared to controls (Chapter 2: Fig. 11). One of these genes was *Cdkn1c*, which was overexpressed in *Arx* KO cortices when compared to controls and at e14.5 is overexpressed specifically in the VZ (ventricular zone) and SVZ (subventricular zone). *Cdkn1c* is a cell cycle dependent kinase inhibitor that regulates cell cycle progression. Expression of the protein results in cell cycle exit (Sherr CJ and JM Roberts 1999). *Cdkn1c* was determined to be a direct transcriptional target of Arx and therefore the effector protein by which *Arx* regulates proliferation and cell cycle exit in cortical progenitor cells. In agreement with this conclusion overexpression of *Cdnk1c* in the cortex causes progenitor cells to exit the cell cycle and differentiate (Tury A et al. 2011). Furthermore, mice with a loss of *Cdnk1c* have an increase of proliferation of RGCs and IPCs with a greater effect on IPCs (Mairet-Coello G et al. 2012). Together this data provides the most direct evidence for *Arx* regulating cell cycle exit through repression of *Cdnk1c* in cortical progenitor cells.

The microarray expression profiles of *Arx* knockouts from different cortical and subcortical regions provides clear evidence that Arx regulates different genes in different cell types during different stages of development (Fulp CT et al. 2008; Colasante G et al. 2009)(Chapter 2: Fig. 11). For example *Cdkn1c* did not appear as a target on either of the two microarrays of the ventral telencephalon, but it does in the dorsal telencephalon (Fulp CT et al. 2008; Colasante G et al. 2009)(Chapter 2: Fig. 11). In fact, comparing the two microarrays done by the same group but in different regions revealed only 5 target genes found in both the dorsal and ventral telencephalon (Colasante G et al. 2009)(Chapter 2: Fig. 11). This is not completely surprising given that *Arx* is expressed at different developmental stages of the cell types formed from the ventral telencephalon verses the

dorsal telencephalon. In the dorsal telecephalon, *Arx* is expressed in actively dividing progenitor cells correlating with a regulatory role in the cell cycle. In the ventral telencephalon *Arx* is expressed in the interneurons as they are born, during migration, and into maturation, so it makes sense that in addition to another cohort of transcription factors it would also regulate signaling receptors and cytoskeletal regulatory proteins. From this data, our lab hypothesized that Arx is regulating different groups of genes in different cell types explaining how varying mutations and/or a loss of the protein can have differential effects in diverse brain regions. Supporting this hypothesis is work from the Golden lab that found *Arx* with a polyalanine expansion mutation was sufficient for normal excitatory neuron development but not interneuron development (Nasrallah MP et al. 2012). The differential effect was apparently due to the Arx polyalanine tract expansion mutation loosing the ability to repress a subset of its target genes, but not others. This finding was reported to be due to a failure of Arx to bind to one of its cofactors (Tle1) (Nasrallah MP et al. 2012). Another member of the Golden lab also found that *Arx* has different binding preferences for different DNA sequences when it is bound to different proteins, indicating it may bind with different cofactors in different cell types (Cho G et al. 2012).

To further understand the network of genes regulated by *Arx,* Quille and colleagues performed chromatin immunoprecipitation assays on promoter arrays from both whole brain tissue and a neuroblastoma (N2a) cell line and compared the resulting targets (Quille ML et al. 2011). Interestingly, this experiment did not pull down *Cdkn1c*, but did pull down *Cdkn1a*, another cyclin dependent kinase inhibitor in the same family of proteins with similar functions (Quille ML et al. 2011). Because the whole brain was

used in this assay its impossible to know in what cell type Arx binds to *Cdkn1a*. It remains possible that Arx binds to the promoter of *Cdkn1a* in the cortical progenitor cells and regulates their cell cycle exit through expression of that gene or Arx could be regulating *Cdkn1a* in a different cell type. Given our RT-PCR analysis in the dorsal telencephalon showing there was no increase in the expression of *Cdkn1a* in the *Arx* knockout as compared to controls, it seems most likely Arx is regulating *Cdkn1a* in a different cell type (Chapter 2: Fig. 11).

Loss of *Arx* in the progenitor cells changes the structure of the cortex

The radial glia (RGCs) and intermediate progenitor cells (IPCs) give rise to all of the excitatory neurons that will form the adult cortex. Therefore, by regulating cell cycle exit in these two cortical progenitor populations *Arx* regulates both the number and types of excitatory neurons produced in the cortex during development. There is currently some debate in the field regarding whether IPCs can produce all of the excitatory neuron subtypes in the cortex or whether they can only produce superficial layer neurons (for review see (Kriegstein A et al. 2006; Pontious A et al. 2008)). Our finding of a loss of superficial neurons in the adult cortex in the $Arx^{-/Y}$ $Emx1^{Cre}$ mice with a relative preservation of deeper neurons is consistent with the hypothesis that intermediate progenitor cells (IPCs) produce only upper layer neurons (Kriegstein A et al. 2006; Pontious A et al. 2008)(Chapter 2: Fig. 10).

In turn this loss of upper layer neurons in the cortex seems to result in a loss of connectivity in the brain as evidenced by the decrease in major white matter tracts, the corpus callosum and the anterior commissure, that connect distant cortical regions

(Chapter 2: Fig.1; Chapter 3: Fig. 9). In order to prove that the change is these white matter tracts was a direct result of the loss of these upper layer neurons in the cortex more experiments will need to be performed. For example a retrograde or anterograde label (DiI or Neurobiotin) injected into the upper cortical layers in the *Arx*$^{-/Y}$ *Emx1*^{Cre} mice and wild type littermate controls could map projections of layer 2/3 axons to see if fewer are found in the corpus callosum or the anterior commissure in the mutant mice. I performed a series of these proposed experiments, but was unable to specifically label only layer 2/3 neurons, likely due to a technical issues with the injection methods employed. Alternative methods include: a replication deficient lentivirus expressing GFP injected into superficial cells in an adult brain and targets traced; permanently labeling layer 2-3 neurons by crossing the *Arx*$^{-/Y}$ *Emx1*^{Cre} line with a Satb2 or Cux1 reporter mouse; or using *in utero* electroporation of a Tau-GFP construct at e15.5 to label the projections of the superficial layer neurons specifically. This embryonic method of labeling could be useful for looking at these cells at different points of development to determine if perhaps these cells do project early in development but are unable to maintain those projections.

Defects in the corpus callosum, either agenesis or hypoplasia, can be the result of a primary failure of axons to cross the midline, or due to a primary loss or depletion in the number of neurons producing the axons destined to cross the midline. Based on my data I hypothesize that the corpus callosum is thinner due to decreased generation of callosal projecting neurons in the superficial layers of the cortex. Therefore, no change would be found in the remaining neuronal projections over the course of development because the cells that are formed most likely project and are maintained normally. This is how a transcription factor that is expressed only at one time point early in the

development of these cortical cells can have a profound effect on the ultimate structure and function of the cortex.

Arx$^{-/Y}$ *Emx1*^{Cre} mice have slow background EEG

Our studies also provide some insight into the role of Arx in excitatory neurons and how this influences electrical activity in the brain. Since *Arx* was only lost in the excitatory neurons of the neocortex in *Arx*$^{-/Y}$ *Emx1*^{Cre} mice it was not surprising that the total number of interneurons and relative number of the two main subtypes of interneurons was preserved in these mutants (Chapter 3: Fig. 1). Most interestingly, unlike all other *Arx* mutant mouse models, the *Arx*$^{-/Y}$ *Emx1*^{Cre} mice do not appear to have seizures, further supporting the interneuron origin underlying epileptogenesis in these mice. Even without seizures, the *Arx*$^{-/Y}$ *Emx1*^{Cre} mice have an abnormal EEG pattern with an increase in slower frequencies and a decrease of faster frequencies (Chapter 3: Fig. 1). This slow EGG pattern is indicative of brain dysfunction and is seen in many developmental disorders, particularly epileptic encephalopthies, such as Lennox-Gastaut syndrome, Dravet's syndrome, and West syndrome (Kandel ER et al. 2000; Zupanc ML 2009). West syndrome is caused by various mutations in *ARX* including polyalanine tract expansions and duplications, missense mutations, and deletions (Turner G et al. 2002; Hirose S and A Mitsudome 2003; Kato M et al. 2003; Kato M et al. 2004; Wohlrab G et al. 2005; Demos MK et al. 2009; Cossee M et al. 2011). In addition, this increase in slower frequencies and decrease of faster frequencies is also consistent with the EEGs of children and adults with Attention Deficit Hyperactivity Disorder (ADHD) (Barry RJ et al. 2010; van Dongen-Boomsma M et al. 2010; Loo SK and S Makeig 2012; Woltering S

et al. 2012; Clarke AR et al. 2013) and our mutant mice appear hyperactive. Therefore, the *Arx*$^{-/Y}$ *Emx1*^{Cre} mice have an abnormal EEG background consistent with particular *ARX* mutations in humans and ADHD patients.

This increase of slower frequencies and a decrease of faster frequencies seen in the *Arx*$^{-/Y}$ *Emx1*^{Cre} mice is the opposite of the *Arx*$^{-/Y}$ *Dlx5/6*^{Cre} mice, which have a decrease of slower frequencies and an increase of faster frequencies. In the *Arx*$^{-/Y}$ *Dlx5/6*^{Cre} mice, *Arx* is lost only in the ganglionic eminence and its derivatives, the cortical interneurons, which generally have inhibitory roles in cortical circuits. The result is fewer interneurons in the cortex, which presumably results in the observed decreased inhibition relative to excitation in the cortex. This imbalance of inhibition relative to excitation is thought to be the cause of seizures in these mice and in *ARX* patients. In the *Arx*$^{-/Y}$ *Emx1*^{Cre} mice the opposite is true, loss of Arx causes a loss of layer 2/3 pyramidal cells which are excitatory and the interneurons are spared so presumably there would be an increase in the inhibition in these cortices relative to the excitation. These intriguing results provide the first data that the removal of particular cell types from the cortex can cause specific changes in murine cortical EEG patterns. This represents, to the best of my knowledge, the first example where the relative loss of inhibition in the cortex decreases slow EEG frequencies and increases fast frequencies while a relative loss of excitation only in the cortex induces an EEG shift to slower frequencies and a decrease of fast frequencies.

Described above is one possible theory to explain our observations regarding the disparate EEGs of these two *Arx* conditional knockout mice. To further validate this

theory we would have to first show that there actually is a relative loss of inhibition or excitation in the cortices of these two conditional knockout mice. This could be done by recording field potentials in cortical slices of each of these mice. If these EEGs did correlate with relative inhibition of excitation in the cortex then the next step would be to find or generate additional mutant mice which are missing either particular excitatory or inhibitory cells, preferably distinct from those lost in the mice we generated and from other genetic mutations and examine the EEG recordings and field potentials of these mutant mice as well. If particular EEG changes could be found to correlate with loss of particular cell types in the cortex then EEGs in people could be used to diagnose more diseases and hopefully lead to more specific treatments.

Behavioral Phenotype of *Arx*$^{-/Y}$ *Emx1*^{Cre} mice

Patients with *ARX* mutations exhibit a spectrum of phenotypes with some mutations having major structural brain malformations and others having normal appearing brains. However, all *ARX* patients have some type of seizure disorder and some level of intellectual disability (Marsh ED and JA Golden 2012). The *Arx*$^{-/Y}$ *Emx1*^{Cre} mice do not have seizures and have a normal lifespan, unlike most other *Arx* mutant mice, but they do have morphological changes of their brains (Chapter 2: Fig. 1; Chapter 3: Fig. 1). Their cortex is smaller and thinner with a specific loss of superficial excitatory neurons and their amygdala is smaller with fewer neurons in the basolateral amygdala. They also have defects of white matter tracts in the brain including the corpus callosum and the anterior commissure. Given these various anomalies we next sought to determine if these morphological changes correlated with possible behavior anomalies. Since most

mutations of *ARX* in people result in some form of intellectual disability we first tested the learning and memory of the $Arx^{-/Y}$ $Emx1^{Cre}$ mice. To our surprise, the mice had normal learning in all modalities tested. Spatial learning and memory, fear based learning, and reversal learning were all normal (Chapter 3: Fig. 4). This is most consistent with the fact that these mice do not have hippocampal defects. In rodents the hippocampus drives much of the learning phenotype and it is normal in these animals.

The $Arx^{-/Y}$ $Emx1^{Cre}$ mice were also put through several anxiety tests and they were found to be less anxious, more exploratory, and more active than their wild type littermates (Chapter 3: Fig. 6). This anxiolytic and hyperactive phenotype could be the result of the loss of neurons in the cortex or the amygdala or the loss of connections within the limbic system. These mice also have a social deficit, an autistic feature, which could also be related to this loss of neurons in the cortex and amygdala or a loss of cortical connections (Chapter 3: Fig. 8).

Three other *Arx* mutant mice ($Arx^{(GCG)7/Y}$, $Arx^{PL/Y}$, $Arx^{(GCG)10+7}$) have been behaviorally phenotyped by two other labs and they have some similarities and differences to the $Arx^{-/Y}$ $Emx1^{Cre}$ mice. The other three *Arx* mutant mice all have impaired spatial learning and fear-based learning (Kitamura K et al. 2009; Price MG et al. 2009). The $Arx^{(GCG)7/Y}$ and $Arx^{PL/Y}$ mice are more anxious than their wild type littermates, while the $Arx^{(GCG)10+7}$ mice are less anxious, more active, and have social deficits similar to the $Arx^{-/Y}$;$Emx1^{Cre}$ mice (Kitamura K et al. 2009; Price MG et al. 2009). The $Arx^{(GCG)7/Y}$ mice and the $Arx^{(GCG)10+7}$ mice have severe seizures and die at a young age (Kitamura K et al. 2009; Price MG et al. 2009). Only a few $Arx^{PL/Y}$ mice have seizures,

which are much less severe than the *Arx*$^{(GCG)7/Y}$ and *Arx*$^{(GCG)10+7}$ mice and they have a normal lifespan (Kitamura K et al. 2009). None of these *Arx* mutants have exactly the same behavioral phenotype as the *Arx*$^{-/Y}$ *Emx1*^{Cre} mice, but this is to be expected since the *Arx*$^{-/Y}$ *Emx1*^{Cre} mouse is a conditional knockout that only affects part of the brain. While the other mutations may only affect part of the function of *Arx*, but are present in the whole brain.

The morphological phenotype of these mutant mice also differs. The *Arx*$^{(GCG)7/Y}$, *Arx*$^{PL/Y}$, and *Arx*$^{(GCG)10+7}$ mice do not have the thinner cortex with an abnormal layer structure and agenesis of the corpus callosum that is seen in the *Arx* knockout mouse and the *Arx*$^{-/Y}$ *Emx1*^{Cre} mouse, which could indicate that cortical progenitor cell proliferation is not affected by these particular mutations to *Arx* (Kitamura K et al. 2009; Price MG et al. 2009). However, the *Arx*$^{(GCG)7/Y}$, *Arx*$^{PL/Y}$, and *Arx*$^{(GCG)10+7}$ mice have a loss of interneurons in the cortex, hippocampus, and striatum while the *Arx*$^{-/Y}$ *Emx1*^{Cre} mice have normal numbers of interneurons. Interestingly, *Arx*$^{-/Y}$ *Dlx5/6*^{Cre} mice, where Arx is only removed from the GE derived cortical interneurons, also do not have a thinner cortex with abnormal layering and agenesis of the corpus callosum. This also shows that this morphological phenotype is caused by changes to the cortical progenitor cells and not the interneurons (Marsh E et al. 2009).

The *Arx*$^{(GCG)7/Y}$, *Arx*$^{PL/Y}$, and *Arx*$^{(GCG)10+7}$ mice all have some degree of epilepsy, learning deficits, and a loss of interneurons although given their seizure frequency this can be difficult to assess, whereas the *Arx*$^{-/Y}$ *Emx1*^{Cre} mice have none of these characteristics (Kitamura K et al. 2009; Price MG et al. 2009). Therefore, we can

hypothesize that loss of interneurons is necessary for the development of epilepsy and learning deficits both in these mice and presumably in human *ARX* patients. The *Arx*$^{-/Y}$ *Emx1*^{Cre} mice provide negative evidence that the epilepsy in *ARX* patients is caused by problems with interneuron development and not the brain malformations seen in these patients. These mice also provide evidence that the behavioral and cognitive deficits seen in *ARX* patients might not be caused by the epilepsy. If this is true then the current clinical dogma that controlling the epilepsy of these patients early on will improve their cognitive and behavioral outcomes is incorrect and these patients may have the same behavioral and cognitive deficits regardless of how well their epilepsy is controlled.

The morphological and behavioral phenotype of the *Arx*$^{-/Y}$ *Emx1*^{Cre} mice makes them a reasonable model to investigate the pathobiology underlying patients with mild *ARX* mutations such as those with nonsyndromic X-linked intellectual disability, Proud syndrome, Partington syndrome, and females with *ARX* mutations (Suri M 2005; Shoubridge C et al. 2010). These mice could be used in future studies to understand how the brains of these patients are altered and how these changes led to their particular behavioral phenotypes. Once their phenotype is better understood they could also be used to evaluate treatment options for these patients.

Connecting anxiety and autistic behaviors to changes in development

The other behaviors (low anxiety, hyperactivity, and social deficits) seen in various *Arx* mutant mice (*Arx*$^{-/Y}$ *Emx1*^{Cre}, *Arx*$^{(GCG)7/Y}$, *Arx*$^{PL/Y}$, and *Arx*$^{(GCG)10+7}$) are more difficult to attribute to a particular function of *Arx* or to particular groups of neurons in the cortex. One reason for this is that these behaviors are controlled by the limbic

system, which involves the entorhinal and pyriform cortex, amygdala, hippocampus, and the connections between them. It has been reported that *Arx* is expressed in cells in the adult amygdala, but its function in the amygdala has not been investigated (Poirier K et al. 2004). We have shown that in the $Arx^{-/Y}$ $Emx1^{Cre}$ mice there are fewer neurons in the basolateral amygdala. It would be interesting to look at whether other *Arx* mutant mice also have a loss of neurons in the basolateral amygdala or perhaps to examine other amygdala nuclei. If there is found to be consistent loss of neurons in the basolateral amygdala of the *Arx* mutant mice then this could be a potential explanation for the changes in anxiety and social behaviors in these mice.

A possible future direction of this work would be to examine which particular neurons are lost from the basolateral amygdala of the $Arx^{-/Y}$ $Emx1^{Cre}$ mice or from other *Arx* mutant mice. I would hypothesize that excitatory neurons are lost in the $Arx^{-/Y}$ $Emx1^{Cre}$ mice because interneurons are born in the ventral areas of the brain that do not express Emx1 and these mice have normal numbers of interneurons in the cortex. To test this we could stain amygdala sections from the $Arx^{-/Y}$ $Emx1^{Cre}$ mice for Tbr1 or Mef2c or do *in situ* hybridizations for *Foxp2* or *Meis2*, which should all mark excitatory neurons in the amygdala and compare the numbers of those cells in the mutant mice to their wild type littermates (Remedios R et al. 2007; Waclaw RR et al. 2010; Cocas LA et al. 2011). We could also label *GAD67*, Parv, or SST as we did with the cortex to confirm that there is no loss of GABAergic neurons subtypes in the amygdala of these mice. Performing similar studies on the other *Arx* mutant mice to determine which, if any, of the neuronal subtypes are lost could also be informative in understanding both the role of *Arx* in development and the consequences of specific neuronal loss to behavior. If these

experiments were done, I would hypothesize that the $Arx^{(GCG)7/Y}$ and $Arx^{PL/Y}$ mutant mice would have a loss of interneurons and/or GABAergic projections neurons in the amygdala and no loss of excitatory cells similar to what has been demonstrated in the cortex. Perhaps the loss of different subtypes of neurons in the amygdala could explain the differences in anxiety behaviors seen in the different *Arx* mutant mice.

Another future direction of this work could be to examine whether connections between the cortex and amygdala are lost in the $Arx^{-/Y}$ $Emx1^{Cre}$ mice either because of a loss of neurons in the cortex or a loss of neurons in the amygdala. As with the white matter tract studies, a labeling study using DiI or Neurobiotin in the dorsolateral prefrontal cortex or anterior cingulate cortex could determine if there are fewer projections to or from the amygdala in the $Arx^{-/Y}$ $Emx1^{Cre}$ mice. Conversely injections into the basolateral and lateral amygdala could be performed to trace the cortical-amygdala projections. If the $Arx^{-/Y}$ $Emx1^{Cre}$ mice are missing connections between the cortex and the amygdala then the other *Arx* mutant mice should also be examined to determine if they are missing the same connections and if they are missing connections between the cortex and the amygdala that could be another explanation for the anxiety, hyperactivity, and social deficits and could bring us closer to understanding the human behavioral phenotype.

Ideally, to learn if any behavioral deficit could be correlated with specific cellular or regional dysfunction related to *Arx* loss, one could use a more specific Cre line to remove *Arx* either from the cortex, cortical subregions, such as prefrontal or somatosensory, the amygdala or particular subnuclei. If such specific Cre lines could be

developed the anxiety, hyperactivity, and social deficit behaviors of the resulting mice could be examined and correlated with the underlying structural changes in the cortex, amygdala or connections between the two.

Arx has different functions in different parts of the brain

Previous research on *Arx* has focused on where and when it is expressed during development and what happens to the brain when it is absent or mutated (Kitamura K et al. 2002; Kitamura K et al. 2009; Price MG et al. 2009). There has also been research into what genes *Arx* regulates and how different mutations change its DNA binding and repressive activities (McKenzie O et al. 2007; Colasante G et al. 2009; Quille ML et al. 2011; Cho G et al. 2012; Nasrallah MP et al. 2012; Shoubridge C et al. 2012). These studies provide one explanation for the spectrum of phenotypes seen in human patients, a close though not perfect genotype-phenotype correlation. For example an Arx protein with a polyalanine expansion can bind to three of its known target genes (*Lmo1*, *Shox2*, and *Ebf3*) but it can only repress *Shox2* and *Lmo1* (McKenzie O et al. 2007; Nasrallah MP et al. 2012). While an Arx protein with a mutation in its homeodomain cannot bind to or repress any of these three target genes (Cho G et al. 2012; Shoubridge C et al. 2012). Therefore, the phenotype of the homeodomain mutations is worse because the protein is completely non-functional whereas the polyalanine expansion Arx mutation is partially functional.

However, another explanation for the spectrum of phenotypes could be that *Arx* has different functions in different cell types and some of the functions can be accomplished by some mutations of *Arx,* but not by others. This would occur if different

cell types have different cofactors that *Arx* interacts with to regulate different groups of genes and some mutations may abolish binding to some cofactors but not others. Our lab recently found that *Arx* with a polyalanine expansion has reduced binding to its known cofactor Tle1, which could explain why it can no longer bind to the promoter regions of *Shox2* and *Ebf3* (Nasrallah MP et al. 2012). Therefore, a future direction for the field would be to look for cofactors of Arx and try to determine if different cell types at different points in development express particular cofactors and this correlates with the expression of particular groups of genes associated with particular cellular functions.

Our data has already provided some evidence for this alternative explanation for the spectrum of *ARX* phenotypes. We have shown that Arx functions to regulate cell cycle exit of progenitor cells in the cortex by regulating a distinct cohort of genes, particularly *Cdkn1c*, from those already shown to be regulated in interneurons. Therefore, loss of *Arx* in the cortical progenitor cells results in changes in the structure and function of the cortex that are different from the changes in function that result from the loss of *Arx* in interneurons. When *Arx* is lost in the cortical progenitor cells the adult animal has a thinner cortex and agenesis of the corpus callosum, but does not have seizures. Whereas the removal of *Arx* from interneurons results in an animal with a normal appearing cortex that has fewer interneurons and does have seizures, which it often succumbs to before adulthood (Marsh E et al. 2009).

Prior to the results presented here, *Arx* was known to function in cortical proliferation and differentiation, but the exact mechanism was not known. We have now revealed that *Arx* is regulating the cell cycle exit of cortical progenitor cells in the cortex

by repressing the cyclin dependent kinase inhibitor *Cdkn1c*. This results in premature exit of progenitor cells from the cell cycle, which ultimately results in a thinner cortex due to loss of neurons from the superficial layers. We have correlated this finding in adult mutant mice with lower anxiety, hyperactivity, and social deficits, providing evidence for the cell types and circuits that are involved in these behaviors in mice and presumably in humans. Hence, these mice can serve as a model of mild human *ARX* patients and could aid in the understanding of both the physiology of the disease and be used to test possible treatments for these behavioral symptoms.

BIBLIOGRAPHY

Albarran-Zeckler RG, Brantley AF, Smith RG. 2012. Growth hormone secretagogue receptor (GHS-R1a) knockout mice exhibit improved spatial memory and deficits in contextual memory. Behav Brain Res 232:13-19.

Alvarez IS, Schoenwolf GC. 1992. Expansion of surface epithelium provides the major extrinsic force for bending of the neural plate. J Exp Zool 261:340-348.

Angelo M, Plattner F, Irvine EE, Giese KP. 2003. Improved reversal learning and altered fear conditioning in transgenic mice with regionally restricted p25 expression. Eur J Neurosci 18:423-431.

Arnold SJ, Huang GJ, Cheung AF, Era T, Nishikawa S, Bikoff EK, Molnar Z, Robertson EJ, Groszer M. 2008. The T-box transcription factor Eomes/Tbr2 regulates neurogenesis in the cortical subventricular zone. Genes Dev 22:2479-2484.

Azim E, Jabaudon D, Fame RM, Macklis JD. 2009. SOX6 controls dorsal progenitor identity and interneuron diversity during neocortical development. Nat Neurosci 12:1238-1247.

Bale TL, Contarino A, Smith GW, Chan R, Gold LH, Sawchenko PE, Koob GF, Vale WW, Lee KF. 2000. Mice deficient for corticotropin-releasing hormone receptor-2 display anxiety-like behaviour and are hypersensitive to stress. Nat Genet 24:410-414.

Barkovich AJ, Guerrini R, Kuzniecky RI, Jackson GD, Dobyns WB. 2012. A developmental and genetic classification for malformations of cortical development: update 2012. Brain 135:1348-1369.

Barry RJ, Clarke AR, Hajos M, McCarthy R, Selikowitz M, Dupuy FE. 2010. Resting-state EEG gamma activity in children with attention-deficit/hyperactivity disorder. Clin Neurophysiol 121:1871-1877.

Bayer SA, Altman J. 1991. Development of the endopiriform nucleus and the claustrum in the rat brain. Neuroscience 45:391-412.

Bielle F, Griveau A, Narboux-Neme N, Vigneau S, Sigrist M, Arber S, Wassef M, Pierani A. 2005. Multiple origins of Cajal-Retzius cells at the borders of the developing pallium. Nat Neurosci 8:1002-1012.

Bonneau D, Kaplan J, Girard G, Dufier JL. 1992. Autosomal inheritance of "senile" retinitis pigmentosa. A report of a family with consanguinity. Clin Genet 42:199-200.

Bonneau D, Toutain A, Laquerriere A, Marret S, Saugier-Veber P, Barthez MA, Radi S, Biran-Mucignat V, Rodriguez D, Gelot A. 2002. X-linked lissencephaly with absent

corpus callosum and ambiguous genitalia (XLAG): clinical, magnetic resonance imaging, and neuropathological findings. Ann Neurol 51:340-349.

Bourin M, Hascoet M. 2003. The mouse light/dark box test. Eur J Pharmacol 463:55-65.

Bragin A, Jando G, Nadasdy Z, Hetke J, Wise K, Buzsaki G. 1995. Gamma (40-100 Hz) oscillation in the hippocampus of the behaving rat. J Neurosci 15:47-60.

Britanova O, Akopov S, Lukyanov S, Gruss P, Tarabykin V. 2005. Novel transcription factor Satb2 interacts with matrix attachment region DNA elements in a tissue-specific manner and demonstrates cell-type-dependent expression in the developing mouse CNS. Eur J Neurosci 21:658-668.

Buschert J, Hohoff C, Touma C, Palme R, Rothermundt M, Arolt V, Zhang W, Ambree O. 2013. S100B overexpression increases behavioral and neural plasticity in response to the social environment during adolescence. J Psychiatr Res.

Chenn A, Walsh CA. 2002. Regulation of cerebral cortical size by control of cell cycle exit in neural precursors. Science 297:365-369.

Chioca LR, Antunes VD, Ferro MM, Losso EM, Andreatini R. 2013. Anosmia does not impair the anxiolytic-like effect of lavender essential oil inhalation in mice. Life Sci 92:971-975.

Cho G, Nasrallah MP, Lim Y, Golden JA. 2012. Distinct DNA binding and transcriptional repression characteristics related to different ARX mutations. Neurogenetics 13:23-29.

Clarke AR, Barry RJ, Dupuy FE, McCarthy R, Selikowitz M, Johnstone SJ. 2013. Excess beta activity in the EEG of children with attention-deficit/hyperactivity disorder: A disorder of arousal? Int J Psychophysiol.

Cobos I, Broccoli V, Rubenstein JL. 2005. The vertebrate ortholog of Aristaless is regulated by Dlx genes in the developing forebrain. J Comp Neurol 483:292-303.

Cocas LA, Georgala PA, Mangin JM, Clegg JM, Kessaris N, Haydar TF, Gallo V, Price DJ, Corbin JG. 2011. Pax6 is required at the telencephalic pallial-subpallial boundary for the generation of neuronal diversity in the postnatal limbic system. J Neurosci 31:5313-5324.

Colasante G, Collombat P, Raimondi V, Bonanomi D, Ferrai C, Maira M, Yoshikawa K, Mansouri A, Valtorta F, Rubenstein JL, Broccoli V. 2008. Arx is a direct target of Dlx2 and thereby contributes to the tangential migration of GABAergic interneurons. J Neurosci 28:10674-10686.

Colasante G, Sessa A, Crispi S, Calogero R, Mansouri A, Collombat P, Broccoli V. 2009. Arx acts as a regional key selector gene in the ventral telencephalon mainly through its transcriptional repression activity. Dev Biol 334:59-71.

Colasante G, Simonet JC, Calogero R, Crispi S, Sessa A, Cho G, Golden JA, Broccoli V. 2013. ARX Regulates Cortical Intermediate Progenitor Cell Expansion and Upper Layer Neuron Formation Through Repression of Cdkn1c. Cereb Cortex.

Cole JT, Mitala CM, Kundu S, Verma A, Elkind JA, Nissim I, Cohen AS. 2010. Dietary branched chain amino acids ameliorate injury-induced cognitive impairment. Proc Natl Acad Sci U S A 107:366-371.

Collombat P, Mansouri A, Hecksher-Sorensen J, Serup P, Krull J, Gradwohl G, Gruss P. 2003. Opposing actions of Arx and Pax4 in endocrine pancreas development. Genes Dev 17:2591-2603.

Colombo E, Collombat P, Colasante G, Bianchi M, Long J, Mansouri A, Rubenstein JL, Broccoli V. 2007. Inactivation of Arx, the murine ortholog of the X-linked lissencephaly with ambiguous genitalia gene, leads to severe disorganization of the ventral telencephalon with impaired neuronal migration and differentiation. J Neurosci 27:4786-4798.

Colombo E, Galli R, Cossu G, Gecz J, Broccoli V. 2004. Mouse orthologue of ARX, a gene mutated in several X-linked forms of mental retardation and epilepsy, is a marker of adult neural stem cells and forebrain GABAergic neurons. Dev Dyn 231:631-639.

Cossee M, Faivre L, Philippe C, Hichri H, de Saint-Martin A, Laugel V, Bahi-Buisson N, Lemaitre JF, Leheup B, Delobel B, Demeer B, Poirier K, Biancalana V, Pinoit JM, Julia S, Chelly J, Devys D, Mandel JL. 2011. ARX polyalanine expansions are highly implicated in familial cases of mental retardation with infantile epilepsy and/or hand dystonia. Am J Med Genet A 155A:98-105.

Crawley JN. 2007. Mouse behavioral assays relevant to the symptoms of autism. Brain Pathol 17:448-459.

Crawley JN. 2007. What's wrong with my mouse? : behavioral phenotyping of transgenic and knockout mice. Hoboken, N.J.: Wiley-Interscience.

d'Isa R, Clapcote SJ, Voikar V, Wolfer DP, Giese KP, Brambilla R, Fasano S. 2011. Mice Lacking Ras-GRF1 Show Contextual Fear Conditioning but not Spatial Memory Impairments: Convergent Evidence from Two Independently Generated Mouse Mutant Lines. Front Behav Neurosci 5:78.

Deacon RM. 2006. Digging and marble burying in mice: simple methods for in vivo identification of biological impacts. Nat Protoc 1:122-124.

Dehay C, Kennedy H. 2007. Cell-cycle control and cortical development. Nat Rev Neurosci 8:438-450.

Demos MK, Fullston T, Partington MW, Gecz J, Gibson WT. 2009. Clinical study of two brothers with a novel 33 bp duplication in the ARX gene. Am J Med Genet A 149A:1482-1486.

Erlander MG, Tillakaratne NJ, Feldblum S, Patel N, Tobin AJ. 1991. Two genes encode distinct glutamate decarboxylases. Neuron 7:91-100.

Fairless AH, Dow HC, Toledo MM, Malkus KA, Edelmann M, Li H, Talbot K, Arnold SE, Abel T, Brodkin ES. 2008. Low sociability is associated with reduced size of the corpus callosum in the BALB/cJ inbred mouse strain. Brain Res 1230:211-217.

Faux C, Rakic S, Andrews W, Britto JM. 2012. Neurons on the move: migration and lamination of cortical interneurons. Neurosignals 20:168-189.

Faux C, Rakic S, Andrews W, Yanagawa Y, Obata K, Parnavelas JG. 2010. Differential gene expression in migrating cortical interneurons during mouse forebrain development. J Comp Neurol 518:1232-1248.

Ferrai C, Munari D, Luraghi P, Pecciarini L, Cangi MG, Doglioni C, Blasi F, Crippa MP. 2007. A transcription-dependent micrococcal nuclease-resistant fragment of the urokinase-type plasminogen activator promoter interacts with the enhancer. J Biol Chem 282:12537-12546.

Fowler SC, Zarcone TJ, Vorontsova E, Chen R. 2002. Motor and associative deficits in D2 dopamine receptor knockout mice. Int J Dev Neurosci 20:309-321.

Frantz GD, McConnell SK. 1996. Restriction of late cerebral cortical progenitors to an upper-layer fate. Neuron 17:55-61.

Friocourt G, Kanatani S, Tabata H, Yozu M, Takahashi T, Antypa M, Raguenes O, Chelly J, Ferec C, Nakajima K, Parnavelas JG. 2008. Cell-autonomous roles of ARX in cell proliferation and neuronal migration during corticogenesis. J Neurosci 28:5794-5805.

Friocourt G, Parnavelas JG. 2011. Identification of Arx targets unveils new candidates for controlling cortical interneuron migration and differentiation. Front Cell Neurosci 5:28.

Friocourt G, Poirier K, Rakic S, Parnavelas JG, Chelly J. 2006. The role of ARX in cortical development. Eur J Neurosci 23:869-876.

Fulp CT, Cho G, Marsh ED, Nasrallah IM, Labosky PA, Golden JA. 2008. Identification of Arx transcriptional targets in the developing basal forebrain. Hum Mol Genet 17:3740-3760.

Gal JS, Morozov YM, Ayoub AE, Chatterjee M, Rakic P, Haydar TF. 2006. Molecular and morphological heterogeneity of neural precursors in the mouse neocortical proliferative zones. J Neurosci 26:1045-1056.

Gecz J, Cloosterman D, Partington M. 2006. ARX: a gene for all seasons. Curr Opin Genet Dev 16:308-316.

Gilbert SF. 2010. Developmental biology. Sunderland, Mass.: Sinauer Associates.

Golub MS, Germann SL. 2001. Long-term consequences of developmental exposure to aluminum in a suboptimal diet for growth and behavior of Swiss Webster mice. Neurotoxicol Teratol 23:365-372.

Gotz M, Barde YA. 2005. Radial glial cells defined and major intermediates between embryonic stem cells and CNS neurons. Neuron 46:369-372.

Gotz M, Sommer L. 2005. Cortical development: the art of generating cell diversity. Development 132:3327-3332.

Grillon C, Southwick SM, Charney DS. 1996. The psychobiological basis of posttraumatic stress disorder. Mol Psychiatry 1:278-297.

Hamiwka LD, Wirrell EC. 2009. Comorbidities in pediatric epilepsy: beyond "just" treating the seizures. J Child Neurol 24:734-742.

Han Q, Feng J, Qu Y, Ding Y, Wang M, So KF, Wu W, Zhou L. 2013. Spinal cord maturation and locomotion in mice with an isolated cortex. Neuroscience.

Harris L, Dixon C, Cato K, Heng YH, Kurniawan ND, Ullmann JF, Janke AL, Gronostajski RM, Richards LJ, Burne TH, Piper M. 2013. Heterozygosity for nuclear factor one x affects hippocampal-dependent behaviour in mice. PLoS One 8:e65478.

Hermann BP, Lin JJ, Jones JE, Seidenberg M. 2009. The emerging architecture of neuropsychological impairment in epilepsy. Neurol Clin 27:881-907.

Hevner RF, Neogi T, Englund C, Daza RA, Fink A. 2003. Cajal-Retzius cells in the mouse: transcription factors, neurotransmitters, and birthdays suggest a pallial origin. Brain Res Dev Brain Res 141:39-53.

Heyser CJ, Vishnevetsky D, Berten S. 2013. The effect of cocaine on rotarod performance in male C57BL/6J mice. Physiol Behav 118:208-211.

Hirose S, Mitsudome A. 2003. X-linked mental retardation and epilepsy: pathogenetic significance of ARX mutations. Brain Dev 25:161-165.

Innocenti GM, Price DJ. 2005. Exuberance in the development of cortical networks. Nat Rev Neurosci 6:955-965.

Itoh Y, Masuyama N, Nakayama K, Nakayama KI, Gotoh Y. 2007. The cyclin-dependent kinase inhibitors p57 and p27 regulate neuronal migration in the developing mouse neocortex. J Biol Chem 282:390-396.

Jin XL, Guo H, Mao C, Atkins N, Wang H, Avasthi PP, Tu YT, Li Y. 2000. Emx1-specific expression of foreign genes using "knock-in" approach. Biochem Biophys Res Commun 270:978-982.

Kandel ER, Schwartz JH, Jessell TM. 2000. Principles of neural science. New York: McGraw-Hill, Health Professions Division.

Kato M, Das S, Petras K, Kitamura K, Morohashi K, Abuelo DN, Barr M, Bonneau D, Brady AF, Carpenter NJ, Cipero KL, Frisone F, Fukuda T, Guerrini R, Iida E, Itoh M, Lewanda AF, Nanba Y, Oka A, Proud VK, Saugier-Veber P, Schelley SL, Selicorni A, Shaner R, Silengo M, Stewart F, Sugiyama N, Toyama J, Toutain A, Vargas AL, Yanazawa M, Zackai EH, Dobyns WB. 2004. Mutations of ARX are associated with striking pleiotropy and consistent genotype-phenotype correlation. Hum Mutat 23:147-159.

Kato M, Das S, Petras K, Sawaishi Y, Dobyns WB. 2003. Polyalanine expansion of ARX associated with cryptogenic West syndrome. Neurology 61:267-276.

Kitamura K, Itou Y, Yanazawa M, Ohsawa M, Suzuki-Migishima R, Umeki Y, Hohjoh H, Yanagawa Y, Shinba T, Itoh M, Nakamura K, Goto Y. 2009. Three human ARX mutations cause the lissencephaly-like and mental retardation with epilepsy-like pleiotropic phenotypes in mice. Hum Mol Genet 18:3708-3724.

Kitamura K, Yanazawa M, Sugiyama N, Miura H, Iizuka-Kogo A, Kusaka M, Omichi K, Suzuki R, Kato-Fukui Y, Kamiirisa K, Matsuo M, Kamijo S, Kasahara M, Yoshioka H, Ogata T, Fukuda T, Kondo I, Kato M, Dobyns WB, Yokoyama M, Morohashi K. 2002. Mutation of ARX causes abnormal development of forebrain and testes in mice and X-linked lissencephaly with abnormal genitalia in humans. Nat Genet 32:359-369.

Kornack DR, Rakic P. 1995. Radial and horizontal deployment of clonally related cells in the primate neocortex: relationship to distinct mitotic lineages. Neuron 15:311-321.

Kowalczyk T, Pontious A, Englund C, Daza RA, Bedogni F, Hodge R, Attardo A, Bell C, Huttner WB, Hevner RF. 2009. Intermediate neuronal progenitors (basal progenitors) produce pyramidal-projection neurons for all layers of cerebral cortex. Cereb Cortex 19:2439-2450.

Krass M, Runkorg K, Wegener G, Volke V. 2010. Nitric oxide is involved in the regulation of marble-burying behavior. Neurosci Lett 480:55-58.

Kriegstein A, Noctor S, Martinez-Cerdeno V. 2006. Patterns of neural stem and progenitor cell division may underlie evolutionary cortical expansion. Nat Rev Neurosci 7:883-890.

Kwan KY, Sestan N, Anton ES. 2012. Transcriptional co-regulation of neuronal migration and laminar identity in the neocortex. Development 139:1535-1546.

Kwon GS, Hadjantonakis AK. 2007. Eomes::GFP-a tool for live imaging cells of the trophoblast, primitive streak, and telencephalon in the mouse embryo. Genesis 45:208-217.

Lafaucheur L, Missohou A, Ecolan P, Monin G, Bonneau M. 1992. Performance, plasma hormones, histochemical and biochemical muscle traits, and meat quality of pigs administered exogenous somatotropin between 30 or 60 kilograms and 100 kilograms body weight. J Anim Sci 70:3401-3411.

Lagercrantz H, Ringstedt T. 2001. Organization of the neuronal circuits in the central nervous system during development. Acta Paediatr 90:707-715.

Lawson A, Anderson H, Schoenwolf GC. 2001. Cellular mechanisms of neural fold formation and morphogenesis in the chick embryo. Anat Rec 262:153-168.

Le Magueresse C, Monyer H. 2013. GABAergic interneurons shape the functional maturation of the cortex. Neuron 77:388-405.

Lin CH, Jao WC, Yeh YH, Lin WC, Yang MC. 2009. Hemocompatibility and cytocompatibility of styrenesulfonate-grafted PDMS-polyurethane-HEMA hydrogel. Colloids Surf B Biointerfaces 70:132-141.

Lodato S, Rouaux C, Quast KB, Jantrachotechatchawan C, Studer M, Hensch TK, Arlotta P. 2011. Excitatory projection neuron subtypes control the distribution of local inhibitory interneurons in the cerebral cortex. Neuron 69:763-779.

Loo SK, Makeig S. 2012. Clinical utility of EEG in attention-deficit/hyperactivity disorder: a research update. Neurotherapeutics 9:569-587.

Lyden D, Young AZ, Zagzag D, Yan W, Gerald W, O'Reilly R, Bader BL, Hynes RO, Zhuang Y, Manova K, Benezra R. 1999. Id1 and Id3 are required for neurogenesis, angiogenesis and vascularization of tumour xenografts. Nature 401:670-677.

Mairet-Coello G, Tury A, Van Buskirk E, Robinson K, Genestine M, DiCicco-Bloom E. 2012. p57(KIP2) regulates radial glia and intermediate precursor cell cycle dynamics and lower layer neurogenesis in developing cerebral cortex. Development 139:475-487.

Malatesta P, Hartfuss E, Gotz M. 2000. Isolation of radial glial cells by fluorescent-activated cell sorting reveals a neuronal lineage. Development 127:5253-5263.

Manzini MC, Walsh CA. 2011. What disorders of cortical development tell us about the cortex: one plus one does not always make two. Curr Opin Genet Dev 21:333-339.

Marin O. 2013. Cellular and molecular mechanisms controlling the migration of neocortical interneurons. Eur J Neurosci 38:2019-2029.

Marsh E, Fulp C, Gomez E, Nasrallah I, Minarcik J, Sudi J, Christian SL, Mancini G, Labosky P, Dobyns W, Brooks-Kayal A, Golden JA. 2009. Targeted loss of Arx results in a developmental epilepsy mouse model and recapitulates the human phenotype in heterozygous females. Brain 132:1563-1576.

Marsh ED, Golden JA. 2012. Developing Models of Aristaless-related homeobox mutations. In: Noebels JL, Avoli M, Rogawski MA, Olsen RW, Delgado-Escueta AV, editors. Jasper's Basic Mechanisms of the Epilepsies 4th ed. Bethesda (MD).

McKenzie O, Ponte I, Mangelsdorf M, Finnis M, Colasante G, Shoubridge C, Stifani S, Gecz J, Broccoli V. 2007. Aristaless-related homeobox gene, the gene responsible for West syndrome and related disorders, is a Groucho/transducin-like enhancer of split dependent transcriptional repressor. Neuroscience 146:236-247.

Medina L, Legaz I, Gonzalez G, De Castro F, Rubenstein JL, Puelles L. 2004. Expression of Dbx1, Neurogenin 2, Semaphorin 5A, Cadherin 8, and Emx1 distinguish ventral and lateral pallial histogenetic divisions in the developing mouse claustroamygdaloid complex. J Comp Neurol 474:504-523.

Meyer G, Perez-Garcia CG, Abraham H, Caput D. 2002. Expression of p73 and Reelin in the developing human cortex. J Neurosci 22:4973-4986.

Miller FD, Gauthier AS. 2007. Timing is everything: making neurons versus glia in the developing cortex. Neuron 54:357-369.

Miwa JM, Walz A. 2012. Enhancement in motor learning through genetic manipulation of the Lynx1 gene. PLoS One 7:e43302.

Miyoshi G, Fishell G. 2011. GABAergic interneuron lineages selectively sort into specific cortical layers during early postnatal development. Cereb Cortex 21:845-852.

Molyneaux BJ, Arlotta P, Menezes JR, Macklis JD. 2007. Neuronal subtype specification in the cerebral cortex. Nat Rev Neurosci 8:427-437.

Moy SS, Nadler JJ, Perez A, Barbaro RP, Johns JM, Magnuson TR, Piven J, Crawley JN. 2004. Sociability and preference for social novelty in five inbred strains: an approach to assess autistic-like behavior in mice. Genes Brain Behav 3:287-302.

Munn E, Bunning M, Prada S, Bohlen M, Crabbe JC, Wahlsten D. 2011. Reversed light-dark cycle and cage enrichment effects on ethanol-induced deficits in motor coordination assessed in inbred mouse strains with a compact battery of refined tests. Behav Brain Res 224:259-271.

Muzio L, Di Benedetto B, Stoykova A, Boncinelli E, Gruss P, Mallamaci A. 2002. Conversion of cerebral cortex into basal ganglia in Emx2(-/-) Pax6(Sey/Sey) double-mutant mice. Nat Neurosci 5:737-745.

Nadler JJ, Moy SS, Dold G, Trang D, Simmons N, Perez A, Young NB, Barbaro RP, Piven J, Magnuson TR, Crawley JN. 2004. Automated apparatus for quantitation of social approach behaviors in mice. Genes Brain Behav 3:303-314.

Nasrallah MP, Cho G, Simonet JC, Putt ME, Kitamura K, Golden JA. 2012. Differential effects of a polyalanine tract expansion in Arx on neural development and gene expression. Hum Mol Genet 21:1090-1098.

Nguyen L, Besson A, Heng JI, Schuurmans C, Teboul L, Parras C, Philpott A, Roberts JM, Guillemot F. 2006. p27kip1 independently promotes neuronal differentiation and migration in the cerebral cortex. Genes Dev 20:1511-1524.

Nieto M, Monuki ES, Tang H, Imitola J, Haubst N, Khoury SJ, Cunningham J, Gotz M, Walsh CA. 2004. Expression of Cux-1 and Cux-2 in the subventricular zone and upper layers II-IV of the cerebral cortex. J Comp Neurol 479:168-180.

Noctor SC, Martinez-Cerdeno V, Ivic L, Kriegstein AR. 2004. Cortical neurons arise in symmetric and asymmetric division zones and migrate through specific phases. Nat Neurosci 7:136-144.

Pedley TA. 1980. Interictal epileptiform discharges: discriminating characteristics and clinical correlations. American Journal Electroencephalographic Technology 20:101-119.

Phillips RG, LeDoux JE. 1992. Differential contribution of amygdala and hippocampus to cued and contextual fear conditioning. Behav Neurosci 106:274-285.

Poirier K, Van Esch H, Friocourt G, Saillour Y, Bahi N, Backer S, Souil E, Castelnau-Ptakhine L, Beldjord C, Francis F, Bienvenu T, Chelly J. 2004. Neuroanatomical distribution of ARX in brain and its localisation in GABAergic neurons. Brain Res Mol Brain Res 122:35-46.

Pontious A, Kowalczyk T, Englund C, Hevner RF. 2008. Role of intermediate progenitor cells in cerebral cortex development. Dev Neurosci 30:24-32.

Price DJ, Kennedy H, Dehay C, Zhou L, Mercier M, Jossin Y, Goffinet AM, Tissir F, Blakey D, Molnar Z. 2006. The development of cortical connections. Eur J Neurosci 23:910-920.

Price MG, Yoo JW, Burgess DL, Deng F, Hrachovy RA, Frost JD, Jr., Noebels JL. 2009. A triplet repeat expansion genetic mouse model of infantile spasms syndrome, Arx(GCG)10+7, with interneuronopathy, spasms in infancy, persistent seizures, and adult cognitive and behavioral impairment. J Neurosci 29:8752-8763.

Proud VK, Levine C, Carpenter NJ. 1992. New X-linked syndrome with seizures, acquired micrencephaly, and agenesis of the corpus callosum. Am J Med Genet 43:458-466.

Puelles L, Kuwana E, Puelles E, Bulfone A, Shimamura K, Keleher J, Smiga S, Rubenstein JL. 2000. Pallial and subpallial derivatives in the embryonic chick and mouse telencephalon, traced by the expression of the genes Dlx-2, Emx-1, Nkx-2.1, Pax-6, and Tbr-1. J Comp Neurol 424:409-438.

Quille ML, Carat S, Quemener-Redon S, Hirchaud E, Baron D, Benech C, Guihot J, Placet M, Mignen O, Ferec C, Houlgatte R, Friocourt G. 2011. High-throughput analysis of promoter occupancy reveals new targets for Arx, a gene mutated in mental retardation and interneuronopathies. PLoS One 6:e25181.

Remedios R, Huilgol D, Saha B, Hari P, Bhatnagar L, Kowalczyk T, Hevner RF, Suda Y, Aizawa S, Ohshima T, Stoykova A, Tole S. 2007. A stream of cells migrating from the caudal telencephalon reveals a link between the amygdala and neocortex. Nat Neurosci 10:1141-1150.

Ross ME. 2011. Cell cycle regulation and interneuron production. Dev Neurobiol 71:2-9.

Rudy B, Fishell G, Lee S, Hjerling-Leffler J. 2011. Three groups of interneurons account for nearly 100% of neocortical GABAergic neurons. Dev Neurobiol 71:45-61.

Sankoorikal GM, Kaercher KA, Boon CJ, Lee JK, Brodkin ES. 2006. A mouse model system for genetic analysis of sociability: C57BL/6J versus BALB/cJ inbred mouse strains. Biol Psychiatry 59:415-423.

Sansom SN, Livesey FJ. 2009. Gradients in the brain: the control of the development of form and function in the cerebral cortex. Cold Spring Harb Perspect Biol 1:a002519.

Schaeren-Wiemers N, Gerfin-Moser A. 1993. A single protocol to detect transcripts of various types and expression levels in neural tissue and cultured cells: in situ hybridization using digoxigenin-labelled cRNA probes. Histochemistry 100:431-440.

Schienle A, Ebner F, Schafer A. 2011. Localized gray matter volume abnormalities in generalized anxiety disorder. Eur Arch Psychiatry Clin Neurosci 261:303-307.

Sessa A, Mao CA, Colasante G, Nini A, Klein WH, Broccoli V. 2010. Tbr2-positive intermediate (basal) neuronal progenitors safeguard cerebral cortex expansion by controlling amplification of pallial glutamatergic neurons and attraction of subpallial GABAergic interneurons. Genes Dev 24:1816-1826.

Sessa A, Mao CA, Hadjantonakis AK, Klein WH, Broccoli V. 2008. Tbr2 directs conversion of radial glia into basal precursors and guides neuronal amplification by indirect neurogenesis in the developing neocortex. Neuron 60:56-69.

Sherr CJ, Roberts JM. 1999. CDK inhibitors: positive and negative regulators of G1-phase progression. Genes Dev 13:1501-1512.

Shinnar S, Hauser WA. 2002. Do occasional brief seizures cause detectable clinical consequences? Prog Brain Res 135:221-235.

Shoubridge C, Fullston T, Gecz J. 2010. ARX spectrum disorders: making inroads into the molecular pathology. Hum Mutat 31:889-900.

Shoubridge C, Tan MH, Seiboth G, Gecz J. 2012. ARX homeodomain mutations abolish DNA binding and lead to a loss of transcriptional repression. Hum Mol Genet 21:1639-1647.

Silverman JL, Yang M, Lord C, Crawley JN. 2010. Behavioural phenotyping assays for mouse models of autism. Nat Rev Neurosci 11:490-502.

Soriano E, Del Rio JA. 2005. The cells of cajal-retzius: still a mystery one century after. Neuron 46:389-394.

Suri M. 2005. The phenotypic spectrum of ARX mutations. Dev Med Child Neurol 47:133-137.

Takahashi T, Goto T, Miyama S, Nowakowski RS, Caviness VS, Jr. 1999. Sequence of neuron origin and neocortical laminar fate: relation to cell cycle of origin in the developing murine cerebral wall. J Neurosci 19:10357-10371.

Takahashi T, Nowakowski RS, Caviness VS, Jr. 1995. The cell cycle of the pseudostratified ventricular epithelium of the embryonic murine cerebral wall. J Neurosci 15:6046-6057.

Takiguchi-Hayashi K, Sekiguchi M, Ashigaki S, Takamatsu M, Hasegawa H, Suzuki-Migishima R, Yokoyama M, Nakanishi S, Tanabe Y. 2004. Generation of reelin-positive marginal zone cells from the caudomedial wall of telencephalic vesicles. J Neurosci 24:2286-2295.

Tarabykin V, Stoykova A, Usman N, Gruss P. 2001. Cortical upper layer neurons derive from the subventricular zone as indicated by Svet1 gene expression. Development 128:1983-1993.

Thomas A, Burant A, Bui N, Graham D, Yuva-Paylor LA, Paylor R. 2009. Marble burying reflects a repetitive and perseverative behavior more than novelty-induced anxiety. Psychopharmacology (Berl) 204:361-373.

Thomson AM, Lamy C. 2007. Functional maps of neocortical local circuitry. Front Neurosci 1:19-42.

Tottenham N, Hare TA, Quinn BT, McCarry TW, Nurse M, Gilhooly T, Millner A, Galvan A, Davidson MC, Eigsti IM, Thomas KM, Freed PJ, Booma ES, Gunnar MR, Altemus M, Aronson J, Casey BJ. 2010. Prolonged institutional rearing is associated with atypically large amygdala volume and difficulties in emotion regulation. Dev Sci 13:46-61.

Turner G, Partington M, Kerr B, Mangelsdorf M, Gecz J. 2002. Variable expression of mental retardation, autism, seizures, and dystonic hand movements in two families with an identical ARX gene mutation. Am J Med Genet 112:405-411.

Tury A, Mairet-Coello G, DiCicco-Bloom E. 2011. The cyclin-dependent kinase inhibitor p57Kip2 regulates cell cycle exit, differentiation, and migration of embryonic cerebral cortical precursors. Cereb Cortex 21:1840-1856.

Tury A, Mairet-Coello G, DiCicco-Bloom E. 2012. The multiple roles of the cyclin-dependent kinase inhibitory protein p57(KIP2) in cerebral cortical neurogenesis. Dev Neurobiol 72:821-842.

van Dongen-Boomsma M, Lansbergen MM, Bekker EM, Kooij JJ, van der Molen M, Kenemans JL, Buitelaar JK. 2010. Relation between resting EEG to cognitive performance and clinical symptoms in adults with attention-deficit/hyperactivity disorder. Neurosci Lett 469:102-106.

van Lookeren Campagne M, Gill R. 1998. Tumor-suppressor p53 is expressed in proliferating and newly formed neurons of the embryonic and postnatal rat brain: comparison with expression of the cell cycle regulators p21Waf1/Cip1, p27Kip1, p57Kip2, p16Ink4a, cyclin G1, and the proto-oncogene Bax. J Comp Neurol 397:181-198.

Vorhees CV, Williams MT. 2006. Morris water maze: procedures for assessing spatial and related forms of learning and memory. Nat Protoc 1:848-858.

Waclaw RR, Ehrman LA, Pierani A, Campbell K. 2010. Developmental origin of the neuronal subtypes that comprise the amygdalar fear circuit in the mouse. J Neurosci 30:6944-6953.

Whittington MA, Cunningham MO, LeBeau FE, Racca C, Traub RD. 2011. Multiple origins of the cortical gamma rhythm. Dev Neurobiol 71:92-106.

Wilson D, Sheng G, Lecuit T, Dostatni N, Desplan C. 1993. Cooperative dimerization of paired class homeo domains on DNA. Genes Dev 7:2120-2134.

Wohlrab G, Uyanik G, Gross C, Hehr U, Winkler J, Schmitt B, Boltshauser E. 2005. Familial West syndrome and dystonia caused by an Aristaless related homeobox gene mutation. Eur J Pediatr 164:326-328.

Woltering S, Jung J, Liu Z, Tannock R. 2012. Resting state EEG oscillatory power differences in ADHD college students and their peers. Behav Brain Funct 8:60.

Wonders C, Anderson SA. 2005. Cortical interneurons and their origins. Neuroscientist 11:199-205.

Woo NH, Lu B. 2006. Regulation of cortical interneurons by neurotrophins: from development to cognitive disorders. Neuroscientist 12:43-56.

Wood MA, Kaplan MP, Park A, Blanchard EJ, Oliveira AM, Lombardi TL, Abel T. 2005. Transgenic mice expressing a truncated form of CREB-binding protein (CBP) exhibit deficits in hippocampal synaptic plasticity and memory storage. Learn Mem 12:111-119.

Xu X, Roby KD, Callaway EM. 2010. Immunochemical characterization of inhibitory mouse cortical neurons: three chemically distinct classes of inhibitory cells. J Comp Neurol 518:389-404.

Yang F, Liu WP, He MX, Tang QL, Zhao S, Zhang WY, Xia QJ, Li GD. 2006. [Real-time fluorescence quantitative PCR in detecting ribosome protein S13 (RPS13) gene expression in NK/T cell lymphoma]. Sichuan Da Xue Xue Bao Yi Xue Ban 37:464-466.

Yang M, Crawley JN. 2009. Simple behavioral assessment of mouse olfaction. Curr Protoc Neurosci Chapter 8:Unit 8 24.

Zimmer C, Tiveron MC, Bodmer R, Cremer H. 2004. Dynamics of Cux2 expression suggests that an early pool of SVZ precursors is fated to become upper cortical layer neurons. Cereb Cortex 14:1408-1420.

Zupanc ML. 2009. Clinical evaluation and diagnosis of severe epilepsy syndromes of early childhood. J Child Neurol 24:6S-14S.